Synthesis of mesoporous nanomaterials from natural sources as low-cost nanotechnology

Zur Erlangung des akademischen Grades eines

DOKTORS DER NATURWISSENSCHAFTEN

von der Fakultät für

Bauingenieur-, Geo- und Umweltwissenschaften
der Karlsruher Institute für Technologie (KIT)

genehmigte

DISSERTATION

von

Dipl.-Chem.
Mehdi Adjdir

aus Oran

Tag der mündlichen Prüfung: 20.10.2010
Hauptreferent: PD. Dr. Detlef Eckhardt
Koreferent : Prof. Dr. Thomas Neumann

Karlsruhe 2010

Acknowledgments

I am profoundly grateful to Dr. Peter G Weidler for his patient guidance, support, encouragement and suggestions throughout this research and in the same time I appreciate his arrangement of facilities and equipments.

I acknowledge supports from Deutscher Akademischer Austausch Dienst (DAAD) for the scholarship in the program Research Grants for Doctoral Candidates under the matriculation: A/05/55364.

I am grateful to my PhD supervisor Prof. Dr. Detlef Eckhardt for having accepted me after and for his constructive criticism of the work and knowledge.

I would like to acknowledge other committee members including Prof. Dr. Heinz-Günter Stosch, Prof. Dr. Thomas Neumann, Prof. Dr. Harald Müller, Prof. Dr. Frank Schilling and PD Dr. Katja Emmerich for their guiding provided extensive knowledge and expanded my scientific point of view.

I would like to thank all my colleagues Nebatti Chergui-AEK, Ali-Dahmen Tewfik, Dr. Frank Friedrich, Dr. Cherifa Bachir and Carlos Azucena for the precious help and discussions, Dr. Hartmut Gliemann, Dr. Annett Steudel, Julia Scheiber, Andre Petershans, Mohamed Aymen Youssef and Mahmoud Bekri for the precious help for the continuous encouragement, and the pleasant atmosphere to this thesis.

Special thanks go to Marita Heinle for the ICP-OES measurements, Astrid Biedermann and Christian Biedermann for the precious help.

I also would like to thank all of my lab members at institute for Functional Interfaces, Karlsruhe Institute of Technology (KIT) for their valuable discussions, helps and comments.

I am finally deeply grateful to my father Djaber, my sisters Mokhtaria; Samar; Faiza and Nawel, my wife Karima and my kids Soumia and Youcef-yahia for support, understanding, encouragement, motivation and building up inspiration.

I dedicate this work to my deceased mother Adjdir-Nora Mimouna

Contents

LIST OF FIGURES

LIST OF TABLES

LIST OF ABREVIATION

MCM:	Mobil Composition of Matter or Mobil Crystalline Material
SBA-15:	Santa Barbara amorphous -15
ZSM-5:	Zeolite Socony Mobil -5
NaP:	$Na_6Al_6Si_{10}O_{32}\cdot 12H_2O$, Gismondine type framework (GIS)
XRD:	X-ray diffraction
FWHM:	Full Width at Half Maximum
XRF:	X-ray fluorescence
TEM:	Transmission Electron Microscopy
SAED:	Selected Area Electron Diffraction pattern
SEM:	Scanning Electron Microscopy
EDXS:	Energy Dispersive Analysis by X-ray Spectroscopy
BET:	Brunauer–Emmett–Teller
NLDFT:	Non-Local Density Functional Theory
FT-IR:	Fourier Transform Infrared
ICP-OES:	Inductively Coupled Plasma Optical Emission Spectrometer
CTAB:	Hexadecyltrimethylammoniumbromide
ATR-FT-IR:	Attenuated Total Reflectance-Fourier Transform Infrared
IUPAC:	International Union of Pure and Applied Chemistry
cmc:	Critical Micelle Concentration
μm:	Micrometer
ppm:	Parts Per Million
mmol:	Millimole
wt.%:	Weight percentage

Abstract

The study focuses on the MCM-41 material (MCM = Mobil Composition of Matter). This material shows a hexagonal array of uniform mesopores with sizes ranging from 2 to 10 nm. Their extraordinary high surface around 1000 m^2/g and distinct adsorption properties open up many potential applications in catalysis, catalytic supports, energy, adsorbents, host–guest chemistry, sensors and drug delivery.

The MCM-41 nanomaterial is usually synthesized by using laboratory reagents as silicate sources such as cab-o-sil M5 fumed silica, sodium silicate and tetramethylammonium silicate and ludox (colloidal silica). For aluminium source sodium aluminates are used. These laboratory reagents are still expensive for a large scale production, and it is found in the literature that the higher aluminium content in the MCM-structure decreases their crystallinity. This work is undertaken to solve: first the problem of cost by replacing these expensive laboratory reagents by others more effective; secondly how to conserve their physical properties cited above; thirdly how to increase the aluminium content in the MCM-structure with the preservation of the crystallinity.

The volclay a low-cost mass clay material is used as model for a natural source. The volclay contains smectite as the dominating clay mineral and other minerals like quartz, muscovite and feldspars. This clay mineral is taken to replace both the synthetic silicon and aluminium in the synthesis of nanomaterials. The silicon and aluminium are extracted from volclay by applying the alkaline fusion process as a first step. This process consists of fusion of a volclay-NaOH mixture at 550 °C for 1 h, where all different phases which constitute volclay are dissolved. In the second step, the fused volclay-NaOH is mixed with water under stirring. In a third step, two phases are obtained after centrifugation, a sedimented phase which is called residual-1 and a liquid phase which is called supernatant-1. This supernatant-1 is used as silicon and aluminium source for the synthesis of Al-MCM-41. The product was afterwards characterized with different techniques such as X-Ray Diffraction (XRD), Nitrogen Adsorption-desorption, and Infra Red-spectroscopy (IR). To examine whether all soluble species have been dissolved, a second supernatant-2 was obtained after centrifuging the solution prepared from the residual-1 and water. This solution is called supernatant-2 and is further used as silicon and aluminium source for the synthesis of MCM-41 nanomaterials. Comparison of the physical properties of MCM-41 from laboratory reagent and from supernatant-1 and -2 reveals that the MCM-41 from supernatant-1 and -2 present a better ordered structure, a higher specific surface area of around 1060 m^2/g and 1040 m^2/g

respectively compared to MCM-41 from laboratory reagents, where its specific surface area is around 540 m^2/g. The aluminium content in the MCM-41 framework from supernatant-1 is higher than that found in MCM-41 laboratory reagents. The Si/Al ratio increased approximately 4-fold in favour of the MCM-41 from supernatant-1 with the preservation of MCM-structure crystallinity. The pore size for the MCM-41 from laboratory reagents, MCM-41 from supernatant-1 and 2 was constant at around 3.8 nm.

In addition, an Algerian bentonite was used and compared to volclay. This Algerian bentonite undergoes the same alkaline fusion treatment as volclay with the same treatment parameters such as clay/NaOH weight ratio, temperature and treatment time. According to different analysis, no impurities which belong to Algerian bentonite were detected in MCM-41 from this source. The specific surface area of MCM-41 from bentonite is around 460 m^2/g smaller than the ones found from both supernatant-1 and supernatant-2 derived from the volclay and similar to that one found by using the laboratory reagent where the Si/Al is around 50. The alkaline fusion at 550 °C is an alternative to produce cheap silicon and aluminium. From different results obtained in this work, the use of the silicon and aluminium obtained from the alkaline fusion increase the aluminium content in the nanomaterials framework and enhance the physical properties of the nanomaterials either mesoporous or microporous. The fusion process can be applied on a large kind of clays and even waste materials which contain silicon and aluminium.

Zusammenfassung

Diese Arbeit handelt von einem mesoporösen Material, das als MCM-41 (Mobil Composition of Matter) bezeichnet wird. Dieses Material weist eine hexagonale Anordnung von einheitlichen parallel angeordneten zylindrischen Mesoporen auf, deren Größen zwischen 2 und 10 nm liegen. Die außerordentlich hohe Oberfläche und deren besonderen Adsorptionseigenschaften eröffnen viele potentielle Anwendungen u.a. in Katalyse, Katalysematerialien, Energiebereich, Adsorbentien, Host-Guest Chemie, Sensoren und kontrollierte Arzneimittelabgabe.

Das MCM-41 Nanomaterial wird üblicherweise aus Reinstchemikalien synthetisiert. Als Siliziumquelle werden u.a. cab-o-sil M5 fumed silica, Na-Silicate, tetramethylammonium Silicate und Ludox (kolloidales Silica) verwendet. Das Aluminium wird aus Aluminaten gewonnen. Die Reinstchemikalien sind jedoch für eine industrielle Großproduktion sehr teuer. Diese Arbeit wurde unternommen, um dieses Kostenproblem zu beheben und diese teuren Chemikalien durch preiswertere zu ersetzen. Volclay, ein kostengünstiger Massenrohstoff auf Basis von Schichtsilcaten (Tone, Clays), wurde als Modellsubstanz eines natürlichen Ausgangsmaterials verwendet. Der Volclay enthält Smektit als dominierendes Tonmineral (reich an Al und Si) und andere Minerale wie Quarz, Muskovit und Feldspäte.

Das Silizium und Aluminium wurden aus dem Volclay in einem ersten Schritt durch einen basischen Aufschluss extrahiert. Dieser Prozess besteht aus einer einstündigen Behandlung der Volclay-NaOH Mischung bei 550 °C, bei dem die mineralischen Bestandteile des Volclay aufgelöst werden. Im zweiten Schritt wird das aufgeschlossene Volclay-NaOH Gemisch mit Wasser vermischt. In einem 3. Schritt erhält man zwei Phasen durch Zentrifugation, ein Sediment, das Residual-1 und einen Überstand, der Supernatant-1 genannt wird. Dieser Überstand Supernatant-1 wird als Si- und Al-Quelle zur Synthese von Al-MCM-41 verwendet. Das so erhaltene Produkt wurde mit verschiedenen Analysemethoden, wie XRD (Röntgenbeugung), BET (N_2 Gassorption) und IR-Spektroskopie charakterisiert.

Zur Beantwortung der Frage zur Effizienz des Prozesses, also ob alle löslichen Anteile in Lösung gingen, wurde in einer weiteren Zentrifugation des Residual-1/Wassergemisches ein Supernatant-2 hergestellt. Diese Lösung wurde für eine weitere Synthese von MCM-41 herangezogen.

Der Vergleich der Eigenschaften der MCM-41 Nanomaterialien hergestellt aus Reinstchemikalien und den verschiedenen Lösungen (Supernatant-1 und -2), die aus dem Aufschluss des Volclay gewonnen wurden, zeigen höhere spezifische Oberflächen mit 1060

m^2/g und 1040 m^2/g, als die von Reinstchemikalien herrührenden MCM-41 Proben mit ca. 540 m^2/g.

Der Al-Gehalt ist in den MCM-41 Proben, die aus Supernatant-1 hergestellt wurden, höher als in den herkömmlich produzierten. Das Si/Al-Verhältnis vergrößerte sich fast 4-fach. Dagegen lagen die Porenweite aller Proben bei ca. 3.8 nm.

Zusätzlich wurde als Vergleich zum Volclay ein Bentonit aus Algerien getestet. Dieser Bentonit wurde unter den identischen Bedingungen aufgeschlossen. In den MCM-41 Endprodukten konnten keine Verunreinigungen, die aus dem Bentonit stammen könnten, gefunden werden. Die spezifische Oberfläche dieser MCM-Phasen war jedoch um ca. 460 m^2/g kleiner als die der Produkte, die aus den Supernatant-1 und Supernatant-2 Lösungen des Volclays hergestellt wurden.

Introduction

The family of mesoporous M41S material consists of three types, MCM-41, MCM-48 and MCM-50. The M41S assures a bright future due to their properties with a well-defined pore size between 2-20 nm and their extraordinary high specific surface up to 1000 m^2/g and distinct adsorption properties due to their pore volume around 0.9 cm^3/g. The number of publications on MCM-41 (MCM is the abbreviation for **M**obil **C**rystalline **M**aterial) has experienced considerable growth since their first appearance in 1990. This growth is attributed to their wide use in different field of industry.

Zeolite has extensive applications in basic science, petrochemical science, energy conservation/storage, medicine, chemical sensor, air purification, environmentally benign composite structure and waste remediation. Despite these catalytically desirable properties of zeolites, they become inadequate when reactants with sizes above the dimensions of the pores have to be processed. In this case the rational approach to overcome such a limitation would be to maintain the porous structure, which is responsible for the benefits described above. The mesoporous materials can resolve these problems and can be used in catalysis, catalytic supports, sensors, adsorbents, host–guest chemistry, energy, drug delivery. However, the use of synthetic zeolite and MCM-41 in these areas are restricted due to prohibitive production cost.

The challenge was the use of a natural source as precursor for the synthesis of nanomaterials either mesoporous or microporous. The use of waste and natural materials as silicon and aluminium precursors is considered as direct synthesis and by their use not only the problem of storage will be resolved but also the problem of mesoporous cost. To achieve this aim, some questions have been raised, for example which kind of natural source should be used? Or is this natural source adequate to be used as nanomaterials precursor?

Referring to the literature, many attempts are focused on the use of a waste source, such as fly and bottom ashes, rice husk, instead of the laboratory reagents to reduce the cost of mesoporous materials. The use of ash and bottom ash, as silicon and aluminium source, in large scale can cause the same problem caused when ash and bottom ash are produced (see Chapter 1). Concerning rice husk, the problem comes from their treatment to extract the silicon and aluminium, they used toxically chemical reagent in addition to thermal treatment for several hours (Chapter 1). Referring to the literature, very limited works are focused on the use of natural ores as silicon and aluminium precursors for the synthesis of mesoporous. Zhu et al., (2002) were the first who investigated the combination between pillared clays and

quaternary ammonium bromide. Recently, Kang et al., (2005) reported the synthesis of Al-MCM-41 by using water glass (or silicate sodium) as Si source and meta-kaolin as Al sources. In this work and contrary to Kang et al, we tried for the first time to use volclay, which is a low-cost mass clay, as both silicon and aluminium source. An overview of this work and the route towards a solution to the above stated problems is given in the following flow sheet (Fig.1).

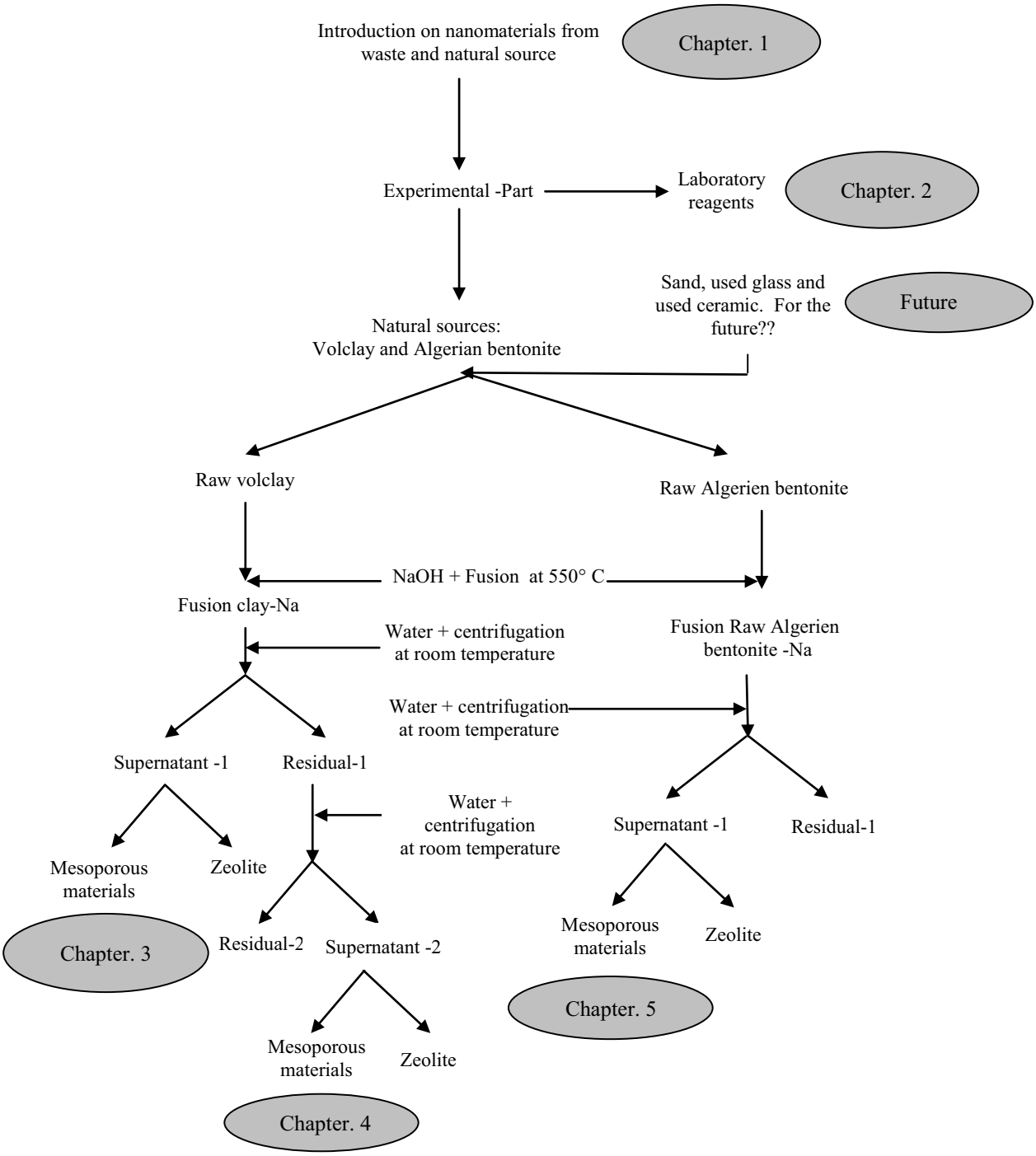

Fig.1. Flow sheet of the different production steps of MCM-41 and zeolite from clay

In the following paragraphs, a description of the chapters of this work will be given.

First in Chapter 1, a detailed description of MCM-41 material and its different synthesis methods has been carried out. In this part comprehensive, chronologic review about the use of waste and natural sources as silicon and aluminium precursor as presented fly and bottom ashes, rice husk, kaolin, diatomite, pumicite attapulgite and volclay, the characterisation of the starting source cited above and optimisation of synthesis parameters, was considered.

In chapters 2, the production of MCM-41 from laboratory reagents with different substitutions of aluminium and boron is explained. Different characterization techniques are described, which accounts for the most important MCM-41 properties.

Chapter 3, and 4 are focused on the use of volclay as new challenge instead laboratory reagents. In the 3rd chapter, the focus is done on the optimisation of different NaOH forms (powder or pastille), which exhibit a marked difference in pricing, and on the kind of treatment of volclay- sodium hydroxide. This treatment consists on the fusion of volclay and sodium hydroxide mixture at 550 °C for 1 h, the fused mixture is combined with water under stirring, then the solution is centrifuged and two different phases are obtained, a solution which is called supernatant-1 and a sediment which is called residual-1, where 1 is referred to the 1st centrifugation and so forth. The supernatant-N (where N is the number of centrifugation steps) is characterized with Inductively Coupled Plasma Optical Emission Spectrometer (ICP-OES). According to the result obtained from ICP-OES, the supernatant-1 is used as silicon and aluminium source for the synthesis of Al-MCM-41. The product is afterwards characterized with different techniques such as XRD, BET, and IR-spectroscopy.

The aim of the 4th chapter is to examine whether all soluble species have been dissolved. A second supernatant solution was obtained by centrifuging the solution prepared from the residual-1 and water. The supernatant-2 is then used as silicon and aluminium precursor in the synthesis of Al-MCM-41. Another question is raised: is the silicon and aluminium extraction process, developed in chapter 3, effective for all kind of clay mineral? (e.g. Algerian bentonite) The answer of this question is given in chapter 5.

At the end of this work a summary is given, where the answers and the most important results are given.

Chapter 1.

Ordered mesoporous materials from chemical reagents, natural and waste sources

1.1 Introduction

International Union of Pure and Applied Chemistry (IUPAC) classifies three categories for pore sizes in solids. Pore size distributions larger than 50 nm are macroporous. Materials having pores between 2 nm to 50 nm represent mesoporous material. Materials with pore size distribution less than 2 nm are related to microporous materials. Mesoporous are silicates or heteroatom–silicates, their structure is made up of a framework of $[SiO_4]^{4-}$ and $[AlO_4]^{5-}$ or $[T^mO_4]^{m-8}$ (T ≡ Al, B, Ti, Zn, Cu….) tetrahedra linked to each other at the corners by sharing their oxygens (Fig.1.1.1).

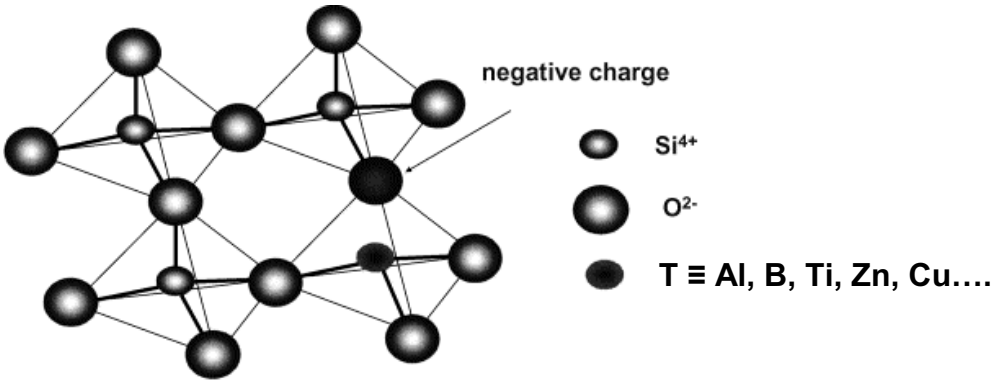

Fig.1.1.1. Idealized structure of MCM-41 framework of silicon and heteroatom tetrahedral units

The tetrahedra make up a one-dimensional, with lots of pores and open spaces. It displays an ordered structure with uniform mesopores arranged into a hexagonal, honeycomb-like lattice (Fig.1.1.2a and b).

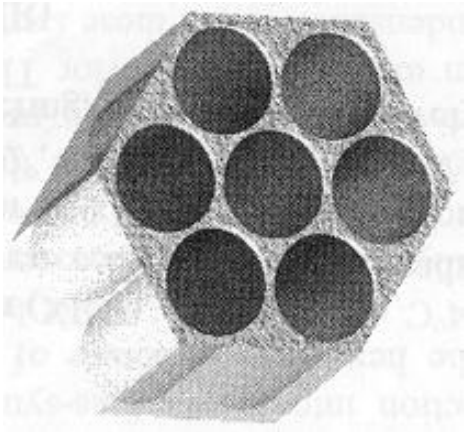

Fig.1.1.2a. Schematic representation of MCM-41

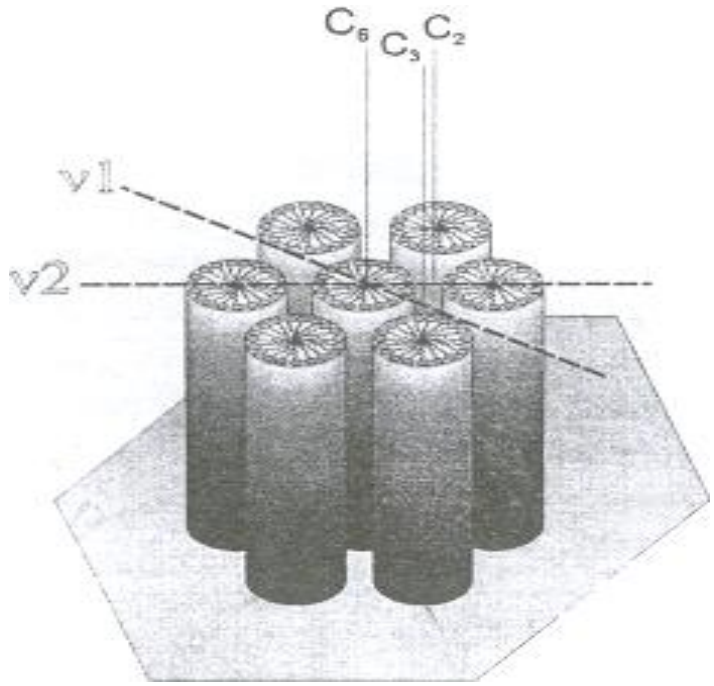

Fig.1.1.2b. Schematic representation of MCM -41 micelles arrangement

Mesoporous materials belong to a new family of material with sizes intermediate to those usually studied by chemists and material scientist, and therefore mesoporous materials pose new challenge in their synthesis and characterization. The first report on the formation of "low bulk density silica" was reported by Chiola et al., (1971). The findings were filed as a patent for Sylvania Electric Product Inc. According to their research, the silica is obtained through the reaction of cetyltrimethylammonium bromide and tetraethylorthosilicates. Nevertheless, the Sylvania Electric researchers did not give any importance on the silica characterization. In 1992, researchers at the Mobil Oil Company reported a novel family of materials called M41S (Beck et al., 1991; Kresge et al., 1992; Beck et al., 1992). The family of mesoporous M41S material consists of three types, as summarized in Table 1.1.1, Fig.1.1.3.

Table 1.1.1. Different phases of M41S family

Material type	Phase
MCM-41	hexagonal
MCM-48	Cubic
MCM-50	lamellar

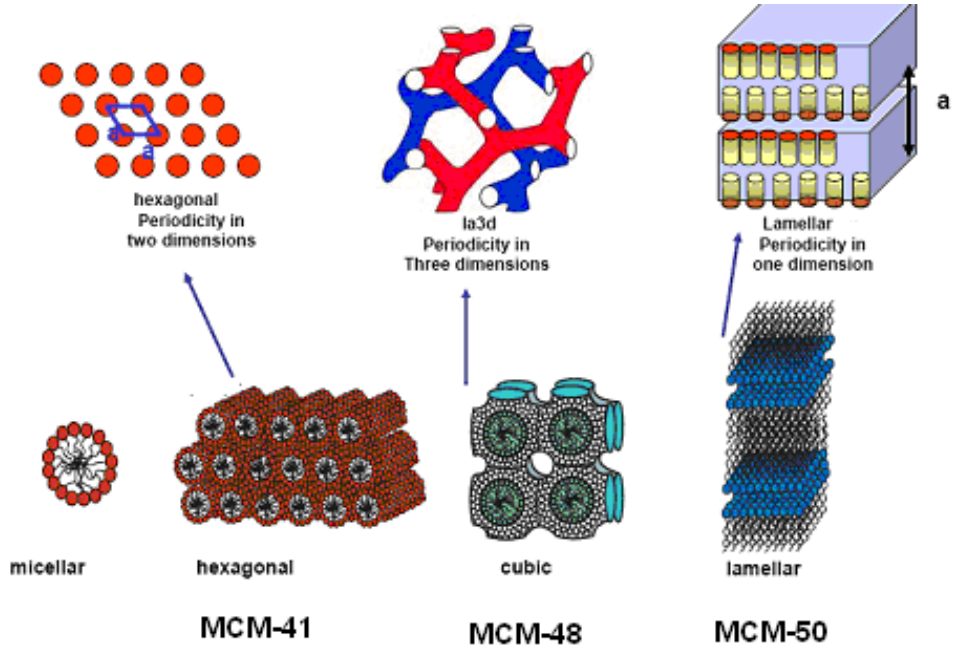

Fig.1.1.3. Different phases of M41S family

The M41S assures a bright future due to their properties with a well-defined pore size between 2-20 nm and their extraordinary high surface up to 1000 m^2/g and distinct adsorption properties due to their pore volume around ca 0.9 cm^3/g. The number of publications on MCM-41 has experienced considerable growth since their first appearance in 1990. This growth is attributed to their wide useful in different field of industry. In catalysis (Zhao et al., 2005; Hu et al., 2006; Li et al., 2006), catalytic supports (Perathoner et al., 2006), energy (Gao et al., 2002; Sun et al., 2007), adsorbents (He et al., 2009; Akasaka et al., 2009), host–guest chemistry (Parala et al., 2000; Lee et al., 2005), sensors (Shimizu et al., 2004; Dai et al., 2007), drug delivery (Salonen and Lehto, 2008; Angelos et al., 2008).

1.2 Synthesis parameters of mesoporous materials

1.2.1 Introduction

The concept of micelle from lat. Micella meaning "small bit" was introduced for the first time by McBain and Soldate (1942) to describe colloidal aggregates obtained from the salts of fatty acids in aqueous solution. One of the most used properties of micelles is their ability to solubilize hydrophobic substances, thereby altering their physical properties and chemical. A micelle is an aggregate formed by self association of a number of organic surfactant molecules, also called surfactants (SURface ACTive AgeNT). These molecules are organic compounds with antagonistic properties.

1.2.2 Properties of surfactant and micelles

Surfactants are amphiphilic molecules which contain a polar head group and a nonpolar tail (Fig.1.1.4). In general, the tail is a chain of hydrocarbon groups. When the amphiphilic molecules are dispersed in a single solvent, such as water, the hydrophobic characteristic of the hydrocarbon chains drives the amphiphilic molecules to self-assemble into some structures. In these structures, the hydrophobic tails are shielded from unfavourable interactions with the polar solvent by the hydrophilic polar head group.

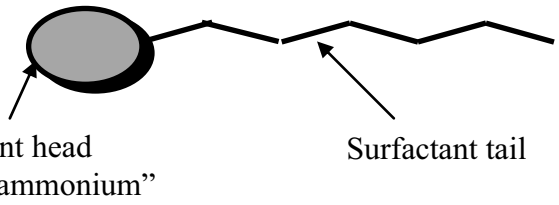

Fig.1.1.4. Schematic illustration of the reversible monomer-surfactant. The black circles represent the surfactant heads (hydrophilic moieties) and the black curved lines represent the surfactant tails (hydrophobic moieties)

A surfactant, when present at low concentrations in a system, adsorbs onto surfaces or interfaces significantly changing the surface or interfacial free energy. Surfactants usually act to reduce the interfacial free energy, although there are occasions when they are used to increase it (Rosen, 1989). When surfactant molecules are dissolved in water at concentrations above the critical micelle concentration (cmc)**,** they form aggregates known as micelles. In a micelle, the hydrophobic tails flock to the interior in order to minimize their contact with water, and the hydrophilic heads remain on the outer surface in order to maximize their contact with water (see Figure.1.1.5) (Chevalier and Zemb, 1990; Tanford, 1980). The micellization process in water results from a delicate balance of intermolecular forces including hydrophobic, steric, electrostatic, hydrogen bonding, and van der Waals interactions. The main attractive force results from the hydrophobic effect associated with the nonpolar surfactant tails, and the main opposing repulsive force results from steric interactions and electrostatic interactions between the surfactant polar heads. Whether micellization occurs and, if so, at what concentration of monomeric surfactant, depends on the balance of the forces promoting micellization and those opposing it (Tanford, 1980).

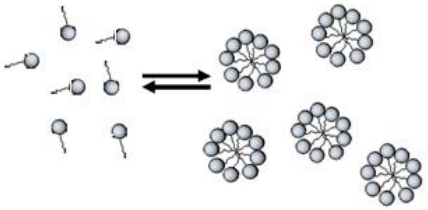

Fig.1.1.5. Schematic illustration of the reversible monomer-micelles

1.2.3 Liquid crystalline phases

The earliest liquid crystalline phase that is formed by spherical micelles is the micellar cubic, denoted by the symbol (I_1). This is a highly viscous, optically isotropic phase in which the micelles are arranges on a cubic lattice. At higher amphiphile concentrations the micelles fuse to form cylindrical aggregates of indefinite length, and these cylinders are arranged on a long-ranged hexagonal lattice. This lyotropic liquid crystalline phase is known as the hexagonal phase, and is generally denoted by the symbol (H_I). Cubic phase denoted as (V_1) appears when the amphiphile concentrations increase. At higher concentrations of amphiphile the lamellar phase is formed. This phase is denoted by the symbol (L_α). This phase consists of amphiphilic molecules arranged in bilayer sheers separated by layers of water (Fig.1.1.6).

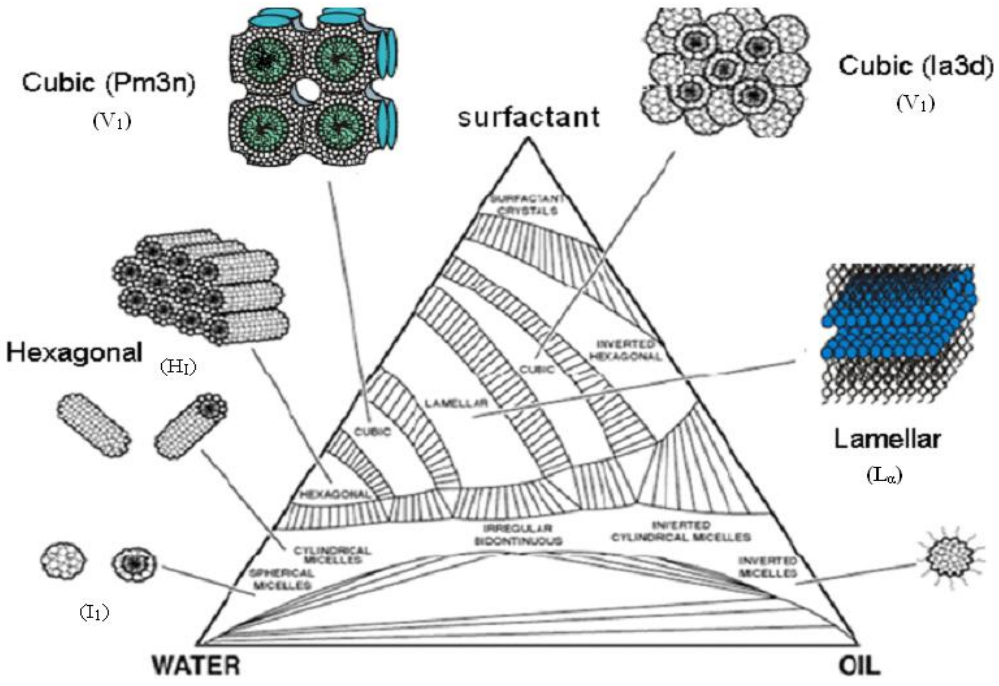

Fig.1.1.6. Diagram surfactant/water/oil and different liquid crystalline phases

1.2.4 Principles of synthesis

A typical synthesis of MCM-41 requires a minimum of four reagents: a solvent (water and/or ethanol), a silica precursor (tetraethyl orthosilicate (TEOS), tetramethyl orthosilicate (TMOS), tetrabutyl orthosilicate (TBOS), Ludox), an ionic (anionic or cationic) or non-charged surfactant and a catalyst. Depending on the protocol, the reaction could occur in an acidic or basic medium, with different silica/surfactant ratios. The mixture is stirred, aged at room temperature and placed in a static autoclave for several hours at 100 °C. The surfactant template is removed by calcination.

1.2.5 Effect of substitution of different elements

The discovery of mesoporous materials offers new possibilities for using large molecules such as those commonly used in the production of fine chemicals and petrochemicals. Many researches on MCM-41 have been focused on the incorporation of different elements like Al, B, Zn, Cu, Ti and on the grafting of different active functions in order to modify the framework of MCM-41 mesoporous materials and to generate catalytic sites needed for different type of reactions. The aluminosilicate mesoporous molecular sieves have received much attention for their strong Brønsted and Lewis acidity. Many efforts have been made to optimize the silicate sources such as cab-o-sil M5 fumed silica, sodium silicate and tetramethylammonium silicate (Liu et al., 1996), cab-o-sil M5 fumed silica and sodium silicate (Yanagisawa et al., 1990). The aluminium source has been studied by Borade and Clearfiled (1995), Occelli et al., (1998) and Badamali et al., (2000) who have reported that the sodium aluminate source incorporates aluminium to a maximum amount in the framework sites. In addition, density and the strength of acid sites are found to be significantly higher when sodium aluminate is applied. The aluminium containing MCM-41 can be synthesized by both direct and post-treatment synthesis using a wide range of Si/Al ratios, depending on different synthetic conditions. The typical characteristic of Al-MCM-41 such as highly ordered mesoporosity; large surface area; high thermal stability and acidity allow the possibility of applying these materials as catalyst in the synthesis and conversion of large molecules. The catalytic activity of aluminium containing MCM-41 is attributed to the presence of acidic sites arising from the AlO_4 tetrahedral units in the framework. These acid sites may be Brønsted or Lewis in character depends on the nature of treatment. A purely MCM-41 framework is electronically neutral due to (+4) charge of Si and four (-1) charges from oxygen atoms. However, the substitution of another element such as aluminium atom

affects the charge density of the framework. As a result, purely siliceous MCM-41 loses neutrality when lattice Si^{+4} cations are replaced by Al^{+3} cations. This requires the Al atoms to be tetra-coordinated and consequently becomes negatively charged. The distribution of tetrahedral Si and Al atoms in the framework is generally, governed by Loewenstein and Lowenstein's rule (1953). The rule suggests that AlO_4 tetrahedral in aluminosilicate networks do not share oxygen atoms. Thus, according to that (AlOAl) avoidance principle, Al-MCM-41 is composed of alternating silicon and aluminium atoms and imposes an overall negative charge. The negatively charged framework is balanced by Na^+ ions present in the system (Figure.1.7).

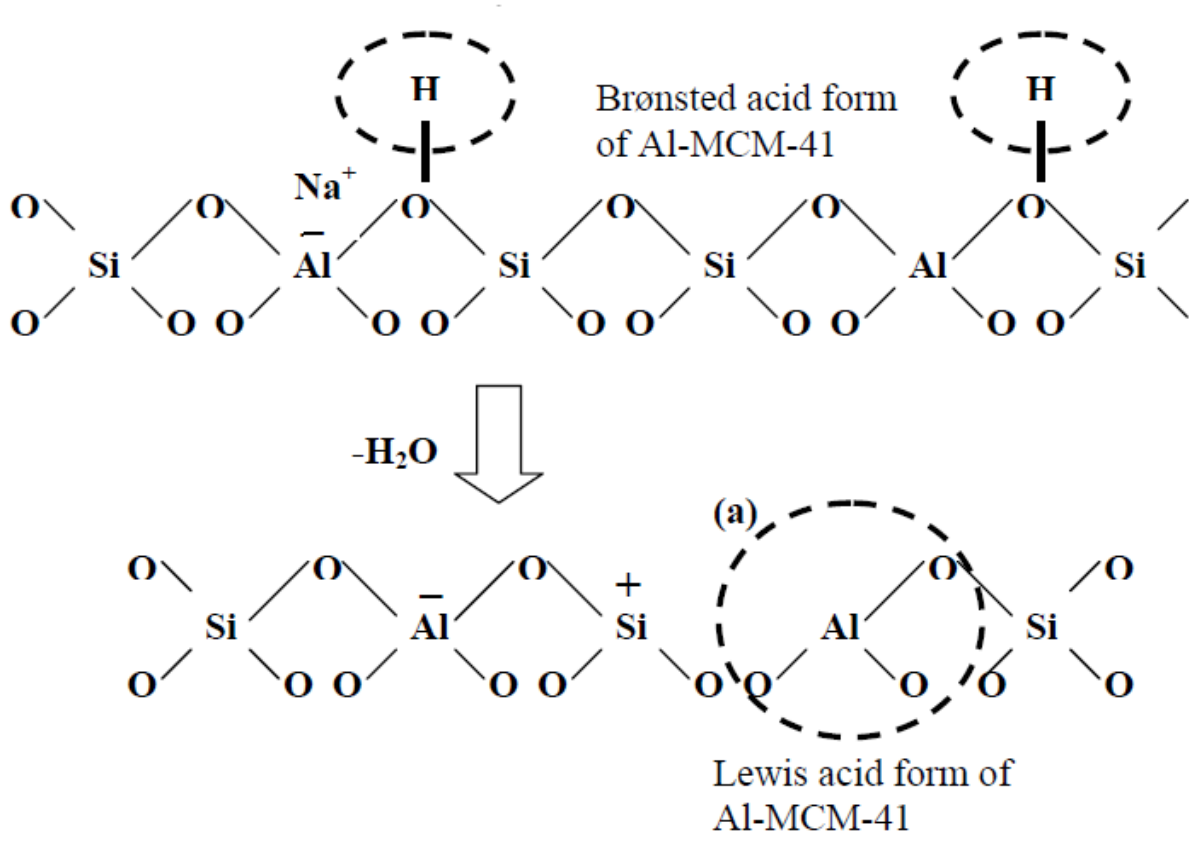

Fig.1.1.7. Scheme for the generation of Brønsted and Lewis acid sites with (a) Distorted Framework Tricoordinated Aluminium in Al-MCM-41

1.2.6 MCM-41 for enzyme stabilization

Enzyme immobilization in MCM-41 was first reported by Diaz and Balkus, and it was found that the enzyme immobilization was dependent on the molecular size of enzymes (Diaz and Balkus, 1996). A recent trend is to modify mesoporous silica in a more delicate way, which can expedite the adsorption of enzymes by enlarging the inlet pore size or controlling the morphologies of materials (Jie et al., 2004; Fan et al., 2003). Immobilized enzymes in mesoporous materials have found applications in biosensors (Liu et al., 1997; Liu et al., 2003, Heilmann et al., 2003 and Xu et al., 2009), peptide synthesis (Shanbhag et al., 2008), and pulp bio-bleaching (Sasaki et al., 2001).

1.2.7 MCM-41 as adsorbent

The separation of precious metals from complex mixtures is difficult, but of great economic importance. The mesoporous NH_2-MCM-41 adsorbent prepared by grafting aminopropyls on MCM-41 has successfully adsorbed gold and palladium and can be used to separate these precious metals from complex solutions containing other metal ions such as cobalt, nickel, copper and zinc. Adsorption is rapid and the adsorbent's capacity for gold is better comparable to most carbonaceous adsorbents including activated carbons. Furthermore, NH_2-MCM-41 can separate palladium from gold solution at pH1.0 (58.5 mg/g) with excellent selectivity and capacity. The sequential adsorption at different pHs enabled the separation first of palladium at pH1.0 (58.5 mg/g) and then gold at pH2.5 (276.0 mg/g) from the solution. A simple acid wash was sufficient to recover the adsorbed palladium and gold as concentrated, high purity (i.e., > 95%) metal salt solutions and the regenerated adsorbent was reused without lost of performance (Lam et al., 2007).

1.2.8 MCM-41 as host-guest

The porosity of MCM-41 makes it an ideal candidate for the loading and encapsulation of metals, metal oxides and semiconductors as well as molecular liquids, e.g. water (Moller and Bein, 1998; Llewellyn et al., 1994; Wu et al., 1994 ; Gross,et al., 1999 and Baker et al 1997). Different pathways have been reported for synthesizing metallic particles within mesoporous silica: impregnation from solution followed by a reduction process (heat-treatment, irradiation, and chemical reduction), gas phase deposition and chemical vapour deposition. Inclusion chemistry is by far the most used route and improvements have been made to increase the amount of loaded material via a functionalization of the mesopores

Moller and Bein, (1998). The functionalization can be achieved by introducing positive charges in the intrachannel surface of the host silica for the accommodation of negatively charged metal complexes. Supported high density stable arrays of highly crystalline nanowires can be produced inside the mesoporous matrix. In the case of the noble metals (Au, Pt, Pd), bundles of nanowires were observed with a diameter.

1.2.9 MCM-41 for the removal of heavy metals

The expanded ordered mesoporous silica MCM-41 and MCM-48 with hexagonal and cubic structures respectively were prepared by post-synthesis method with N-N dimethyldodecylamine (DMDDA) and dodecylamine (DDA). The expanded materials were tested for adsorption of Cd^{2+}, Co^{2+}, Cu^{2+} and Pb^{2+} in aqueous solution. Aminated materials were found to be fast adsorbents for metallic ions cation with affinity for Cu^{2+}, Pb^{2+}, than for Cd^{2+} and Co^{2+} from single solution. In mixed metallic ions cation solutions, competition by the adsorption sites is likely to occur, the adsorption preference is for Cu^{2+} and Pb^{2+}. All materials are very efficient at low metal ions concentration and substantial amounts of Cd^{2+}, Co^{2+}, Cu^{2+} and Pb^{2+}. The capacity order for single solutions is: $Cu^{2+} > Pb^{2+} > Cd^{2+} > Co^{2+}$. On the mixed cations solutions, the adsorption affinity sequence is the same with a competitive mechanism. MCM-41 and MCM-48 expanded with DMDDA have more affinity to remove the cations compared with those expanded with DDA (Benhamou et al., 2009).

1.3 Problem statement

The use of mesoporous materials synthesized from laboratory silicon and aluminium reagents in large scale confronts a serious problem that is their high price, for example 5 g of Al-MCM-41 is approximately 308 € when 1kg of Al-MCM-41 is 6000 €. This problem is a handicap for their use in industry. For this, the need to find solutions to the problem would be greatly desired. Many researchers have devoted studies to replace the expensive source of synthetic silica with one that is cheaper. Later in this chapter, it will be presented the works that have been made by scientists using different natural sources or even waste materials as a source of silica and aluminium and you will find also our contribution to resolve this problem. For a good understanding of this chapter, it will be discussed different propositions to resolve this problem according of their chronological appearance. We will start with the fly ash and rice husk being considered as waste, and then we finished with the natural sources.

1.4 Introduction

1.4.1 Coal fly ash

The use of waste and natural materials as silicon and aluminium precursors is considerate as direct synthesis and by their use not only the problem of their storages will be resolved but also the problem of mesoporous cost. The use of waste source like coal fly ash, which is recognized as "products" "coal combustion products", this term, was coined by the US. Environmental Protection Agency, by many scientists as low cost materials and in order to reduce its important quantity. Coal combustion in the world accounts for about 37% of the total electricity production (Kumar et al., 2001) and, in turn, results in huge amounts of fly ash as waste materials. In 2008, the United States produced more than 130 million tons of coal combustion products. While 43% were used beneficially, nearly 75 million tons were disposed (acaa-usa.org). In the European Union of the EU 15 the production was about 61 million tons in 2007 and in the larger EU of 27 member states the total production is estimated to be about 100 million tons (ecoba). Currently, the energy sector in India generates over 130 Mt of fly ash annually (Burke et al., 2007). The disposal of waste of coal combustion products is one of the many environmental problems affecting our planet. Millions tons of coal fly ashes are stored in landfills in USA and other countries in Europe and due to their properties particularly durability and no biodegradability at all, make their elimination process difficult. In addition, it is known that their fine particles can become airborne by virtue of their very low masses and can cause fibrosis or cancer. Since the major chemical compounds contained in fly ash are SiO_2 and Al_2O_3 (60–70 wt.% and 16–20 wt.%, respectively), resource recovery from coal fly ash is one of the most important issues in waste management at present. Tremendous research effort was put into how to increase the disposal rate of fly ash and how to promote the recycling of fly ash into microporous and mesoporous materials. Therefore, this new way of its utilization is not only the elimination of the storage problem of fly ash but also turns it into useful materials, to contribute to resolve its health's problems and to reduce the electricity bill.

1.4.2 Rice husk

Global production of rice, the majority of which is grown in Asia, is approximately 550 million tons/year. Rice milling industry generates a lot of rice husk during milling of paddy which comes from the fields. This rice husk is mostly used as a fuel in the boilers for processing of paddy. Rice husk is also used as a fuel for power generation. Rice husk ash

(RHA) is about 25% by weight of rice husk when burnt in boilers. It is estimated that about 70 million tons of RHA is produced annually worldwide. This RHA is a great environment threat causing damage to the land and the surrounding area in which it is dumped. This RHA in turn contains around 85% - 90% amorphous silica. Lots of ways are now being thought of for the disposing of RHA through commercial use. RHA is a good super-pozzolan (material with a high silica content of above 85%) and can be used to make special concrete mixes. Recently the new perspectives are inspected, for this kind of waste basing on their chemical composition which is rich on silicon needed for the synthesis of porous materials either microporous materials or mesoporous materials.

1.4.3 Clay and clay mineral

The term "clay" refers to a naturally occurring material composed primarily of fine-grained minerals, which is generally plastic at appropriate water contents and will harden with dried or fired. Although clay usually contains phyllosilicates, it may contain other materials that impart plasticity and harden when dried or fired. Associated phases in clay may include materials that do not impart plasticity and organic matter.

The term "clay mineral" refers to phyllosilicate minerals and to minerals which impart plasticity to clay and which harden upon drying or firing. Currently, minerals known to produce the property of plasticity are phyllosilicates. Because minerals are not defined based on their crystallite size, appropriate phyllosilicates of any grain size may be considered "clay minerals". Likewise, clay minerals are not restricted, by definition, to phyllosilicates. If research reveals that a non-phyllosilicate mineral imparts plasticity to clay and hardens upon drying or firing, this mineral is a "clay mineral". For example, if an oxy-hydroxide mineral in a clay shows plasticity and hardens upon drying or firing, it may be properly referred to as a "clay mineral". Thus, clay is not required to be predominantly composed of phyllosilicates. Minerals that do not impart plasticity to clay and non-crystalline phases (regardless if they impart plasticity or not) are either "associated minerals" or "associated phases", respectively. (Guggenheim. 1995).

The variation, in both chemistry and structure, among the clays leads to their applications in extremely diverse fields. Nevertheless the difference in structural and chemical characteristics can not affect its use as silicon and aluminium precursors in the synthesis of nanomaterials either microporous or mesoporous. The control of fused temperature and period can resolve this problem and increase the yield of silicon and aluminium in the supernatant.

1.5 Synthesis of nanomaterials from fly and bottom ash

1.5.1 Reactivity of coal fly and bottom ashes

The reactivity of the coal fly or bottom ash depends on their particle size. Generally, smaller particles are more easily cooled in the combustor, resulting in more disordered and more reactive species. It is found that the mean particle size of the coal fly ash (ca. 6 μm) was smaller than the bottom ash (ca. 200 μm).

1.5.2 Coal fly and bottom ashes properties

Table 1.5.1 summarizes the chemical compositions of untreated coal fly. The elemental compositions in coal fly and bottom ash used in these studies vary depending on the mineralogical content of the mother rock in which the coal is embedded and on the combustion temperature. Consequently, the chemical compositions of supernatant vary.

Table 1.5.1. Elemental composition (wt.%) of untreated fly ash

Author	Si	Al	Na	K	Fe
Chang et al. (1999)	55.59	31.41	0.88	3.06	18.95
Kumar et al. (2001)	31.36	10.15	0.24	0.45	—
Halina et al. (2007)	65.70	15.50	0.03	1.43	15.70
Chandrasekar et al.(2008)	57.05	23.04	—	—	9.21

1.5.3 Extraction of different elements from fly and bottom ash

Since the initial studies by Höller and Wirsching (1985), many researchers have proposed different hydrothermal activation methods to synthesize different zeolites from fly ash. All these techniques are based on the dissolution of Al–Si-bearing fly ash phases with alkaline solution (mainly NaOH and KOH solutions) and the subsequent precipitation of zeolitic material. In 1993, Shigemoto et al., were the first to report the modification of fly ash by the fusion at 550 °C with base prior to hydrothermal treatment at elevated temperatures and pressures to produce zeolites and concluded that by alkali fusion, silica in the form of quartz and mullite were converted into more soluble form of sodium silicate and other aluminosilicate phases. Chang et al., (1999) were the first to use fusing of fly ash with NaOH at 550 °C to produce mesoporous materials. Kumar et al., (2001), Halina et al., (2007) and Ghandrasekar and Ahn., (2008) used the Chang`s procedure with a slight change instead to use 1:5 as weight ratio between fused powder and water they used 1:4 to extract the silicon and aluminium from fly ash for the synthesis of MCM-41 and SBA-15. In 2006, Hui et al.,

(2006) extracted silicon and aluminium by the dissolution of coal fly ash with alkaline solution (2M NaOH) under 100 °C for 4.5 h. Table 1.5.2 summarizes the chemical compositions of the supernatant.

Table 1.5.2. Chemical composition of supernatant (ppm)

Element	Chang et al		Kumar et al	Halina et al	Chandrasekar et al
	supI	supII			
Si	2740	572	11000	10000	8404
Al	528	161	380	367	244
Na	46000	12000	35000	41600	50910

1.5.4 Synthesis of mesoporous materials from coal fly and bottom ashes

Chang et al., (1999) synthesized mesoporous aluminosilicate (MCM-41) with a homogeneous chemical composition of Si/Al= 13.4. They obtained two supernatant indexed 1 and 2 referring to the water treatment of fused-fly ash-NaOH and sediment respectively. As results, they found a difference in the Si and Al contents in both solutions (see Table 1.3). Referring to the results obtained by Chang et al., (1999), the use of supernatant1 in the synthesis of Al-MCM-41 is not adequate to give the mesoporous materials even it was heat-treated at 115 °C for 150 h because of the high Na ion present. However, they found that the use of supernatant 2 gives a great result and the Al-MCM-41 with Si/Al= 13.5 are obtained after 150 h at 115 °C. They estimated the purity of Al-MCM is between 40- 50% referring to TEM study. Kumar et al., (2001) used the Chang`s procedure with a slight change instead to use 1:5 as weight ratio between fused powder and water they used 1:4 to extract the silicon and aluminium from fly ash for the synthesis of MCM-41 and Al-SBA-15. Unlike the statement given by Chang et al., (1999), Kumar et al., (2001) found that the high concentration of Na ion present in the supernatant1 of the fused fly ash is not critical in the formation of MCM-41 and even SBA-15 and both structures are obtained. Referring to the ^{27}Al- and ^{29}Si-NMR, Kumar et al., (2001) stated that fly ash favours the tetrahedral coordination of silicon and aluminium in the mesoporous framework. Hui et al., (2006) synthesized an ordered MCM-41 at room temperature for 24 h used coal fly ash as starting materials. The extraction of silicon and aluminium was carried out by the dissolution of coal fly ash with alkaline solution (2M NaOH) under 100 °C for 4.5 h. Halina et al., (2007) proposed the synthesis of MCM-41 by using supernatant of coal fly ash (CFA) as started silica precursor. The MCM-41 was synthesis without hydrothermal treatment of the hydrogel; the quaternary ammonium salt was used as structure directing agents. Ghandrasekar et al., (2008) synthesized three mesoporous

materials named MCM-41, SBA-15, and SBA-16. To improve the textural quality of the SBA-15, and SBA-16 they added an additional amounts of sodium meta-silicate.

1.5.5 Molar composition and pH effects on the synthesis of mesoporous materials

The weight composition used by different authors presented in Table 1.5.3 can affect the quality of the final product.

Table 1.5.3. Synthesis parameters of mesoporous materials

Author	Supernatant ml	CTAB g	NH_4O H ml	H_2O ml	pH
Chang et al. (1999)	40	0.755	0.5	15	12.8
Kumar et al. (2001)	38	0.867	0.75	15	10.2
Chandrasekar et al. (2008)	40	1.2	1	15	10

Kumar et al., (2001) found that the adjustment of pH at 10.2 of the synthesis gel reduced the heat-treatment time and temperature from 150 h to 96 h and 115 °C to 97 °C respectively compared to Chang et al., (1999) and led to the additional incorporation of silica and aluminium originally present in the supernatant in the structure. Referring to both Table 1.5.3 and Table 1.5.4, the decrease of the pH from 12.8 to 10 increases slightly the Si/Al ratio. This result can be in disagreement with Kumar`s statement if Si/Al ratios are normalized to 1 unit. The incorporation of aluminium into the siliceous framework of SBA-15 and SBA-16 by direct method was not observed because of the strongly acidic medium (2M HCl), where most of the aluminium remained in the dissolved state. However, the use of supernatant as silicon and aluminium precursors let some of the aluminium to be incorporated into siliceous framework of SBA-15 (Table 1.5.4).

Table 1.5.4. Textural properties of nanomaterials from fly and bottom ash

Parameter	Chang et al.	Kumar et al.		Halina et al.	Chandrasekar et al.		
	MCM-41	MCM-41	SBA-15	MCM-41	MCM-41	SBA-15	SBA-16
Si/ Al	13.4	13.8	653	–	13.9	819.9	320.4
a_0/ nm	4.1	4.46	11.58	3.89	4.6	9.8	12.5
S_{BET}/m^2g^{-1}	735	842	483	740	847	746	603
V_p/cm^3g^{-1}	–	0.75	0.53	0.42	0.7	1.1	0.6
Dp/ nm	2.74	3.7	5.50	2.3	3	7.7	5
Wall tickness/ nm	1.4	0.76	6.08	1.6	1.6	2.1	7.5

Lattice parameter from XRD using the formula, $a_o = 2\ (3)^{1/} * d_{100}$. Determined by a geometrical method (Kruk *et al.,* 1997 and Dabadie *et al.,* 1996) by supposing that the MCM-41 exhibits a hexagonal arrangement of cylindrical pores. ; Dp: pore is given by diameter. wall thikness, a_o-D_{DRX}.

Hui and Chao, (2006) found that the adjustment of the pH during the synthesis played an important role in the formation of MCM. This statement has been also proposed by Kumar et al., (2001) and (2002), Rayalu et al., (2000), Loy et al., (2004). They found also that the incorporation of aluminium under its tetrahedral form increase when pH of the synthesis increases. This result is in agreement with that found by Kumar et al., (2001). These statements are confirmed by ^{27}Al-NMR where a single very strong peak assigned to T_d framework aluminium is observed at ca. 54 ppm for the sample synthesized from fly ash. However, Hui and Chao. (2006) found that the intensity of 52 ppm signal T_d coordination increased with synthesis pH. They suggested that there were more aluminium species incorporated with tetrahedral coordination in the mesoporous framework under a high pH. Halina et al., (2007) stated that the addition of acetic acid at approximate pH value range of 7–13 was found to be beneficial in aiding the gelation process (i.e. condensation – polymerization process) in producing the MCM-41 materials at room temperature. Ghandrasekar et al., (2008) used the pH value proposed by Kumar et al., (2001). The final nanomaterials synthesized by Ghandrasekar et al., (2008) presented a high crystallinity and purity. In most final nanomaterials synthesized by using coal fly no impurity is detected. Hui and Chao. (2006) found a clear trend of an increasing amount of elements incorporated into the samples with synthesis pH value. They suggested that at low pH value most of elements remained in the dissolved state. However, at high pH values more aluminium elements incorporated into sample and a lower degree of polycondensation of silicates species was observed (Voegtlin et al., 1997); thus more organic template cations interacted with aluminium species than SiO^- groups. Consequently more Na^+ ions were present to balance the charge of the samples. (Fig.1.5.1).

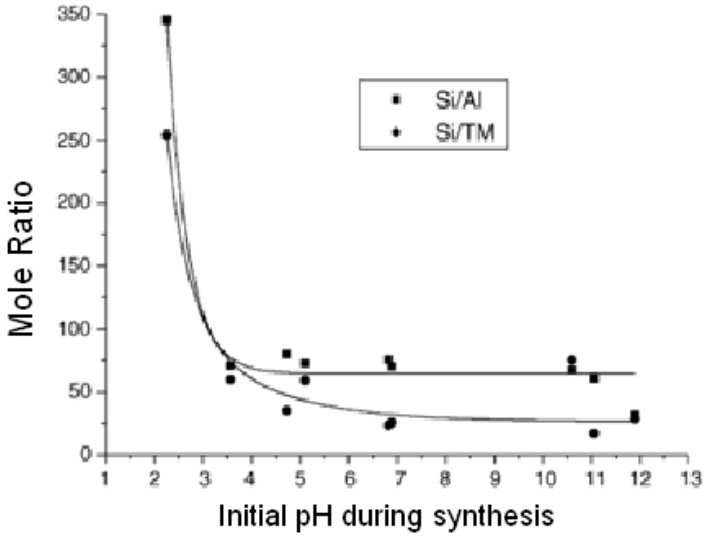

Fig.1.5.1. Si/Al and Si/TM mole ratios of the calcined samples versus initial pH value during synthesis. TM means sum of Na, Al, Ti and Fe elements (Voegtlin et al., 1997)

1.6 Synthesis of nanomaterials from rice husk

1.6.1 Introduction

Because of the need of the cheapest source of silicon for the synthesis of nanomaterials either mesoporous or microporous, rice husk provides abundant and cheap alternatives of silica source. Many researchers try to extract silica with high purity from rice husk. The silica extraction process is simple and inexpensive, making it beneficial to use rice husk as a natural silica source instead of synthetic ones. Silica with high purity in amorphous form and only trace amount of other inorganic impurities can be obtained by leaching with acid or base and calcination (Bajpai et al., 1981; Conradt et al., 1992; Real et al., 1996; Yalcin and Sevinc, 2001; Della et al., 2002; Liou, 2004 and Surachai, 2008). Examples of rice silica preparation methods and the product purity are shown in Table 1.6.1.

Table 1.6.1. Methods of silica preparation from rice husks and yield

Researchers	Methods	Treating substances	Purity (wt.%)
Bajpai et al., 1981	Thermal treatment		88.9
Conradt et al., 1992	Pre-treatment with enzyme or chemicals and thermal treatment	Cellulose enzyme, HCl, H_2SO_4 or NaOH	99.8
Real et al., 1996	Acid leaching and thermal treatment	HCl	99.5
Yalcin and Sevinc, 2001	Chemical and thermal treatment	HCl, H_2SO_4 or NaOH	99.6
Della et al., 2002	Thermal treatment	–	95
Grisdanurak et al., 2003	Acid leaching and thermal treatment	HBr	>99
Liou, 2004	Acid leaching and thermal treatment	HCl	99.7

1.6.2 Extraction of silica from rice husk ash

Silica from rice husk (RH) can be obtained by acid-leaching and pyrolysis (Conradt et al., 1992; Real et al., 1996; Yalcin and Sevinc, 2001; Della et al., 2002; Liou, 2004). Della et al., (2002) developed active silica from rice husk silica. The relative purity of silica increased after burning out the carbonaceous material at different duration and temperatures. Silica powder could be produced after heat treating at 700 °C for 6 h. Chakraverty et al., (1988) and Chakraverty et al., (1990) found that the leaching of RHs in 1N HCl was effective in substantially removing most of the metallic impurities. Acid treatment of RHs prior to combustion does not affect the structural nature (amorphicity) of the silica produced. From the standpoint of the amorphicity of the silica produced, the fusion temperature of 500 °C and combustion time of 6 h are considered optimum for converting RHs into white amorphous silica. After acid leaching, the silica produced was completely white in colour and had high purity. Real et al., (1996) found that the preliminary leaching of RHs with a solution of HCl

before combustion at 600 °C could result in relatively pure silica (approximately 99.5%) that was maintained even after being heated at 800 °C. Acid leaching greatly improves the quality of the silica produced. Other acids, such as H_2SO_4, HNO_3, or their mixture, have also been used in acid pre-treatment (Chakraverty et al., 1988; Conradt et al., 1992, Proctor et al., 2000; Patel et al., 1987 and Sidheswaran and Bhat, 1997). The general leaching effects of H_2SO_4, HNO_3 and HCl are similar, but HCl leaching of RHs is superior to H_2SO_4 and HNO_3 leaching in removing the metallic ingredients (Chakraverty et al., 1988). In some cases, the chemical post treatment of incinerated RHs has also been performed using Hydrochloric acid (HCl) (Conradt et al., 1992).

1.6.3 Synthesis of nanomaterials

Rice husk silica has been used for the synthesis of RH-MCM-41. Grisdanurak et al., (2003) synthesized the RH-MCM-41 from rice husk silica and cetyltrimethylammonium bromide (CTAB) as organic template using an ambient condition. The obtained RH-MCM-41 with various aging time possessed high specific surface area in the range of 750-1100 m^2/g and pore size distribution in the range of 2-4 nm. Nur et al., (2004) prepared mesoporous MCM-41 and MCM-48 from rice husk silica via a mixed cationic-natural templating route using CTAB and Trion x-100 (Tx-100) surfactants. The organization of the surfactants was affected by the concentration of NaOH. MCM-48 was formed when the concentration of NaOH was less than 1.5 M but MCM-41 was obtained when the concentration of NaOH was greater than 1.5 M. Unlike to fly and bottom ash, rice husk can be used only as silicon source which limits the catalytic applications of its nanomaterials due to lack of cooperating between heteroatom. Thereby, it is necessary to increase the active site centres by adding other elements into the structure or dispersing them on the surface. Nur et al., (2005) used Poly (methacrylic acid) (PMAA) and Al-MCM-41 with Si/Al = 20 from rice husk silica as supports for the encapsulation of bulky iron(III)-5,10,15,20-tetra-(4-pyridyl) porphyrin (Fe-TPyP) to be used for oxidation of benzene to phenol. The yield of the oxidation is high when PMAA is used as host. However, the selectivity and generability of Fe-TPyP-MCM-41 is better and higher than that of Fe-TPyP-PMAA. Poh et al., (2006) synthesized sulphide SO_4-AlMCM-41 with SiO_2/Al_2O_3 = 15 from rice ash via impregnation of sulphuric acid using an organic solvent on the surface of H-AlMCM-41. SO_4-AlMCM-41 is used as a solid Brønsted acid. The SO_4-AlMCM-41 was found to be active towards dibenzoylation of biphenyl reaction. Chumee et al., (2009) synthesized RH-MCM-41 by using silica from rice husk and $NaAlO_2$ to increase acidity by adding Al with grafting method. The incorporation of Al with Si/Al ratio of 75 and

25 on the RH-MCM-41 decreased the specific surface area of the result nanomaterials 741 m^2/g and 746 m^2/g respectively compared to the parent RH-MCM-41 around ca. 1231 m^2/g. Ketcome et al., (2009) synthesized MCM-41 from rice husk (RH-MCM-41) and modified it by silylation with either trimethylchlorosilane (TMCS), dimethyl-dichlorosilane (DMCS) or phenyl-trichlorosilane (PTCS) to improve its surface properties. By the silylation technique, hydrophilic functional group such as silanol was substituted by silane groups. Silylated RH-MCM-41 showed higher hydrophobicity than RHMCM-41; therefore, silylated RH-MCM-41 at sufficient concentration and ageing time is favourable material for adsorption and catalytic applications. Bhagiyalakshmi et al., (2009) synthesized mesoporous siliceous MCM-41, MCM-48 and SBA-15 using Rice Husk Ash (RHA) as the silica source. Their defective –OH sites were then grafted with 3-chloropropyl amine hydrochloride (3-CPA) to be used for CO_2 chemisorption. They found that SBA-15/CPA shows maximum of CO_2 adsorption around ca. 1.7 mmol/g at 25 °C, due its high degree of Si–OH compared to MCM-41 and MCM-48 where CO_2 adsorption was 1.5 mmol/g, 1.1 mmol/g respectively. Jullaphan et al., (2009) synthesized a mixed-phase SBA-3 like in SBA-15 bimodal mesoporous silicas (BMS) from rice husk ash. They thought that small pores can promote an interaction between pores materials and guest molecules; whereas the large pores provide high-speed pathways for guest molecules and the products.

1.6.4 Synthesis condition of nanomaterials from rice husk ash

1.6.4.1 Synthesis of MCM-41 and MCM-48

Rice husk ash is used as silica source. The synthesis procedure consists of three parts. The first part (PART A) is to partially dissolve carbonaceous rice hush ash (RHA) to obtain sodium silicate or water glass. Sodium silicate (Na_2SiO_3) is prepared by combining an amount of RHA with NaOH and H_2O. The resulting gel mixture was stirred for 2 h at 80 °C. The mixture is then cooled to room temperature and used in the second part of the synthesis. The second part (PART B) is the preparation of the mixed surfactant solution. The surfactant and H_2O mixture is prepared. The surfactant solution is then cooled to room temperature. Third part (PART C) of the synthesis procedure is the preparation of the gel. The silica source prepared from PART A and the surfactant solution prepared from PART B are quickly poured into a polypropylene bottle. The bottle is capped and shaken rapidly and vigorously. The gel mixture thus obtained is heated at 97 °C for the formation of the surfactant-silica mesophases under static conditions at desired temperature and time. Many molar compositions are proposed for the synthesis of nanomaterials. (Table 1.6.2).

The gel mixture is then cooled to room temperature. Subsequently, the reaction mixture is adjusted to pH10.2 by drop wise addition of acetic acid or sulphuric acid with vigorous stirring. The reaction mixture after the pH adjustment is heated again for another period. The precipitated products, nanomaterials from the reaction mixture are then filtered, washed with distilled water, and dried in an oven overnight.

1.6.4.2 Synthesis of Santa Barbara (SBA) framework

The synthesis procedure consists of three parts. The first part (PART A) is to partially dissolve carbonaceous rice hush ash (RHA) to obtain sodium silicate or water glass. Sodium silicate (Na_2SiO_3) is prepared by combining an amount of RHA with NaOH and H_2O. The resulting gel mixture is stirred at 80 °C. The mixture is then cooled to room temperature and used in the second part of the synthesis. The second part (PART B) is the preparation of the mixed surfactant solution. Triblock copolymer $EO_{20}PO_{79}EO_{20}$ (Pluronic P123) is dissolved with stirring in amount of 2 M HCl at 40 °C. The first part is added to the second one under stirring and temperature for 24 h. Third part (PART C) of the synthesis procedure is the preparation of the gel. The silica source prepared from PART A and the surfactant solution prepared from PART B are quickly poured into a polypropylene bottle. The bottle is capped and shaken rapidly and vigorously. The gel mixture thus obtained is heated for the formation of the surfactant-silica mesophases under static conditions at desired temperature and time. (Table 1.6.2).

Table 1.6.2. Summary of synthesis conditions for nanomaterials

Author	Molar composition
Grisdanurak et al., (2003)	0.147 CTAB :1.00 SiO_2 :2.16 NH_4OH :148.94 H_2O
Nur et al., (2004)	5 SiO2 :(1-2) NaOH :0.85 CTAB :0.15 Tx-10 :400 H_2O
Nur et al.. (2005)	2.295 NaOH :10.015 SiO_2 :1.05 NH_3 :9.1115 CTAB :1.417 $NaAlO_2$
Poh et al., (2006)	6 SiO_2 :1 CTAB :1.5Na_2O :0.15 $(NH4)_2O$:250 H_2O
Ketcome et al., (2009)	0.147 CTAB :1.00 SiO_2 :2.16 NH_4OH :148.94 H_2O
Chumee et al., (2009)	4 SiO2 :0.29 H_2SO_4 :1 CTAB :400 H_2O
Jullaphan et al., (2009)	1 SiO2 :0.088 P123 :4HCl :200 H_2O

1.7 Synthesis of nanomaterial from natural sources

1.7.1 Introduction

Many attempts are focused on the use of a waste source instead of the laboratory reagents. However, very limited works are focused on the use of natural ores as silicon and aluminium precursors for the synthesis of mesoporous. Zhu et al., (2002) were the first who investigated the combination between pillared clays and quaternary ammonium bromide [$CH_3(CH_2)_{n-1}N(CH_3)_3Br$]. Recently, Liu et al., (2003) used NaY and Kaolin as starting materials to synthesis Kaolin/NaY/MCM-41 composites that exhibit good hydrothermal stability. Kang et al., (2005) reported the synthesis of Al-MCM-41 by using water glass (or silicate sodium) as Si source and metakaolin as Al sources. Sanhueza et al., (2006) reported the use of diatomite and pumicite for the synthesis of MCM-41 mesoporous materials. In the case of diatomite, $NaAlO_2$ was used for ratio adjustment. However, Wu et al., (2007) used microcline as silicon and aluminium precursor in the synthesis of mesoporous materials and 13X zeolite as seed for crystal structure on mesoporous walls. Recently, Adjdir et al., (2009) reported for the first time the synthesis of Al-MCM-41 by using volclay as both aluminium and silicon source. They adopted the alkaline fusion and water treatment of fused clay. In another work, Adjdir et al., (2010) used the fused NaOH-volclay sediment of the first water treatment as silicon and aluminium precursor in the synthesis of Al-MCM-41 materials. Yang et al., (2010) used the bentonite as silicon and aluminium source for the synthesis of mesoporous materials Al-MCM-41 by adopting the alkaline fusion to extract silicon and aluminium. In another work Yang et al., (2010) used Natural attapulgite clay mineral as aluminium and silicon source for the synthesis of Al-MCM-41. Ali-dahmane et al., (2010) reported the effect of the mineral phase contents of Algerian bentonite on the structure properties of Al-MCM-41. Example of natural source preparation methods is shown in Table 1.7.1.

Table 1.7.1. Methods of silica preparation from natural source

Researchers	Methods	Source used
Kang et al., 2005	Thermal activation at 850 °C	Kaolin
Sanhueza et al., 2006	−	Diatomite and pumicite
Wu et al., 2007	Na_2CO_3 +Thermal treatment at 820 °C	Microcline
Adjdir et al., 2009	NaOH + Thermal treatment at 550 °C	Volclay (bentonite)
Yang et al., 2010	NaOH + Thermal treatment at 550 °C	China bentonite
Yang et al., 2010	Acid leaching and Thermal treatment 80 °C	Attapulgite
Ali-dahmane et al., 2010	NaOH + Thermal treatment at 550 °C	Algerian bentonite

1.7.2 Clay minerals properties

Table 1.7.2 summarizes the chemical compositions of natural source. The elemental compositions vary depending on the geological conditions. Consequently, the chemical compositions of supernatant vary.

Table 1.7.2. Elemental composition (wt.%) of untreated Natural sources

Author	Source	SiO_2	Al_2O_3	Na_2O	K_2O	Fe_2O_3
Kang et al. (2005)	Kaolin	52.0	45.0	0.2	0.1	0.5
Sanhueza et al. (2006)	Diatomite	93.4	4.0	0.4	0.2	0.9
	Pumicite	74.5	14.3	4.1	4.4	1.2
Wu et al. (2007)	Microcline	65.0	16.4	0.9	13.8	0.7
Adjdir et al. (2009)	Volclay	56.5	18.6	0.9	13.8	0.7
Yang et al. (2010)	China bentonite	66.5	8.3	1.9	0.5	3.6
Yang et al. (2010)	Attapulgite	53.6	7.5	0.1	0.5	2.7
Ali-dahmane et al. (2010)	Algerian bentonite	60.5	18.6	1.2	0.9	2.3

1.7.3 Synthesis of nanomaterials

Kang et al., (2005) for the first time used Kaolin as aluminium source in the synthesis of Al-MCM-41. The kaolin which is clay minerals used after thermal activation at 750 °C for 5 h to obtain metakaolin. The Al-MCM-41 is obtained by mixing a solution of NaOH and metakaolin with water glass as silicon source. The surfactant cetyltrimethylammonium bromide (CTAB) is used as the template. The Al-MCM-41 obtained present a high specific surface area 877 m^2/g, average pore diameter of 2.76 nm and pore volume of 0.78 cm^3/g. Sanhueza et al., (2006) used both diatomite and pumicite sources without any pretreatment. A series of temperature, composition of the initial gel and reaction time are proposed for the synthesis of Al-MCM-41. As results, the used of these natural sources depend on the molar composition used, temperature and reaction time (Table 1.7.3). They found that diatomite gives a better result than pumicite.

Table 1.7.3. Synthesis condition of Al-MCM-41 from diatomite and pumicite

Clay mineral	SiO_2/Al_2O_3	CTAB/ SiO_2	Na/ SiO_2	H_2O/ SiO_2	t(h)	T(K)	Product
Diatomit	8.86	0.1	0.10	250	48	383	MCM-41
Diatomite	8.86	0.1	0.25	330	48	383	MCM-41
Pumicite	8.86	0.1	0.25	330	48	383	AMO
Pumicite	8.86	0.1	0.25	330	96	423	MM

AMO: Amorphous material; MM: mesoporous material

Wu et al., (2007) reported the synthesis of mesoporous aluminosilicate using microcline as silicon and aluminium precursor and the precursor 13X zeolite as seed to improve the thermal and hydrothermal stability of the final product by introducing the secondary building units of zeolite into the mesoporous framework. The microcline was at first mixed with Na_2CO_3 then calcined at 820 °C. The calcined microcline and Na_2CO_3 mixture was used in the synthesis of mesoporous materials. The structural and physical properties of this mesoporous so-called SAR-3. Adjdir et al., (2009) reported the used of volclay as silicon and aluminium precursor for the synthesis of Al-MCM-41. They adopted the fusion process described by Chang et al., (1999) and Kumar et al., (2001). As results, they found that the use of volclay as silicon and aluminium source lead to high quality of Al-MCM-41. The obtained structural and physical properties of Al-MCM-41 from volclay were superior to the one from pure reagents (Table 1.7.4).

Table 1.7.4. Structural and physical properties of different aluminosilicate source Al-MCM-41

Author	Product	a_0 nm	S_{BET} m^2/g	Vp cm^3/g	Dp nm	Wall thickness nm
Wu et al., (2007)	SAR-3	5.07	725	0.67	3.70	1.37
Adjdir et al., (2009)	Al-MCM-41 sup-1	4.53	1060	0.77	3.80	0.73
	Al-MCM-41 sup-2	4.41	1044	0.77	3.70	0.71
Yang et al., (2010)	Al-MCM-41 A1B1C1	4,60	1019	0.72	3.01	1.60
Yang et al., (2010)	Al-MCM-41	4.81	1030	0.96	3.70	1.10
Ali-dahmane et al., (2010)	Al-MCM-41	4.40	464	0.72	3.80	0.60

In another work, Adjdir et al., (2010) believe that not all silicon and aluminum were extracted from the first water treatment of the fused volclay NaOH mixture in supernant-1. For that they applied a second water treatment of the sediment of the first water treatment of the fused volclay NaOH mixture to obtain supernatant-2. Table 1.7.5 summarizes the elemental compositions of supernatant-1 (sup-1) and supernant-2 (sup-2) by ICP-OES.

Table 1.7.5. Elemental compositions of supernatant-1 (sup-1) and supernatant-2 (sup-2) by ICP-OES

Element	sup-1 mg/l	sup-2 mg/l	sup-1 mmol/l	sup-2 mmol/l	sup-1 mol/l*	sup-2 mol/l*	Reduction %
Si	881.9	278.9	31.4	9.9	139.6	44.1	69
Al	64.6	0.9	2.4	<0.1	10.6	0.1	99
K	28.4	5.4	0.7	0.2	3.2	0.6	81
Fe	2,2	0.6	<0.1	<0.1	0.2	<0.1	~70
Na	4758.0	1864.1	206.9	81.1	919.8	360.4	61

* The values were calculated referring to the dilution: 1 ml of supernatant+13,985 ml water+15 µl nitric acid

As conclusion, the originally fused clay can be used more than one time. The physical proprieties of the new Al-MCM-41, such as pore diameter, pore volume, wall thickness and S_{BET} are similar to the Al-MCM-41 produced from the fused material. (Table 1.7.4). Yang et al., (2010) used the bentonite as aluminium and silicon source for the synthesis of Al-MCM-41. They considered for the synthesis of mesoporous materials three synthesis parameters involving mass ratio of bentonite to NaOH (A), leaching time (B) and pH value (C). (Table 1.7.6).

Table 1.7.6. Experimental parameters (Yang et al., 2010)

Bentonite: NaOH ratio (A)	Leaching time (B)	pH value (C)
A1 (1: 1)	B1(12 h)	C1(9)
A2 (1: 1.25)	B2(16 h)	C2(10)
A3 (1: 1.5)	B3(20 h)	C3(11)

Leaching time: the total time of stirring and ageing of fused bentonite and NaOH mixture

As results, they found that the structural and physical properties of the final product depend strongly on these three synthesis parameters and the combination of these experimental parameters leads to mesoporous materials with different structural and physical properties. In another work, Yang et al., (2010) reported the use of natural attapulgite to synthesis mesoporous materials, in this work, the attapulgite was treated with a solution of 8M HCl at 353 K for 2 h, and then cooled to room temperature, the acid-leached sample was used as direct silica and aluminum sources to prepare mesoporous silica MCM-41 under hydrothermal conditions. Compared to the Kumar et al., (2001) where the Si/Al ratio was 13.5, Yang et al., (2010) had successfully decreased the Si/Al ratio to 12,6 which means high aluminum content in the final product with preservation of the MCM-41 structure. They found else that the grinding of the attapulgite before acid-leached played a critical role in the transfer of natural attapulgite to Al-MCM-41. Ali-Dahmane et al., (2010), used an Algerian bentonite as silicon and aluminium sources, and inspected the effect of its mineral phase content on physical properties of MCM-41 such as particle size, specific surface areas, pore size diameters and wall thickness. As results, they found that the fusion process at 550 °C destroyed all mineral phases of the Algerian bentonite which led to different Si/Al ratio in the fused clay-NaOH mixture compared with that obtained from volclay.

1.7.4 Effect of synthesis pH

The adjustment of reaction solution pH is very important for the synthesis of Al-MCM-41 from natural source. Ryoo et al., (1995) found that the long-range structural order and textural uniformity of the mesoporous molecular sieve are markedly improved due to a shift in the reaction equilibrium when acetic acid is repeatedly added during the conversion of sodium silicate and $NMe_3(C_{16}H_{33})Cl$ to a MCM-41 phase. Luechinger et al., (2003) agreed with this statement and found that the variation of acid treatments during the course of the synthesis shows that the optimum method of preparing pure silica MCM-41 from sodium silicate solution is the addition of an appropriate amount of acetic acid all at once after 24 h of synthesis. The acid treatment improves the condensation and coagulation between the silicate species during the synthesis and thereby improves the quality of the final MCM-41. The quality of MCM-41 also depends strongly on the silica precursor. A source with larger silicate species results in a material with better pore characteristics and excellent hydrothermal stability. Wu et al., (2007); Adjdir et al., (2009); Yang et al., (2010), Ali-Dahmane et al., (2010) found that the incorporation of aluminium under its tetrahedral form increase when pH of the synthesis increase and SiO_2 content decrease. As consequence of the increase of the pH, the Brønsted acidity and reactivity of mesoporous materials increase. Galarneau et al., (1998) assumed that, after a certain period of aging, a hexagonal silicate surfactant phase is formed. However, Luechinger et al., (2003) supposed that this phase is neither fully ordered nor fully condensed (Figure.1.7.1, stage (a)). The acid treatment shifts the polymerization/depolymerization equilibrium of the silicate species to a higher degree of condensation (see Figure.1.7.2).

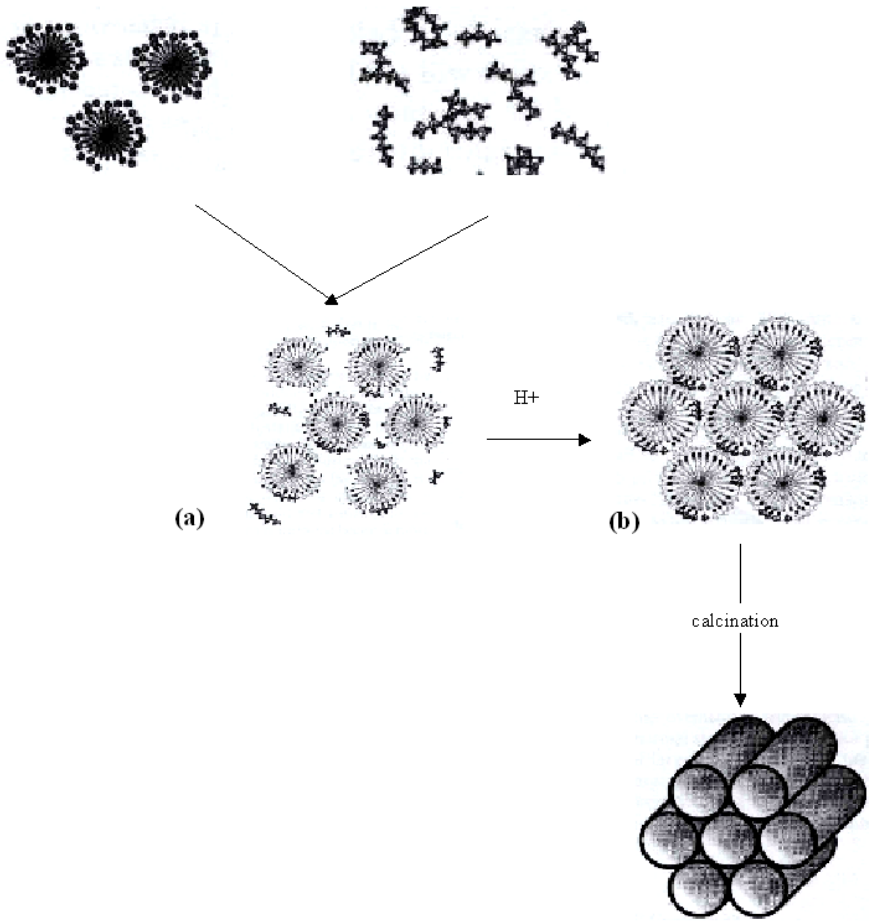

Fig.1.7.1. Schematic representation of the proposed mechanism of MCM-41 formation. (a) hexagonal surfactant silicate mesophase formed from positively charged surfactant molecules and silicate oligomers carrying multiple negative charges, (b) partial protonation of silicate species facilitated approach and condensation between the templatesilicate agglomerates to form a well ordered surfactant silicate mesophase

The acid treatment shifts the polymerization/depolymerization equilibrium of the silicate species to a higher degree of condensation (see Figure.2).

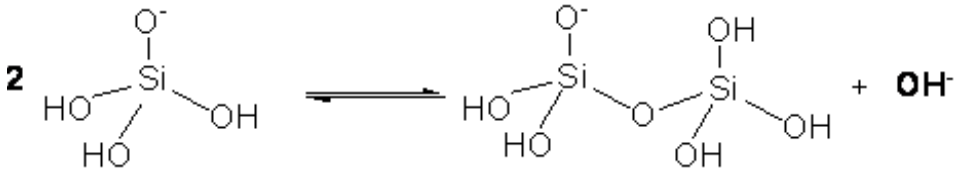

Fig.1.7.2. Shift in polymerization/depolymerization equilibrium of silicate species

It contributes to close the silica-wall around the micelle by the formation of covalent Si–O–Si bonds. As a second effect, lowering the pH leads to protonation of the negatively charged silicate species, thus reducing the electrostatic repulsion between the micelles. This facilitates the approach and the condensation of the micelles. The consequences of these two effects are depicted in stage (b) of Scheme 1. The acid treatment also reduces the amount of charge-compensating Na^+ ions, which remain in the framework of the MCM-41 material. Upon protonation, $Si–O^- Na^+$ units become Si-OH silanol groups.

1.8 Conclusion

Fly and bottom ash can be used as silicon and aluminium source. Nevertheless, as fly and bottom ash are fused; some of the hazardous elements and minor constituents concentrate in the residue, while others are released to the atmosphere in gaseous or particulate form which can reach significant concentrations in the solid, liquid, or gaseous effluents after combustion and cause many health's problems.

Rice husk is used as silicon and aluminium sources by applying an acid treatment. However, the method used to extract the silicon and aluminium from this source does not preserve the environment.

The natural sources, such as volclay; Algerian bentonite and other source which are cited in this chapter, are considerate as an alternative sources to be used as silicon and aluminium precursor. The use of alkaline fusion process reduces the treatment cost (time and temperature), preserves the environment.

The use of natural source and specially volclay would reduced the cost of silicon and aluminium source (1 kg of silicon and aluminium from volclay costs around 0.03 € whereas the same amount of silicon from ludox and aluminium from sodium aluminates cost around 350 €).

Chapter 2.

The synthesis of Al-MCM-41 and B-MCM-41 from laboratory reagents

2.1 Introduction

Since the synthesis of the crystalline mesoporous M41S materials by Mobil's researchers Kresge et al., (1992) and Beck et al., (1992), the following study has focused on the MCM-41 material, which shows a hexagonal array of uniform mesopores with uniform sieves ranging from 2 to 10 nm. Their extraordinary high surface and distinct adsorption properties open up many potential applications in catalysis, separation and nanostructured materials Corma et al., (1997), Vallet-Regi et al., (2001) and Zhang et al., (2001). Many researches on MCM-41 have been focused on the incorporation of different elements like aluminium and boron in order to modify the framework of MCM-41 and to generate catalytic sites needed for different type of reactions. The aluminosilicate mesoporous molecular sieves have received much attention for their strong Brønsted acidity. Many efforts have been made to optimize the silicate sources such as cab-o-sil M5 fumed silica, sodium silicate and tetramethylammonium silicate Liu et al., (1996), cab-o-sil M5 fumed silica and sodium silicate Yanagisawa et al., (1990). The aluminium source has been studied by Borade and Clearfiled (1995), Occelli et al., (1998) and Badamali et al., (2000) who have reported that the sodium aluminates source incorporates aluminium to a maximum amount in the framework sites. In addition, density and the strength of acid sites are found to be significantly higher applying sodium aluminates. The syntheses of Al-MCM-41 by a direct method exhibits considerable hydrothermal stability especially at relatively low Al contents. Al-MCM-41 mesoporous materials prepared via grafting routes are extremely stable in boiling water. Regarding the borosilicate mesoporous molecular sieves, Oberhagemann et al., (1999) used a single silica source, tetramethoxy silane whereas Bonneviot and Kaliaguine (1995) took ludox and sodium silicate to synthesize B-MCM-4. Chu et al., 1985 found that in borosilicate molecular sieves boron occupy the site of the framework aluminium and the protonic form of borosilicate molecular sieves, are less acidic than their aluminosilicate counterparts due to lack of strong Brönsted acidity. In literature no report is available in a comparison between B-MCM-41 and Al-MCM-41 with different content of aluminium and boron. Here we report the synthesis and characterization of MCM-41 materials with different content of aluminium and boron. We have studied the effect of the SiO_2/Al_2O_3 or SiO_2/B_2O_3 ratio from 5 to 150 on the final structure and compared their physical proprieties.

2.2 Experimental

2.2.1 Starting materials

Sodium aluminate (54% Al_2O_3; 41%Na_2O; 5%H_2O; Aldrich) was used as the aluminium sources, boric acid (H_3BO_3 Aldrich) for the provision of boron. Colloidal silica (ludox 40%, Prolabo) served as a silicon source and as surfactant cetyltrimethylammonium bromide ($C_{19}H_{42}NBr$; CTAB, Aldrich; 99%). Tetramethylammonium hydroxide (TMAOH.5H_2O, 25 wt.%, Aldrich) was utilized as a base.

2.2.2 Direct synthesis of Si-MCM-41

The synthesis procedure of Si-MCM-41 was reported in a previous paper of Mokaya (2001) according the following molar composition 1 SiO_2 : 0.25 CTAB : 0.2 TMAOH : 40 H_2O. Tetramethyl-ammonium hydroxide was dissolved in distilled water, and then 2 g of bromide of cetyltrimethylammonium (CTAB) was added into the suspension under stirring. After 30 minutes, Ludox was slowly added, giving rise to white slurry. The reactional mixture was continuously stirred for 2 h. Afterwards the obtained hydrogel was transferred into a Teflon autoclave vessel for the crystallization, which lasted 48 h at 100 °C. Thereafter, the product was washed several times with demineralised water, filtered and dried at 100 °C overnight, afterwards calcined under air at 550 °C for 12 h.

2.2.3 Synthesis of B-MCM-41

The hydrothermal synthesis of B-MCM-41 samples was carried out at 373 K using gel with molar composition of: 1 SiO_2 : 0.25 CTAB : 0.2 TMAOH : y H_3BO_3 : 40 H_2O. The experimental procedure adopted to prepare B-MCM-41 with y= 5; 10; 25; 50; 70 and 150 as a typical case is described as follows. A solution was prepared which contains the hydroxide of tetramethylammonium (TMAOH) in demineralised water, then under stirring 2 g of bromide of cetyltrimethylammonium (CTAB) was added. After 30 minutes silica and finally 0.0193 g of boric acid (H_3BO_3) was added to the solution .The reactional mixture was stirred for 2 hours. The hydrogel obtained is heated at 100 °C during 48 h. The solid obtained was washed several times with demineralised water, filtered and dried at 100 °C overnight, then calcined under air at 550 °C for 12 h.

2.2.4 Synthesis of Al-MCM-41

For this method three solutions were prepared which contain a source of aluminium mixed with an organic hydroxide of quaternary ammonium type (S1), a source of silica (S2) and a surfactant agent (S3). The solvent used in the three solutions is demineralised water. The molar composition was 1 SiO_2 : 0.25 CTAB : 0.2 TMAOH : x Al_2O_3 : 40 H_2O, with x = 5, 10, 25, 50, 70, 150. The gel was kept in a Teflon-lined stainless steel autoclave and heated at 100 °C for two days for crystallization. The solid product obtained was washed, filtered and dried overnight 100 °C. The as-synthesized samples were calcined at 550 °C in air for 12 h.

2.2.5 Characterization

XRD patterns were recorded for all the samples in order to check the formation and structure of Al-MCM-41. The diffraction patterns were recorded in the °2θ range of 1–12° with a step size of 0.02 °2θ and a step time of 5 s on a Bruker D8 diffractometer with CuKα (λ =1.5406Å) radiation equipped with PSD counter. A CuKα anode was powered with 40 kV and 40 mA. A Talc/Vermiculite mixture was applied as internal standard for peak position correction. Single line fitting was performed with the Bruker software Topas 3.0 (polynom 3rd degree as background, pseudo-voigt function as profile function). N_2-sorption measurements were performed at 77 K using a Quantachrome Autosorb1 MP. The samples were degassed at 383 K in vacuum for 24 h before measurements. Specific surface areas were calculated by using the Brunauer–Emmett–Teller (BET) method according to IUPAC (1957). Pore size distribution curves were calculated using two methods. One is the NLDFT equilibrium model

with cylindrical pore shape based on the DFT/Monte Carlo method Lowell et al., (2004) and the other uses the relation $Dp=1.213*d_{100}*(2.2*V_{meso}/(1+2.2*V_{meso}))^{1/2}$ described by Ulagappan et al., (1996). Pore volumes were obtained from the amount of N_2 adsorbed at p/p_o = 0.7 corresponding to a pore width of 7.1 nm in order to exclude inter-particle pores formed by the powder.

The ATR-FT-IR (attenuated total reflection Fourier transformed IR) spectra were obtained on a Bruker IFS66 with DTGS detector and globar source. The ATR device was a Golden Gate single diamond cell and the powder samples were pressed with a torque of 80 cNm on the diamond. Spectra were fitted with Jandel PeakFit software after background subtraction, a Gauss-function was applied for the description of 9 peaks for B-MCM and 6 peaks for Al-MCM-41.

2.3 Results and discussion

In the following chapter we are presenting the XRD and ATR-FT-IR data, which will be discussed in a structural context. In a final chapter the results of the gas adsorption are shown and reviewed.

2.3.1 X-ray diffraction

The XRD patterns of Al-MCM-41 and B-MCM-41 samples prepared with different mass ratios, as presented in (Figure.2.1a and Figure.2.1b), showed typical reflections of hexagonal one-dimensional mesoporous MCM-41 structure (Selvam et al., 2001, Sayari et al., 1995 and Sundaramurthy and Lingappan., 2003). These XRD patterns were characterized by four reflections in a hexagonal space groups denoted as (100), (110), (200) and (210). In the samples with a SiO_2/Al_2O_3 ratio of 5 and 10 and for SiO_2/B_2O_3 with a ratio of 5 these reflections were not well developed, indicating a poor crystallinity for these samples. In contrast, for the samples with SiO_2/Al_2O_3 and SiO_2/B_2O_3 mass ratios of 25 to 150 the reflections were better resolved. This was also observed by Kresge et al., (1992) and Beck et al., (1992). The best structure for Al-MCM-41 and B-MCM-41 was allotted to each mass ratio of 150 which was in agreement with the results found by Oberhagemann et al., (1999), Sayari et al., (1995) and Sundaramurthyand Lingappan (2003). Isomorphous substitution has been shown to be an effective method to modify the MCM-41 materials (Scholle et al., 1984).

*talc/vermiculite mixture was used as internal standard.

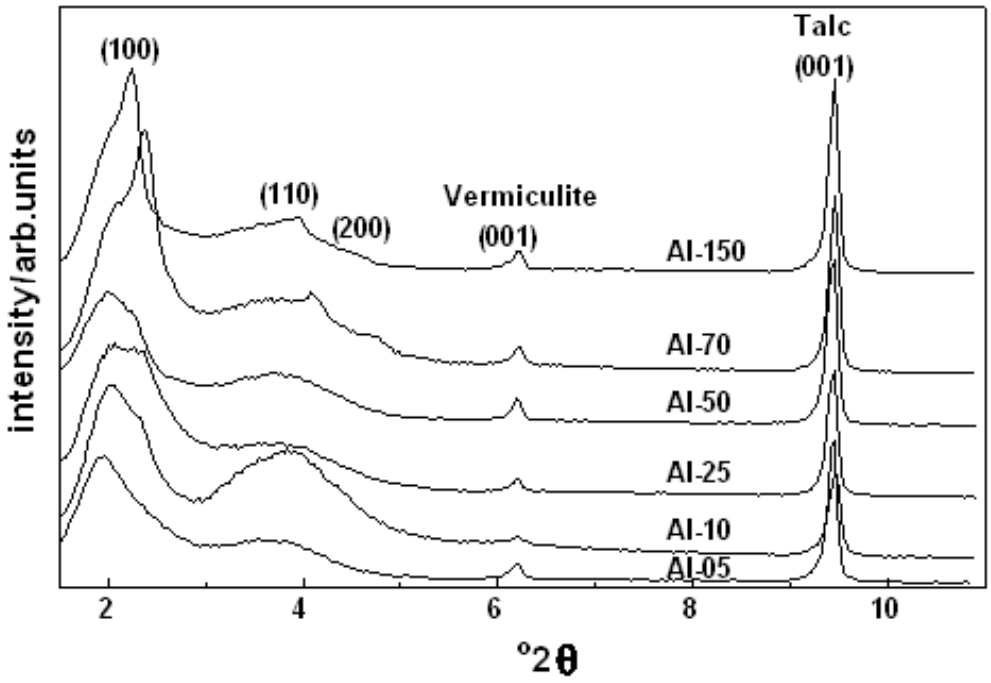

Fig.2.1a. XRD patterns of Al-MCM-41: Al-5; Al-10; Al-25; Al-50; Al-70; Al-150

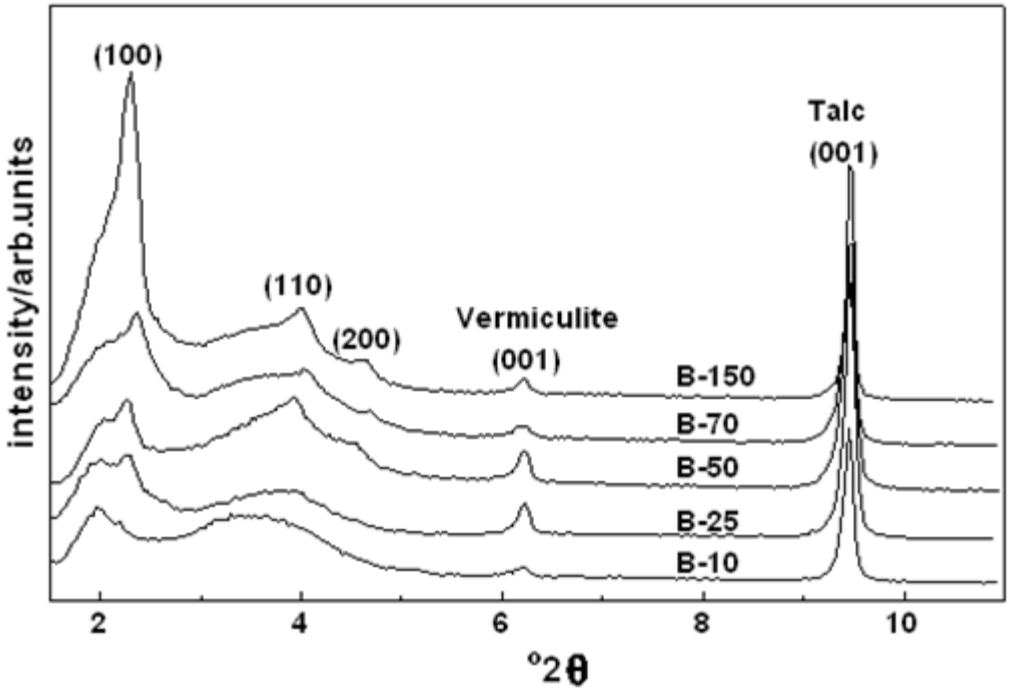

Fig.2.1b. XRD patterns of B-MCM-41: B-5; B-10; B-25; B-50; B-70; B-150

Substitution of elements into the MCM-41 materials could change the T═O═T angle and T═O length (T= Si or substituted element). Kosslick et al., (1993) found that the substitution of Si by tetravalent Ge decreased the T═O═T angle and the T═O bond length. Szostak (1989) found that the unit cell volumes in zeolites crystal structure could also change with substitution. The unit cell volume of B-ZSM-5 decreases with increasing B-content compared to (Si) –ZSM-5 because B was smaller than Si (Szostak, 1989 and Catlow et al., 1995). Contrary to Szostak, the unit cell of B-MCM-41 increases with increasing B-content. For Al-MCM-41 a weak correlation was found. The unit cell of Al-MCM-41 increases with increasing Al-contents. (Table 2.1 and Figure.2.2).

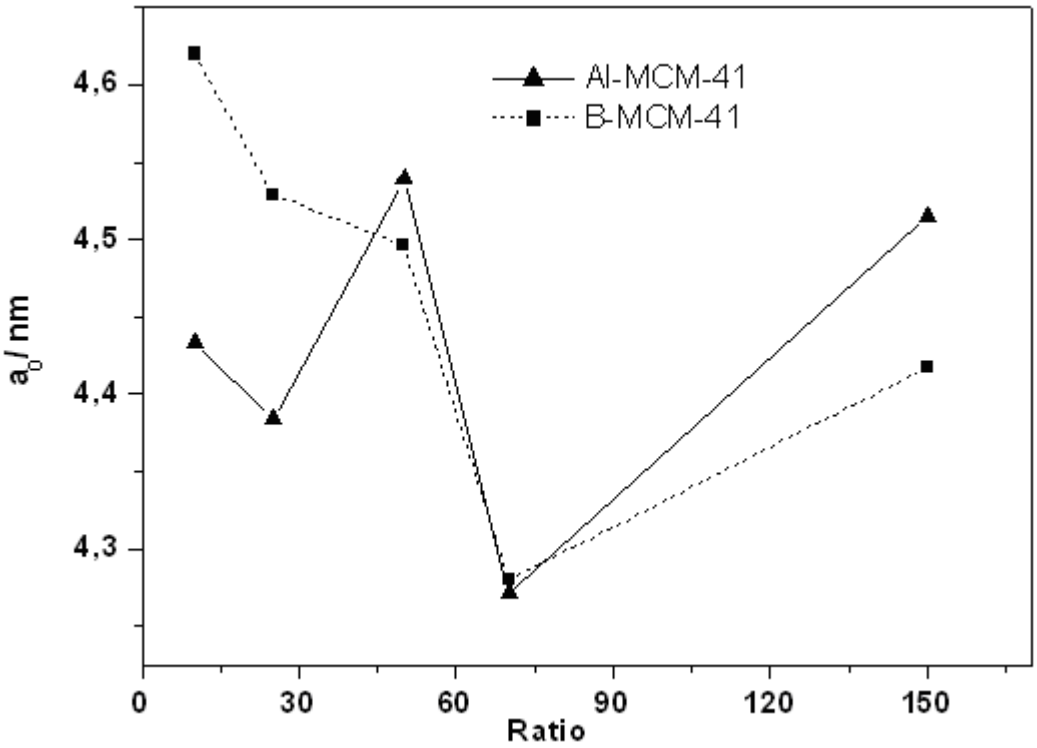

Fig.2.2. Evolution of unit cell versus SiO_2/Al_2O_3 and SiO_2/B_2O_3 ratios

Table 2.1. Results of the XRD data evaluation

ratio	d_{100} (nm)		a_o (nm)		FWHM (° 2θ)	
	SiO_2/B_2O_3	SiO_2/Al_2O_3	SiO_2/B_2O_3	SiO_2/Al_2O_3	SiO_2/B_2O_3	SiO_2/Al_2O_3
150	3.82	3.91	4.42	4.52	0.199	0.184
70	3.71	3.70	4.28	4.27	0.411	0.318
50	3.90	4.25	4.50	4.91	0.229	0.472
25	3.92	3.76	4.53	4.34	0.464	0.560
10	4.00	3.75	4.62	4.33	0.524	0.516

d_{100}: interplanar spacing; a_0: unit cell; FWHM: full width at half maximum

In addition the FWHM of the (100) peak decreased in a progressive way from a mass ration of 10 to 150 for both samples (Figure.2.3a and 2.3b).

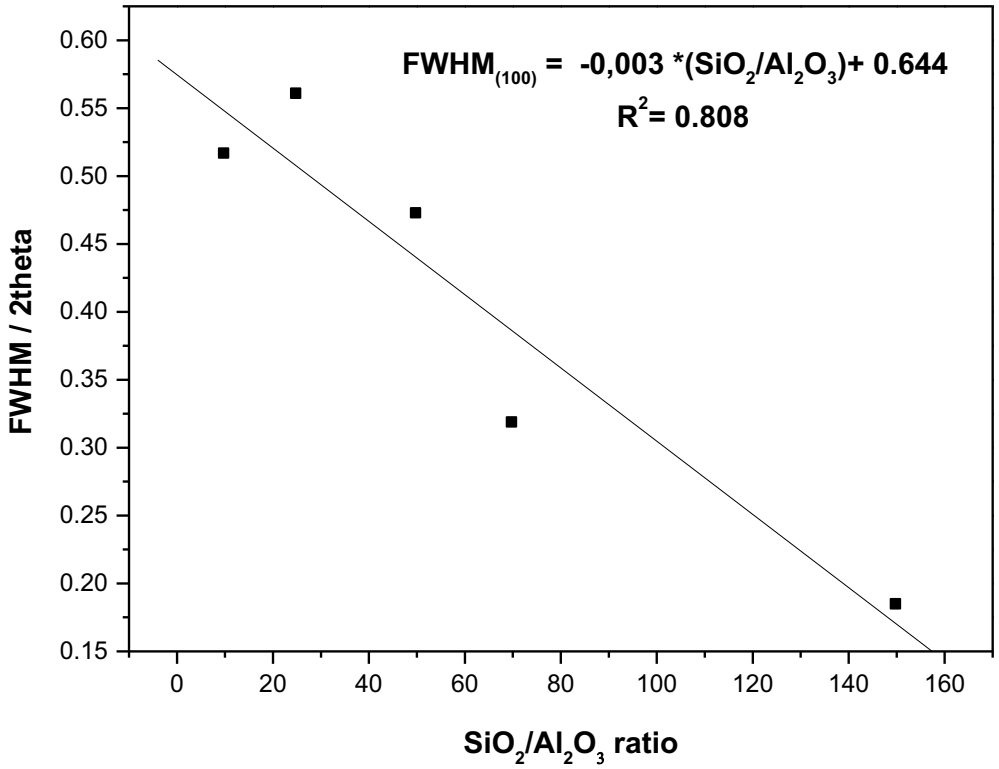

Fig.2.3a. Linear fit of full width at half maximum (FWHM) versus SiO_2/Al_2O_3 ratios

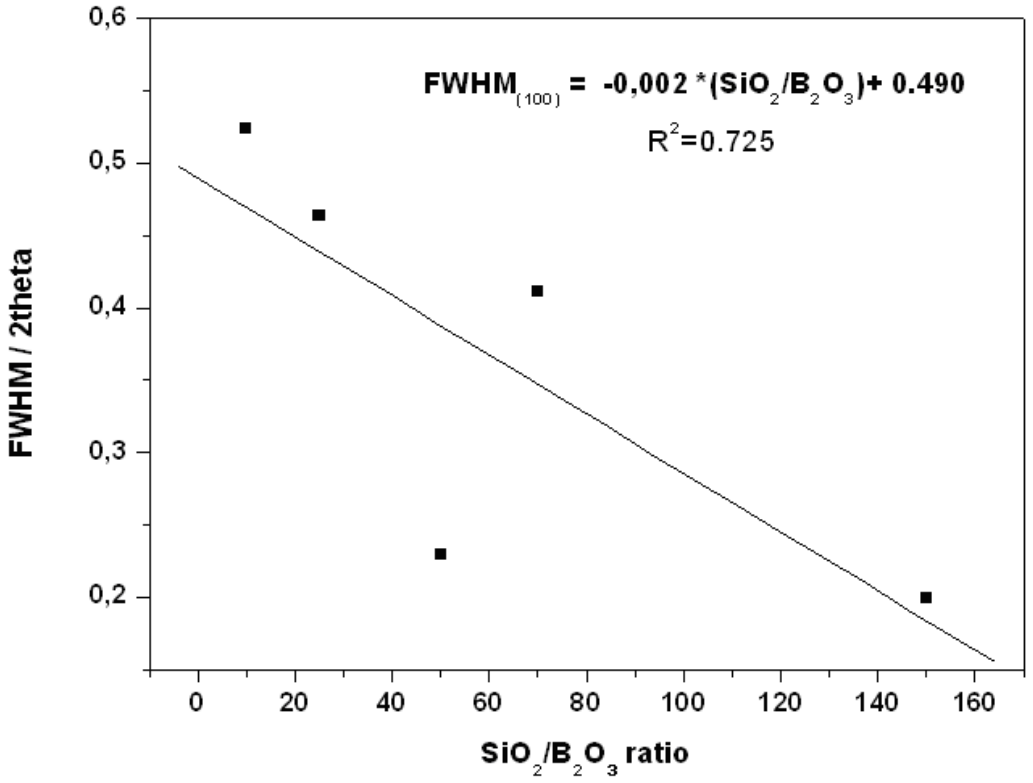

Fig.2.3b. Linear fit of full width at half maximum (FWHM) versus SiO_2/B_2O_3 ratios

This could be interpreted in a slight decrease of the ordered nature of MCM-41 through the incorporation of aluminium and boron into the framework. However, in spite of the substitution by these elements the MCM-41 structure was preserved (Chen et al., 1993 and Vidya et al., 2002).

2.3.2 ATR-FT-IR spectroscopy of mesoporous materials

The ATR-FT-IR method was particularly suited to record IR spectra of mesoporous materials, such as MCM-41, which were known to exhibit unwanted interaction with KBr (Bai et al., 2002). The ATR-FT-IR spectra of Al-MCM-41 (Figure.2.4a, Table 2.2a) exhibited bands in the region between 950-1200 cm^{-1} which could be assigned to antisymmetric stretching of ≡Si−O−T≡, (T= Si or Al) bonds. Bands in the 600-800 cm^{-1} region will involve the corresponding symmetric vibrations. The absorption band at 465 cm^{-1} corresponds to bending vibration of ≡T−O− (T= Si or Al). In addition, there was general tendency for the centre of gravity of the absorption band at 1032-1043 cm^{-1} to shift to higher frequencies with decreasing aluminium content (Milkey, 1960). All these features are typical of aluminosilicate of MCM-41 structure (Meyers et al., 1985 and Chen et al., 1993). The vibrations of SiO_2 tetrahedral unit and its modification due to the incorporation of B in the framework mainly appeared in the region of 450–1390 cm^{-1}. (Figure.2.4b, Table 2.2b).

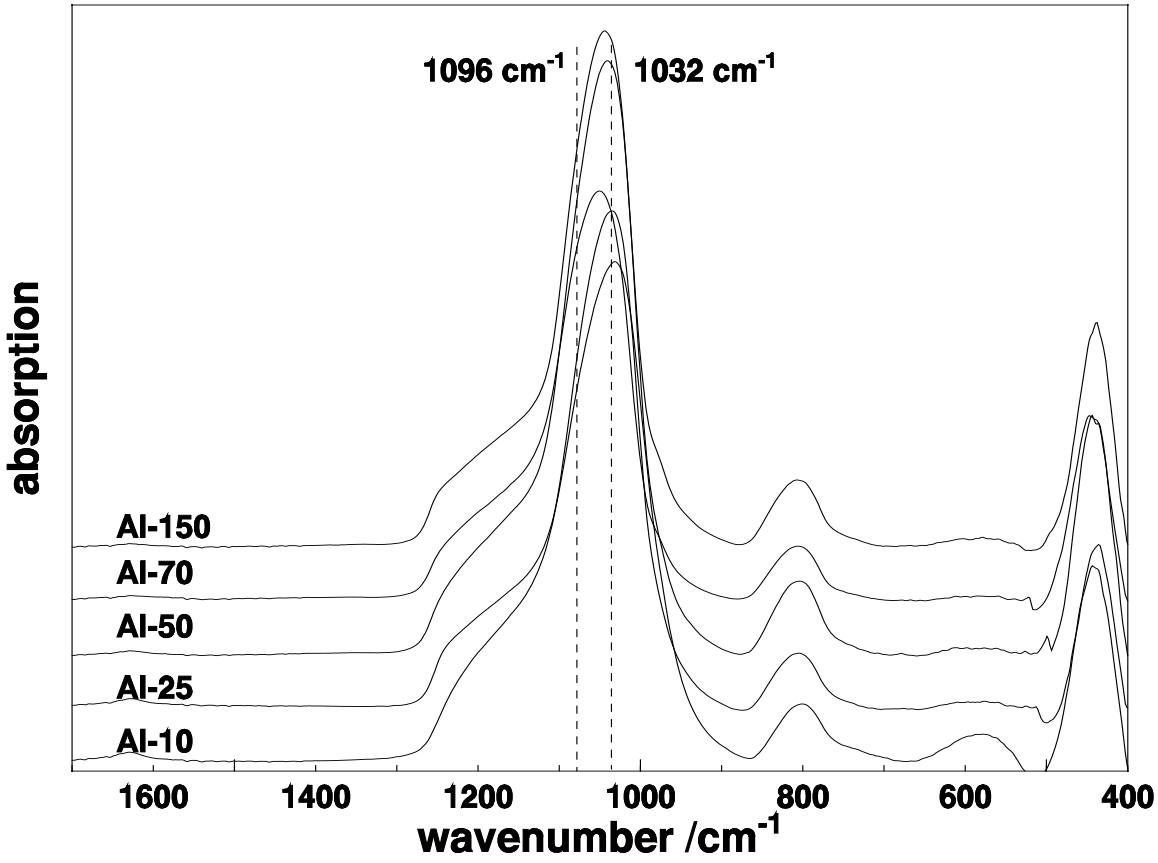

Fig.2.4a. FT-IR spectra of Al-MCM-41 synthesized with various SiO_2/ Al_2O_3 ratios

Table 2.2a. IR band positions of the Al-MCM-41with different content

Ratio	O-Si-O Bending	Si-O-Si sym-stretch	Si-O-Si/Si-O-Al Anti-sym stretching			
SiO_2/Al_2O_3	cm^{-1}	cm^{-1}	cm^{-1}	cm^{-1}	cm^{-1}	cm^{-1}
5	443.0	801.2	1031.9	1093.6	1153.1	1214.4
10	439.1	807.1	1037.5	1087.3	1141.9	1218.4
25	442.5	806.5	1040.0	1090.7	1146.9	1217.3
50	445.5	808.3	1048.1	1093.0	1143.1	1216.4
70	441.2	807.9	1044.8	1090.7	1144.6	1219.4
150	441.9	807.8	1042.8	1090.5	1142.3	1215.9

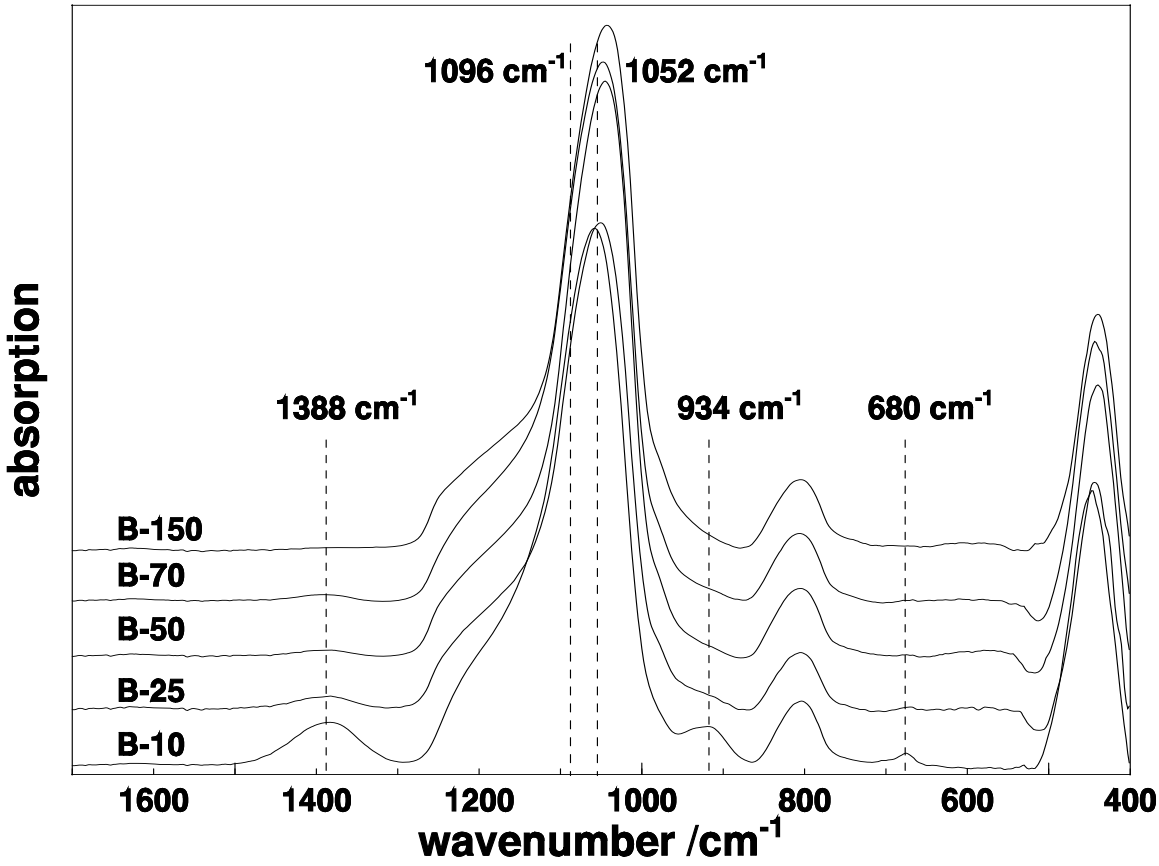

Fig.2.4b. FT-IR spectra of B-MCM-41 synthesized with various SiO_2/B_2O_3 ratios

Table 2.2b. IR band positions of the B-MCM-41with different content

Ratio	O-Si-O Bending	Boron	Si-O-Si sym-stretch	Boron $B^{[4]}$	Si-O-Si/. Si-O-B antisym stretching				Boron $B^{[3]}$
SiO_2/B_2O_3	cm^{-1}	cm^{-1}	cm^{-1}	cm^{-1}	cm^{-1}	cm^{-1}	cm^{-1}	cm^{-1}	cm^{-1}
10	449.2	679.6	806.5	934.1	1052.6	1096.2	1139.7	1209.7	1388.5
25	445.2	674.7	807.6	959.0	1050.0	1096.8	1144.1	1216.5	1392.2
50	442.5		807.4	956.2	1044.2	1091.9	1136.4	1209.8	1391.8
70	443.3		808.9	954.6	1045.1	1091.2	1135.6	1209.1	1395.4
150	441.9		807.8		1042.7	1089.2	1138.1	1217.5	

$B^{[4]}$ tetra-coordination ; $B^{[3]}$ tri-coordination

The location of boron in samples 25-150 was confirmed from the presence of ATR-FT-IR band at 934-954 cm^{-1}, which was characteristic of tetra-coordinated boron $B^{[4]}$ in the MCM-41 framework (Queiroz and Aikawa ,1994 and Eswaramoorthi and Dalai, 2006). This band was completely absent in Al-MCM-41. Moreover, a small intensity band at 1395 cm^{-1} was observed indicating the presence of boron in tri-coordination. A similar observation was reported by Trong et al., (1996) and Zhao et al., (1998) in boron incorporated zeolites as well as mesoporous borosilicate materials. However, for the calcined samples (Figure.2.4b) a minor band also appeared at 1380-1396 cm^{-1} which could be assigned to residual tri-coordinated framework boron $B^{[3]}$. This band formed during the calcinations due to the change of boron coordination from tetrahedral to trigonal (Bai et al., 2002). The relative intensity of the 934 cm^{-1} band, characteristic for $B^{[4]}$ and of the 1390 cm^{-1} band, characteristic for $B^{[3]}$ both increase with increasing boron content. (Figure.2.5).

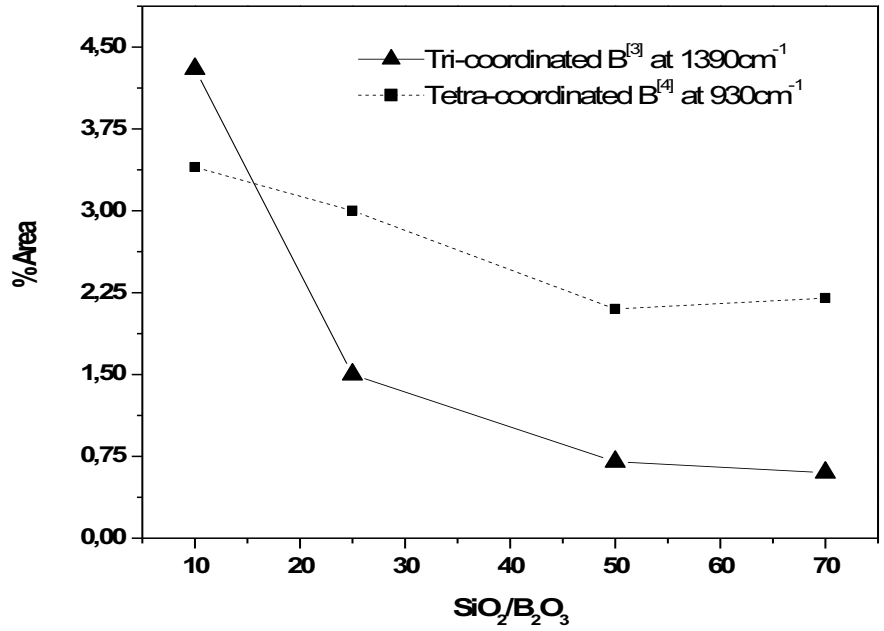

Fig.2.5. Relative intensity of IR bands represents tetra and tri-coordinated boron sites

The position of the band at 1043-1053 cm^{-1} attributed to the Si-O-B bond shifted toward lower wavenumber with decreasing of boron content. For the samples with the highest Si content, i.e. a ratio of 150, the positions for the forgoing bands were identical for both Al and B containing samples. By applying a simple spring-model with a force constant K and the reduced mass μ these shifts could be explained. The wavenumber is proportional to $(K/\mu)^{1/2}$,

an increase in K and a reduction in μ leads to positive shift in band position. Both apply for Boron. The bond length of Si-B shortens, which would be shown in the following section.
Hence the bond strength increased; simultaneously the reduced mass decreased by substituting of Si with B. Table 2.2a and 2b summarize the main Al and B-MCM-41 bands.

2.3.3 Structural discussion

The increasing B content led to increase $B^{[3]}$ tri-coordination of boron in the framework (Fig.2.5) which moreover led to an increase in unit cell and the particle size of the B-MCM-41 materials. Valerio et al., (2000) found that in the case of a proton being the counterion, the tetrahedral BO_4 coordination was unstable and was replaced by silanols groups. These were formed on the adjacent silicon and trigonally coordinated boron. This distance between B and OH (silanols) was longer (0.23 nm) than the corresponding to a tetra-coordinated B. (Figure.2.6).

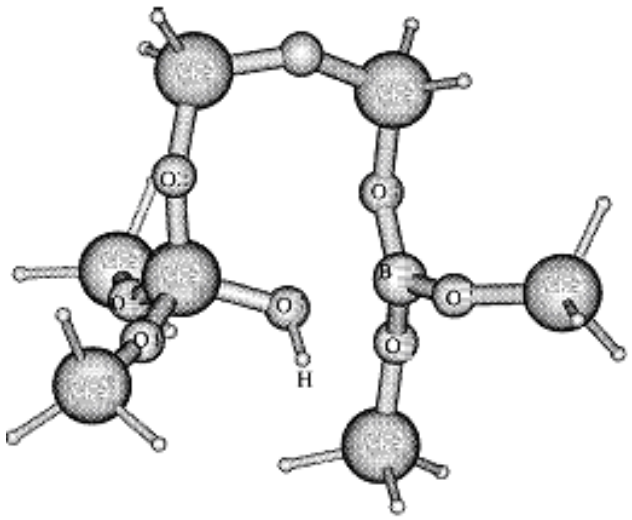

Fig.2.6. Optimized model structures with a proton as boron counterions (Catlow et al., 1995)

The FWHM data from both B- and Al-MCM suggested a less ordered structure for the latter (Table 2.2 and Fig.2.3). The incorporation of boron and aluminium modified the structure from hydrophobic to hydrophilic and gave less well developed structure than Si-MCM-41. The changes in the unit cell dimensions of MCM-41 material as a function of Si-substitution by Al and B were well documented and were useful to characterize such substitution (Fig.2.2). Quantum-chemical calculations suggested that the bond between boron and the protonated framework oxygen atom (silanol group) was much weaker than the Al–O bond in a corresponding Al…O(H)–Si group. The B–O bond in B…..O(H)–Si groups was effectively broken, resulting in trigonal boron in the zeolite framework, $B^{[3]}$. Stave and Nicholas (1995)

have calculated the B–O and Al–O distances in (X)3Si–OH–T(X)3 (X=OSiH3, T=B, Al) cluster models of zeolites ZSM-5 using density functional theory. These authors found a B–O distance of 208.4 pm which is too large for a covalent interaction, while the Al–O bond has a distance of 183.6 pm.

2.3.4 Nitrogen adsorption studies

Substitution of elements into the MCM-41 materials could change the surface properties and the pore structure due to change in the T═O═T angle and T═O length (T= Si or substituted element). Kosslick et al., (1993) found that the substitution of Si by tetravalent Ge decreased the T═O═T angle and the T═O bond length.

The influence of this change was also observed in the N_2 gas adsorption for the samples Al-MCM-41 and B-MCM-41 (SiO_2/Al_2O_3 or B_2O_3=50, 70 and 150) synthesized at 373 K. (Figure.2.7a and 7b).

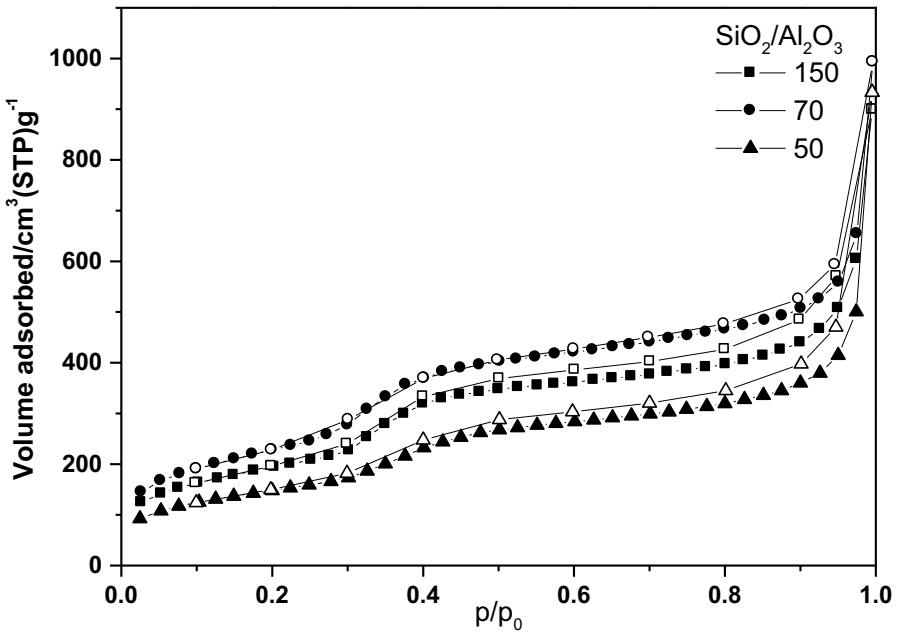

Fig.2.7a. N_2-adsorption-desorption isotherm of Al-MCM-41 with different SiO_2/Al_2O_3 ratios 50 (▲), 70(●) and 150(■). Full symbols adsorption, open symbols desorption

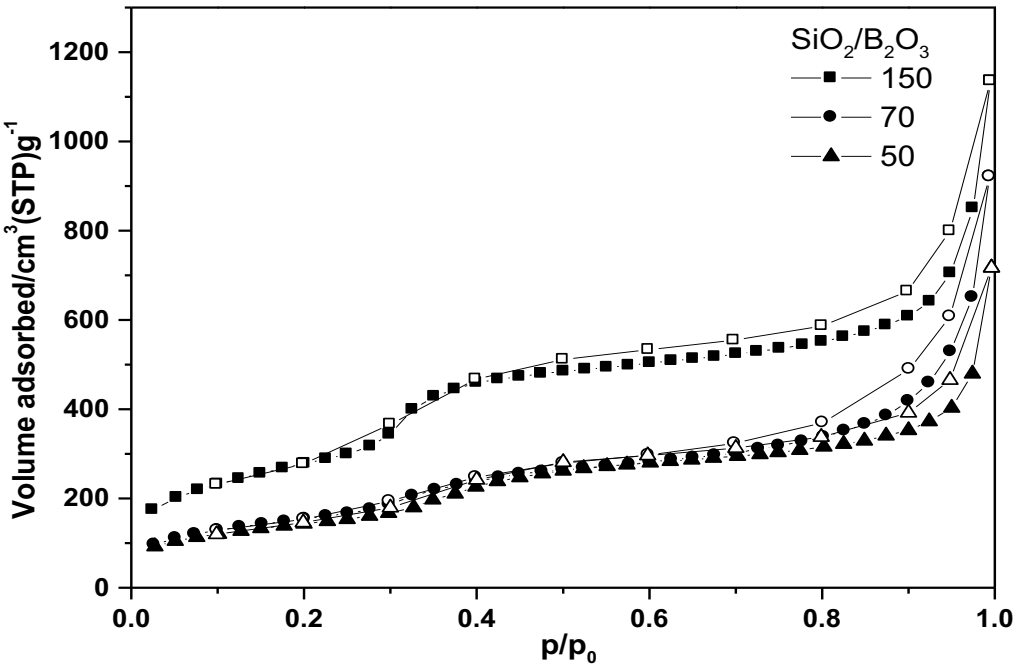

Fig.2.7b. N_2-Adsorption-desorption isotherm of B-MCM-41 with different SiO_2/B_2O_3 ratios 50 (▲), 70(●) and 150(■). Full symbols adsorption, open symbols desorption

The isotherms exhibited type IV isotherms according to the classification of the (IUPAC, 1957). The results obtained were in agreement with the study carried out by Kosslick et al., (1993) and Sayari et al., (1995), which allotted lower specific surface area of the Boron containing samples. During the calcinations process, trigonal B was lost. It could be assumed that this loss has an influence either in the particle size and /or the porosity, indicated by a decrease of SSA of over 500 m²/g when compared to the Si-MCM-41. (Table 2. 3).

Table 2.3. Physical proprieties of MCM-41with different substitution Al and B

Sample	a_0 (nm)	S_{BET} (m^2/g)	V_{meso} (cm^3/g)	Dp_{DFT} (nm)	Dp_{cal} (nm)	bp (nm)
Si-MCM-41	4.48	1273	0.82	4.0	3.9	0.7
B-MCM-41-150	4.42	1052	0.78	3.8	3.6	0.5
B-MCM-41-70	4.28	576	0.48	3.8	3.2	0.9
B-MCM-41-50	4.50	522	0.47	4.1	3.4	0.6
Al-MCM-41-150	4.52	704	0.58	4.1	3.6	0.6
Al-MCM-41-70	4.27	853	0.67	3.8	3.5	0.7
Al-MCM-41-50	4.91	539	0.48	4.0	3.7	0.7

a_0: unit cell; S_{BET}: specific surface area; V_{meso}: mesopore volume (pore width < 7.1 nm); D_{DFT}: porous diameter by DFT- Monte carlo method; $D_{cal:}$ porous diameter by the relation $Dp_{cal} = C*d_{100}\,\rho*V_{meso}/1+\rho\,*V_{meso})^{1/2}$; C=1.213 and ρ = 2.2 cm^3/g bp: wall thickness.

The mesopore volume decreased from 0.82 cm^3/g for the unsubstituted samples to 0.47 cm^3/g for the B and to 0.48 cm^3/g for the Al-containing samples. This could be explained for B-MCM by an expulsion of trigonal Boron which leads to a loss of channels. Boron has shown a strong tendency to be leached out of the lattice during calcinations (Chu et al., 1985). This further confirmed the mesoporous nature of the samples (Branton et al., 1993 and Franke et al., 1993). The pore sizes distributions of all samples were narrow and exhibited a maximum in the range of 3–4 nm. (Figure.2.8a and 8b).

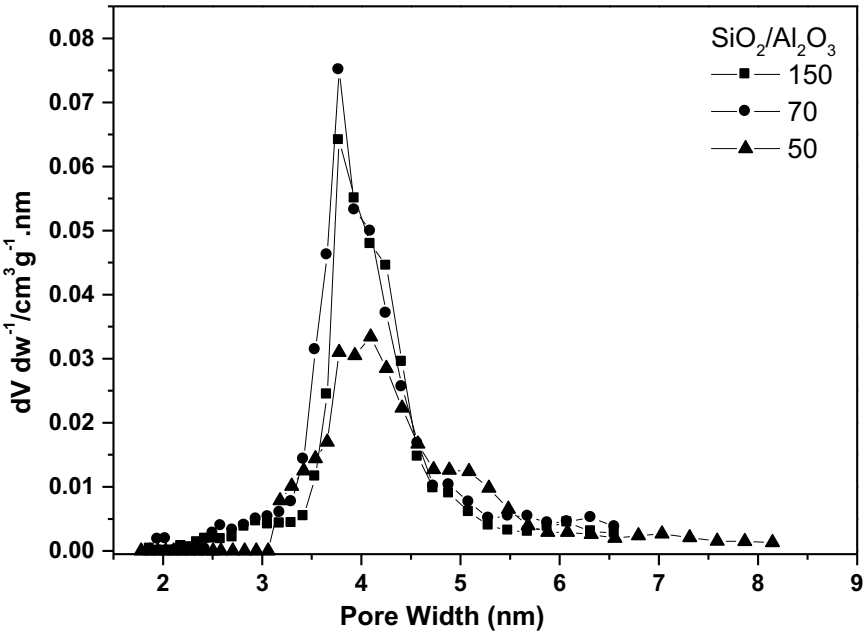

Fig.2.8a. Pore size distributions derived from N_2-adsorption isotherm branch of Al-MCM-41 with different SiO_2/ Al_2O_3 ratios, 50 (▲), 70(●) and 150(■)

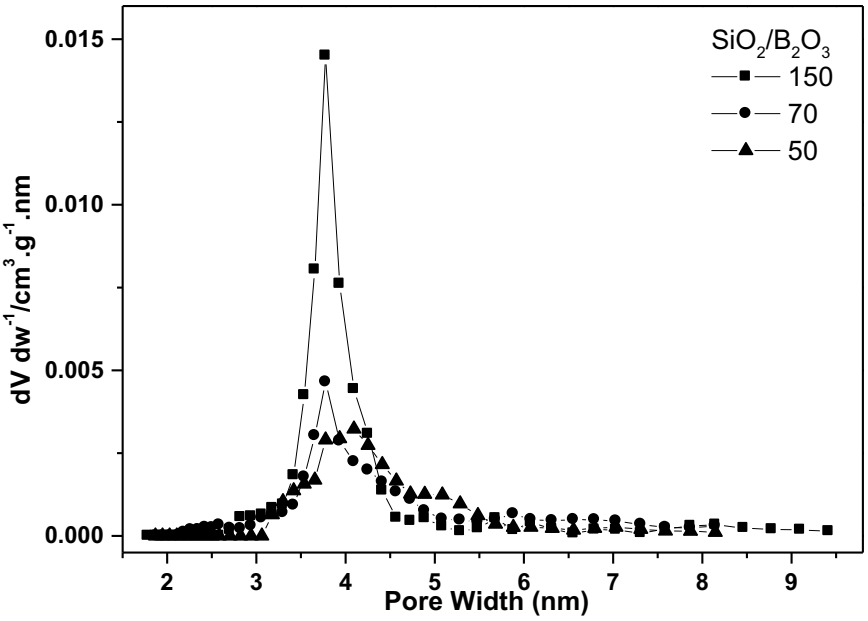

Fig.2.8b. Pore size distributions derived from N2-adsorption isotherm branch of B-MCM-41 with different SiO_2/B_2O_3 ratios, 50 (▲), 70(●) and 150(■)

When compared to siliceous MCM-41, the average pore diameter values of B-MCM-41 samples were slightly less and for Al-MCM-41 about the same (Table 2.3). The comparison of pore size data derived from DFT theory and from the calculation method from (Ulagappan and Rao., 1996) was in good agreement. The pore wall thickness obtained from the XRD data and the gas adsorption values were 0.7 nm for both substitutions, where B-MCM-41 exhibited a slight larger standard deviation. The value of 0.7 nm resembled the one found for Si-MCM-41 (Kresge et al., 1992 and Beck et al., 1992). These values can be only considered as estimations, because there is not yet a definitive method for such pore size or pore wall calculation, respectively because all are implying a smooth cylindrical pore shape. The existence of such a model is a matter of ongoing scientific dispute.

All the textural characteristics of B-MCM-41 and Al-MCM-41 samples revealed that aluminium and boron incorporation slightly decreased the ordered nature of the hexagonal structure of MCM-41. Similar observation was made in XRD analysis. (Figure.2.2.)

2.4 Conclusion

Isomorphous substitution of boron and aluminium in MCM-41 framework was successfully carried out by a direct synthesis method. The change in d-spacing and unit cell parameter compared to siliceous MCM-41 indicated the incorporation of boron or aluminium in the framework. The nitrogen adsorption studies showed that the synthesised M-MCM-41 materials led to a mesoporous material with narrow pore size distribution. The presence of bands at 1380, 920 and 960 cm^{-1} in the ATR-FT-IR spectra of all samples confirmed that B was incorporated into the MCM-41 framework. In addition, the shift of the Si-O-M (M=Al, B) band at around 1043 cm^{-1} gave another strong argument for the incorporation of Al and B. The best structure was allocated to Al- and B-MCM-41 for a mass ratio equal to 150.

A hexagonal structure characteristic for a mesoporous material produced by the direct synthesis method was still obtained for a SiO_2/Al_2O_3 or B_2O_3 ratio of 10. A higher content of Al or B did not further increase the quality of the product.

Chapter 3.

The synthesis of Al-MCM-41 from volclay I:

-a low-cost Al and Si source

3.1 Introduction

Porous materials have experienced a great development in the various fields of application (Sherman, 1999). Among these porous materials, the M41S family which was discovered in beginning of the 1990's by researchers from Mobil and which is composed of three materials MCM-41, MCM-48 and MCM-50 (Kresge et al., 1992; Beck et al., 1992). This class of material has an uniform pore size distribution in the mesopore range, which is tunable between 2 nm and 10 nm, a high specific surface area of up to 1500 m^2/g, and a high porosity (<1 cm^3/g). These proprieties lead the M41S family and especially the MCM-41 which is the best studied member to be used in catalyst (Sayari, 1996) and adsorption (Moller et al., 1998). Several studies proposed to convert the coal fly ash by hydrothermal activation methods to zeolites using alkaline solutions (mainly NaOH and KOH solution) which are analogue to the formation of natural zeolites from volcanic deposits (Singer et al., 1995). Most of the zeolites synthesized by this conversion contain a non-converted part of fly ash and not all aluminium-silicate phases were converted (Moreno et al., 2001). Wakihara et al., (2004) introduced for the first time an alkaline fusion to synthesis the conventional zeolites similar to chabazite or mordenite. This method improved the conversion rate of aluminium-silicate phases and resulted in very interesting types of zeolites. Kumar et al., (2001) synthesized MCM-41 and SBA-15 (Santa Barbara amorphous -15) with a specific surface area of 842 m^2/g and 483 m^2/g respectively from coal fly ash using the fusion method. Kang reported the synthesis of Al-MCM-41 by using water glass (or silicate sodium) as Si source and meta-kaolin as only Al sources (Kang et al., 2005). This paper presents a new way to generate both Si and Al from volclay, a low-cost mass material containing smectite (1 kg of silicium and aluminium from volclay costs around 0.03 € whereas the same amount of silicium from ludox and aluminium from sodium aluminates cost around 52 €), for synthesis of a high structural ordered and cheaper Al-MCM-41 materials under hydrothermal condition by adopting the fusion process.

3.2 Experimental

3.2.1 Starting materials

The volclay used in this study was obtained from Süd-Chemie AG, Germany (Table 3.1). The elemental content was determined by XRF with a MagiXPRO spectrometer from Philips. For the measurements melt tablets were formed by mixing 0.8 g of sample powder with 4.8 g $Li_2B_4O_7$ (Spektromelt A10 from Merck). The volclay contained about 80-wt% montmorillonite, other minerals with around 4 wt.% each were muscovite, quartz, orthoclase, plagioclase, and jarosite. Traces of calcite were also found.

Table 3.1. Chemical composition of volclay

Wt.%	SiO_2	Al_2O_3	Fe_2O_3	TiO_2	CaO	MgO	Na_2O	K_2O	MnO	P_2O_5
Volclay	55.83	18.34	3.52	0.15	1.13	2.24	1.86	0.52	0.01	0.04

The other reactants applied were cetyltrimethylammonium bromide ($C_{19}H_{42}NBr$; CTAB, Aldrich; 99%) as surfactant and ammonium hydroxide, 25% (NH_3, 99,99%, Aldrich) and acetic acid min. 99,8% Aldrich.

3.2.2 Synthesis of Al-MCM-41 from volclay

To extract the Si and Al needed to synthesis Al-MCM-41 from volclay, a fusion process at 550 °C with 1 h duration was adopted which consisted of a treatment of sodium hydroxide with volclay. Two kinds of sodium hydroxide, powder and pastille, which exhibit a marked difference in pricing, were used.

Sample A was a 1:1.2 volclay: NaOH pastille mixture and the second sample B was a 1:1.2 volclay: NaOH powder mixture.

In addition a 2 M sodium hydroxide solution was mixed with 1 g of volclay and heated at 550 °C to obtain a melted mass (sample C). This mass was cooled at room temperature overnight; thereafter 1g of this powder fusion sample was added to 4 g of water and stirred for 1 day at room temperature. The supernatant was obtained by filtration.

Al-MCM-41 from volclay was synthesized according the following procedure (Kumar et al., 2001) 0.91 g $C_{19}H_{42}NBr$, 16 ml of water and 0.8 g NH_4OH aq were combined with 40 ml of supernatant, obtained as described above, and the pH was fixed at 9.5 by addition of acetic acid. The hydrogel was heated at 100 °C. The final material obtained was calcined at 550 °C (heating rate of 2 K/min) up to 6 h under N_2-gas to remove the surfactant ($C_{19}H_{42}N^+$) from the pores of Al-MCM-41.

Al-MCM-41 standard was synthesized by the direct method using Ludox sol as silicium source (Mokaya. 2001).

3.2.3 Characterization

The diffraction patterns were recorded in the °2θ range of 1–70° (step size of 0.02 °2θ, step time of 5 s; Bruker D5000 diffratometer, CuKα, 40 kV and 40 mA), radiation equipped with a graphite monochromator and scintillation counter. A talc/vermiculite mixture was applied as internal standard for peak position correction. For the peak positions the ICCD files 083-1768 for talc and 076-0847 for vermiculite were applied. Bruker Topas 3.0 software was used for the single line fitting of the XRD reflections. The chemical composition was determined with X-ray fluorescence analysis (XRF). The analyses were performed on a MagiXPRO spectrometer (Phillips), equipped with a rhodium X-ray tube (stimulation power: 3.2 KW), using air dry powdered samples fused with lithium tetraborate (mixing ratio 1:7). The loss of ignition was determined separately at 1000 °C (2 h). N_2-adsorption-desorption measurements were performed at 77 K with a Quantachrome Autosorb1 MP. The samples were degassed at 383 K in vacuum for 24 h before measurements. Specific surface areas were calculated by using the Brunauer–Emmett–Teller (BET) method (Brunauer et al., 1938). The pore size distribution curves were calculated using the NLDFT equilibrium model with cylindrical pore shape based on the DFT/Monte Carlo method (Lowell et al., 2004). Pore volumes were obtained from the amount of N_2 adsorbed at $p/p_o = 0.7$ corresponding to a pore width of 7.1 nm in order to exclude inter-particle pores formed by the powder.

The examination of the particle morphology and of the grain size distribution was carried out by the Philips ESEM XL 30 FEG. This kind of SEM uses a chamber atmosphere of 1 – 3 Torr water vapour instead of high vacuum. For high resolution scanning electron microscopy, the samples have been coated with a platinum layer (3 nm) by conventional sputtering to avoid charging. The measurements were carried out using a high resolution LEO 1530 SEM with a Schottky emitter field emission gun under high vacuum (10-6 torr). Acceleration voltages between 10 and 20 kV were applied using an aperture of 20 µ, with 20 kV obtaining the best results. All images were recorded with an In-Column detector (InLens) allowing highest resolution imaging. For noise reduction the pixel averaging mode and a low scan rate were used, the picture resolution being 1024 x 768 pixels.

3.3 Results and discussion

3.3.1 X-ray diffraction and chemical composition

Both the montmorillonite and quartz phases disappeared in all samples except sample C (volclay+NaOH solution 2M) (Fig.3.1). This incomplete dissolution of quartz and montmorillonite was also described by Morino et al., (2001).

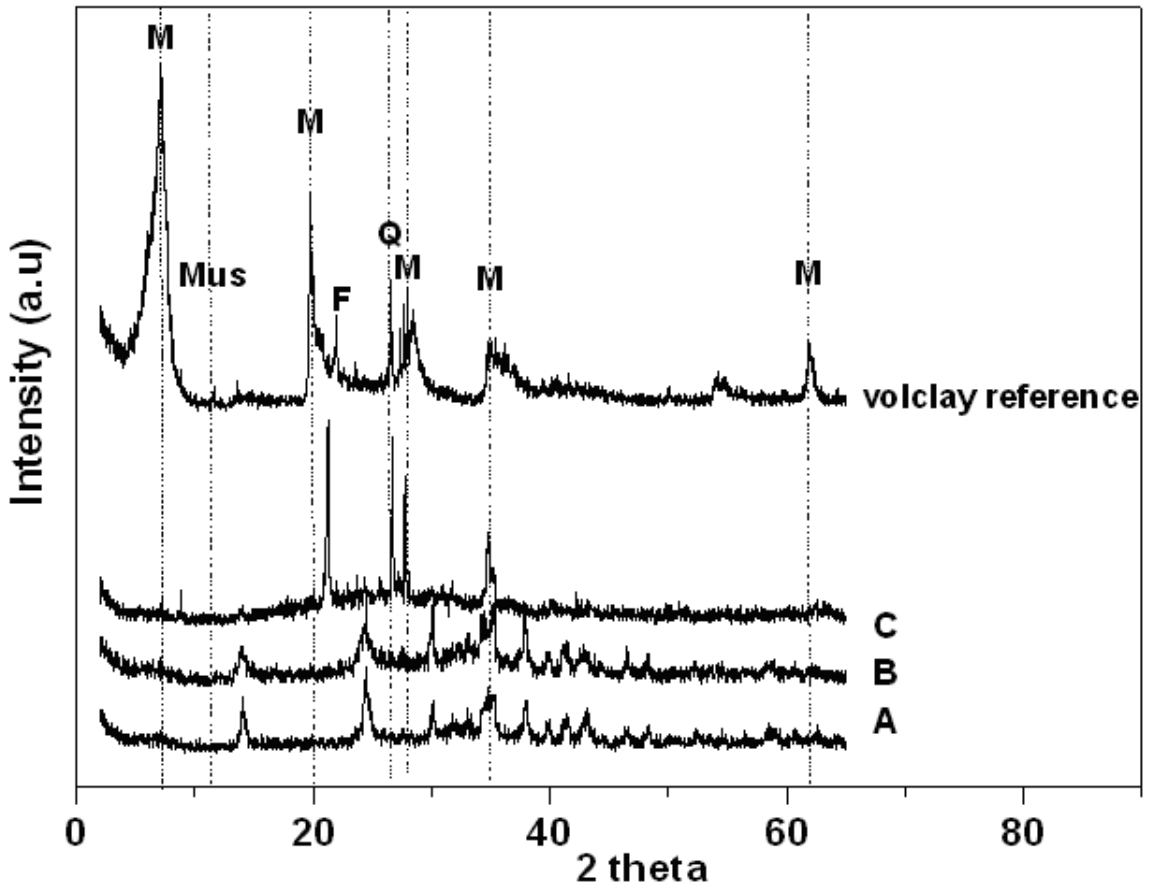

Fig.3.1. XRD patterns; (M) montmorillonite, (F) feldspars, (Q) quartz and (Mus) muscovite. A = 1:1.2 volclay : NaOH pastille mixture; B = 1:1.2 volclay : NaOH powder mixture; C = NaOH solution (2M) with volclay (fused)

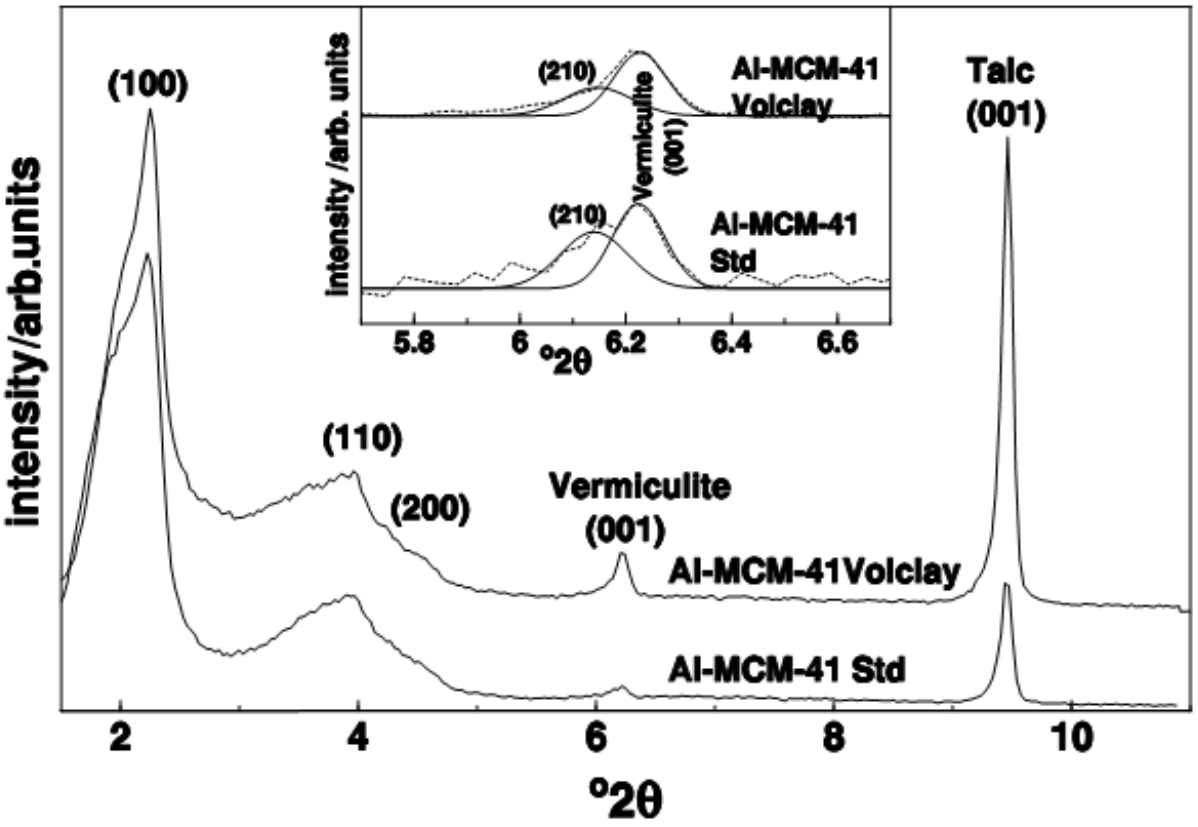

Fig.3.2. XRD pattern of Al-MCM-41 synthesized from volclay and from standard laboratory reagents

The XRD patterns of calcined samples of Al-MCM-41 standard and from volclay (Fig.3.2) displayed reflections consistent with hexagonal indexing typical of the MCM-41 structure in the P6mm space group (Melo et al., 1999). If hexagonal pore symmetry is assumed, the d_{100} – value with 3.91 nm for the standard corresponded to a unit cell parameter a_0 of 4.51 nm. From the d_{100}–value of 3.92 nm for the volclay derived Al-MCM-41 a unit cell parameter a_0 of 4.53 nm was calculated (Table 3.2). The observation of three higher angle reflections, (110), (200), and (210), indicated that the product possessed the symmetrical hexagonal pore structure typical of Al-MCM (Fig.3.2). These results corresponded to those found by Beck et al., (1992). The peak height ratio between (100) and (110) Bragg peak of the Al-MCM-41 synthesized from volclay and the standard differed for both samples (Table 3.2); this result is related with the regularity of the hexagonal structure due to the pH applied and the amounts of silica and aluminium which were reacted at this pH value (Kumar et al., 2001; Mokaya. 2001). Thus the presence of additional mineral phases in the volclay had no impact on the process and the properties of MCM-41.

Table 3.2. Physical properties

Sample	a_0 (nm)	Ratio (100)/(110)	S_{BET} (m^2/g)	V_{meso} (cm^3/g)	D_{DFT} (nm)	bp (nm)
Al-MCM-41 volclay	4.53	0.9	1060	0.77	3.78	0.75
Al-MCM-41 standard	4.51	0.5	704	0.56	3.78	0.73

a_0: unit cell; S_{BET}: specific surface area; V_{meso}: mesoporous volume (pore width < 7.1 nm); D_{DFT} : DFT method pore size distribution; bp: wall thickness = a_o - D_{DFT}.

Wakihara et al., (2004) reported that Na^+ ions (1:1.2 NaOH/fly ashes, comparable to the ratio used in our study) in the precursor solutions favoured the formation of zeolites and hindered the formation of Al-MCM-41. According to the high Si/Al-ratio in the volclay derived Al-MCM-41 (Table 3.3), the concentration of Na^+ ions in the supernatant of volclay seems to be uncritical, and any effect on the synthesis of Al-MCM-41 can be ruled out. The control of the pH during the synthesis is very important and has a strong influence on the Al-MCM-41 synthesis (Luechinger et al., 2003).

Table 3.3. EDAX results of both Al-MCM-41 from volclay and from laboratory standard reagent

Sample	Si (at.%)	Al (at.%)	Si/Al
Al-MCM-41 volclay	11.7	0.75	17
Al-MCM-41 standard	8.3	0.10	63

Since the (200) peak was more pronounced in the volclay Al-MCM-41 in comparison to the standard Al-MCM-41 it can be assumed that most silica and aluminium generated from volclay were reacted . This is supported by the EDAX measurement of the Si and Al amount (Table 3.3). The Si and Al content of MCM-41 from volclay were 11.7 at.% for Si and 0.7 at.% for Al whereas for the Al-MCM-41 standard 8.3 at.% for Si and 0.1 at.% for Al were determined. The Si/Al ratio increased approximately 4-fold in favour of the volclay Al-MCM-41. These results agree with data of Ryoo and Kim (1995) who observed an increase in the yield of MCM-41 based on the amount of silica recovered.

3.3.2 Nitrogen adsorption Studies

The N_2 adsorption-desorption isotherms (Fig.3.3) for calcined Al-MCM-41 synthesized at 100 °C was of type IV according to the classification of IUPAC (Sing et al., 1985) with a pronounced capillary condensation step at relative pressures p/p_0 between 0.3 and 0.4 typical of a material with a uniform and narrow pore distribution. The p/p_0 position of the inflection point is related to the pore diameters in the mesopore size range. The steepness of this step indicates the uniformity of the mesopore size distribution. (Fig.3.4).

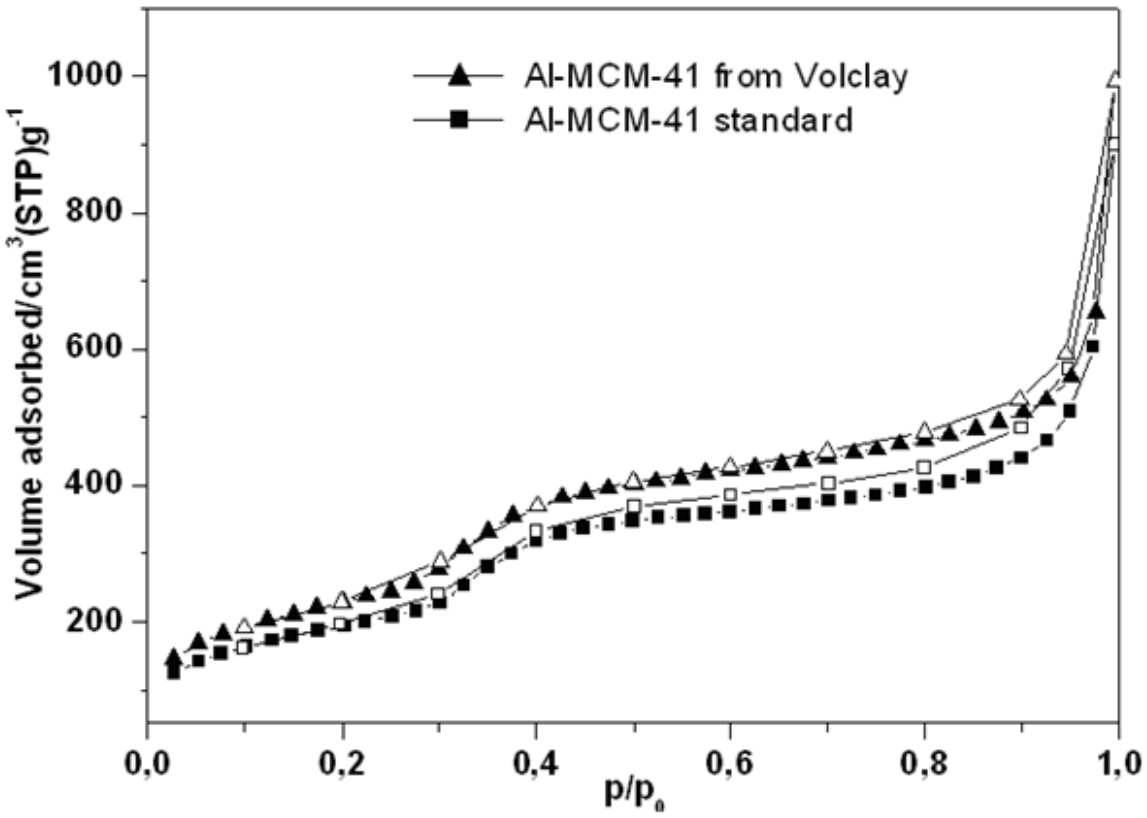

Fig.3.3. N_2-adsorption-desorption isotherm of Al-MCM-41 from volclay (□) and from a standard method (■). Full symbols adsorption, open symbols desorption

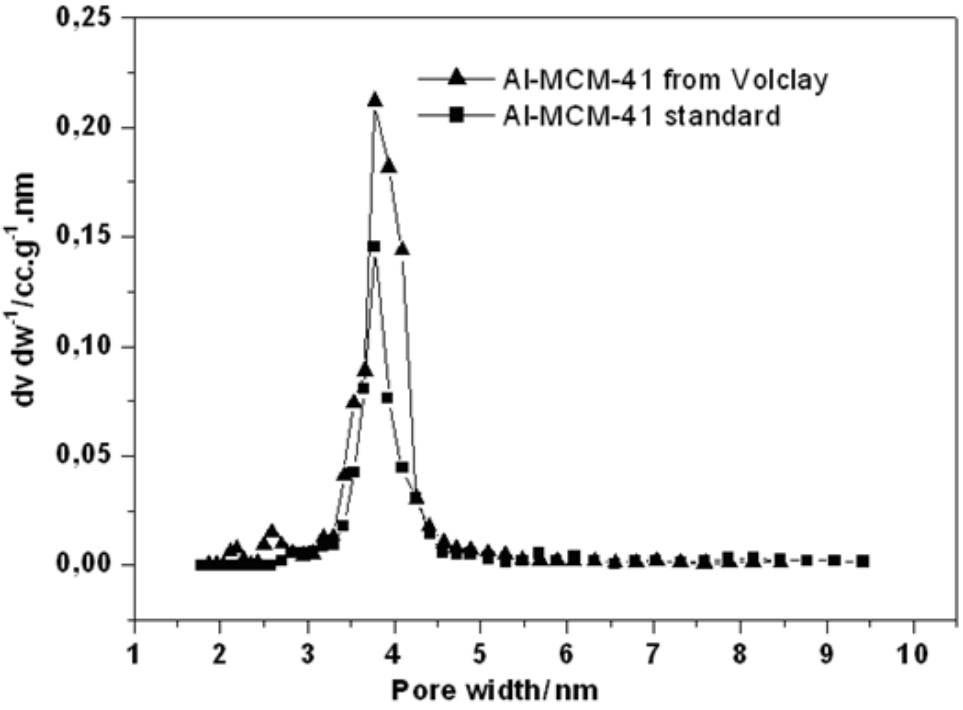

Fig.3.4. Pore size distributions derived from N2-adsorption isotherms calculated by DFT/Monte-Carlo method

The specific surface area of the calcined Al-MCM-41 sample derived from the standard method and from volclay was found to be 704 m^2/g and 1060 m^2/g respectively (Table 3.2). A minor adsorption–desorption hysteresis at a p/p_o of 0.9 for Al-MCM-41 standard can be related to capillary condensation in large meso- or marcopores in the interparticle space. This hysteresis was also observed for the samples prepared at synthesis temperatures of 616 K and 636 K (Kruk et al., 1997). For the volclay derived MCM-41 this hysterics seemed to be absent or of very minor importance. The pore size for volclay MCM-41 and the standard MCM-41 was around 3.8 nm, both calculated by the DFT/Monte-Carlo method (Table 3.2). By subtracting these values from the values of the mean distance of the pores, i.e. a_o as determined by XRD, a wall thickness bp of 0.7 nm for both samples was found. (Table 3.2).

3.3.3 Scanning electron microscopy

The particles (Fig.3.5a- d) were made up of elongated rod-like rounded shapes which in some cases exhibit hexagonal features. Such shapes and features were also described by Pauwels et al., (2001). Evaluation of the rounded particle sizes in (Fig.3.5d) exhibited on average a diameter of 33 +/- 4 nm (n=42). Al-MCM-41 sample synthesised from volclay in (Fig.3.5e and f) consisted of aggregates of spherical particles, similar to the shapes presented in

(Fig.3.5d). This form was characteristic for MCM-41 synthesised under basic conditions (Pauwels et al., 2001; Cheng et al., 1997). The EDAX results of both samples can be found in Table 3.3 and were already discussed above.

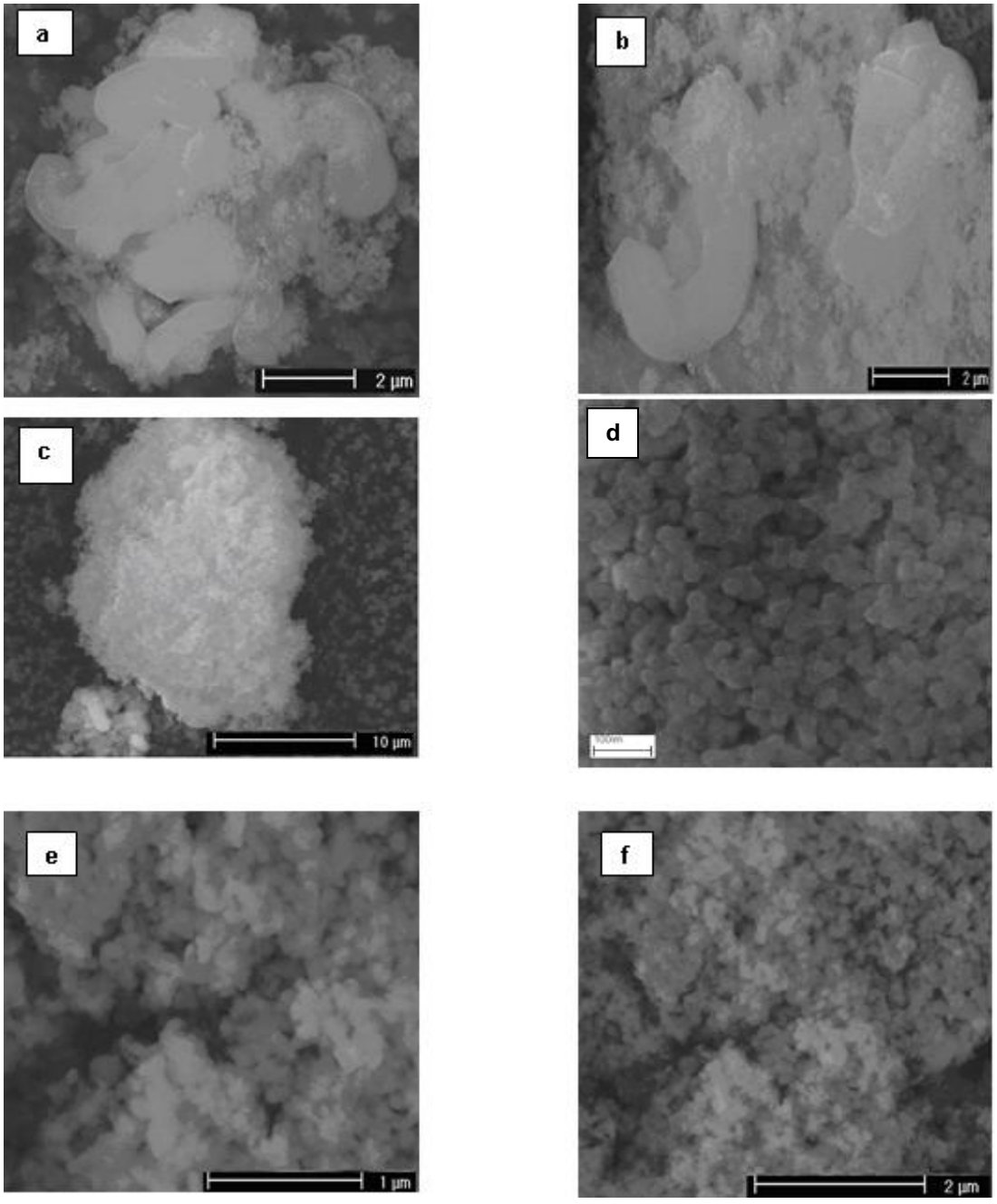

Fig.3.5. SEM of Al-MCM-41. (a-d) samples synthesized by standard method, and (e), (f) for samples synthesized from volclay

3.4 Conclusion

The application of volclay, a low-cost material, as Si and Al source in the MCM-41 synthesis yielded a high quality Al-MCM-41 product. The properties were superior to the ones of an Al-MCM produced by a standard method. The mesoporous Al-MCM-41 had a uniform pore size, a pore diameter of 3.8 nm and a S_{BET} of 1060 m^2/g, which is agrees with the values usually reported for Al-MCM-41 synthesis. Therefore, volclay can be applied as a silicium and aluminium source. The fusion method is efficient to extract the silicium and aluminium from the montmorillonite.

Chapter 4.

The synthesis of MCM-41 nanomaterials from volclay II: increasing process efficiency by iterative water treatment

4.1 Introduction

Molecular sieves, a nanomaterials, collectively known as M41S contain uniform one dimensional channels of 1.6 - 10.0 nm in diameter and a high specific surface area of up to 1000 m^2/g (Kresge et al., 1992; Beck et al., 1992). These materials, of which MCM-41 is the best studied member, are prepared using aggregates of a surfactant to serve as the template, instead of single organic molecules as applied with the conventional sieves. Many attempts are focused on the use of a natural source instead of the laboratory reagents. Singer et al., (1995) proposed to convert the coal fly ash by hydrothermal activation methods to zeolites using alkaline solutions (mainly NaOH and KOH solution) which are analogue to the formation of natural zeolites from volcanic deposits. Chang et al., (1999) have studied the conversion of the coal fly ash to a mesoporous materials aluminosilicate in the hexagonal phase type MCM-41 with the very important incorporation of aluminium (Si/Al = 13.4). Kumar et al., (2001) synthesized MCM-41 and SBA-15 (Santa Barbara amorphous - 15) with a specific surface area of 842 m^2/g and 483 m^2/g, respectively from coal fly ash using the fusion method. Wakihara et al., (2004) introduced for the first time an alkaline fusion to synthesise the conventional zeolites similar to chabazite or mordenite. This method improved the conversion rate of aluminium-silicate phases and resulted in very interesting types of zeolites. Kang et al., (2005) reported the synthesis of Al-MCM-41 by using water glass (or silicate sodium) as Si source and metakaolin as only Al sources. Recently, Adjdir et al. (2009) reported for the first time the synthesis of Al-MCM-41 by using volclay as both aluminium and silicon source. They adopted the alkaline fusion and water treatment of fused clay. After centrifugation two phases were obtained: A liquid phase called supernatant-1 which is used as silica and aluminium source in the synthesis of MCM-41 nanomaterials, and a sediment phase called residual-1. Here for the first time the application of the supernatant-2 obtained from water treatment of residual-1, to synthesise a high structural ordered MCM-41 under hydrothermal condition is reported. In addition, glass tubes instead of autoclaves have been utilized. The original materials employed and the entire design of this MCM-41 production process is cheaper and hence more cost effective than known practices.

4.2 Experimental

4.2.1 Starting materials

The Volclay used in this study constitutes mainly of smectite (dioctahedral) and is obtained from Südchemie AG, Germany (Table 4.1).

Table 4.1. Mineral phase content of Volclay (wt.%) (Composition from Steudel. 2008)

Phases	Sample
	Volclay [wt.%]
Smectite (Na-rich di)	60.0 ± 4.2
Smectite (Ca-rich di)	19.8 ± 3.6
Muscovite/illite	2.8 ± 0.9
Quartz	4.4 ± 0.5
K-feldspars (orthoclase)	4.0 ± 0.9
Plagioclase (albite)	4.1 ± 0.8
Calcite	1.3 ± 0.4
Gypsum	3,6 ± 0,6

In parenthesis the structure model used for Rietveld analysis (di = dioctahedral)

Its chemical composition is listed in Table 4.2.

Table 4.2. Elemental compositions of volclay in weight.%

Wt.%	SiO_2	Al_2O_3	Fe_2O_3	TiO_2	CaO	MgO	Na_2O	K_2O	MnO	P_2O_5	LOI
Volclay	56.50	18.56	3.56	0.15	1.14	2.26	1.88	0.52	0.01	0.04	15.4

The other reactants employed in this study were cetyltrimethylammonium bromide ($C_{19}H_{42}NBr$; CTAB, Aldrich; 99%) as surfactant, and Ammonium hydroxide, 25% (NH_3, 99.99%, Aldrich) and acetic acid min. 99,8% Aldrich.

4.2.2 Synthesis of Al-MCM-41

The Al-MCM-41 was synthesized by using supernatant-2 derived from residual-1. Residual-1 was obtained by the fusion process at 550 °C for 1 h. Volclay was treated with sodium hydroxide in a ratio of 1 : 1.2, volclay: NaOH and heated at 550 °C, to obtain a fusion mass which was cooled at room temperature overnight. The powder fusion samples were mixed with water (1: 4, fusion mass: H_2O; weight ratio) and stirred for 1 day at room temperature. After centrifugation of the mixture for 10 min**,** two different phases were obtained: A solution phase which is called supernatant-1 and a sediment phase which is called residual-1; a second water treatment of the residual-1 is applied to extract silica and aluminium by using the same condition like the mass ratio between water and residual-1, stirring time, and centrifugation

velocity. The liquid solution obtained from the second water treatment is called supernatant-2 its elemental composition is given in Table 4.3.

Table 4.3. Elemental compositions of supernatant-1 (sup-1) and supernatant-2 (sup-2) by ICP-OES

Elements	Sup-1 mg/l	Sup-2 mg/l	sup-1 mmol/l	sup-2 mmol/l	sup-1 mol/l*	sup-2 mol/l*	Reduction %
Si	881.9	278.9	31.4	9.9	139.6	44.1	68
Al	64.6	0.9	2.4	<0.1	10.6	0.1	99
K	28.4	5.4	0.7	0.2	3.2	0.6	81
Fe	2.2	0.6	<0.1	<0.1	0.2	<0.1	~70
Na	4758.1	1864.1	206.9	81.1	919.8	360.4	61

* The values were calculated referring to this dilution: 1ml of supernatant+13.985 ml water+15 µl nitric acid

According to this ICP-OES data of supernatant-2, the synthesis procedure of Al-MCM-41 from supernatant-2 was modified and given as follows. 2.73 g $C_{19}H_{42}NBr$, 16 ml of water and 0.80 g NH_4OH aq were mixed with 120 ml of supernatant-2 and the pH was fixed at 9.5 by the addition of acid acetic. The hydrogel was treated at 100 °C in glass tube instead of autoclave for 48 h. The material obtained was calcined at 550 °C (heating rate of 2 K/min) for up to 6 h under N_2-gas to remove the surfactant ($C_{19}H_{42}N^+$) from the pores of Al-MCM-41.

4.2.3 Characterization

Inductively Coupled Plasma Optical Emission spectrometer (ICP-OES) was used to determine elemental composition in both supernatant solutions. Formation and structure of Al-MCM-41 was checked by XRD. Diffraction patterns were recorded in the 2θ range of 1-70° with a step of 0.02 °2θ and a step time of 5 s on a Bruker D5000 diffractometer with CuKα (λ= 1.5406Å) radiation (40kV, 40mA). Talc/vermiculite mixture was added as internal standard. N_2-gas sorption measurements were performed at 77 K with a Quantachrome Autosorb1 MP. The samples were degassed at 383 K in vacuum for 24 h before measurements. Specific surface areas were calculated by using the BET method (Brunauer et al., 1938). The pore size distribution curves were calculated using the NLDFT equilibrium model with cylindrical pore shape based on the DFT/Monte Carlo method (Lowell et al., 2004). Pore volumes were obtained from the amount of N_2 adsorbed at $p/p_o = 0.7$ corresponding to a pore width of 7.1 nm in order to exclude inter-particle pores formed by the powder particles. Possible differences in particle morphology and of the grain size distribution stemming from the different production processes was carried out by an environmental scanning electron

microscopy (ESEM) using a Philips ESEM XL 30 FEG. This kind of SEM uses a chamber atmosphere of 1-3 Torr water vapour instead of high vacuum.

4.3 Results and discussion

4.3.1 Inductively coupled plasma optical emission spectrometer (ICP-OES)

The results of the ICP-OES analysis of both supernatants are shown in Table 4.3. Differences were found for supernatant-1 and supernatant-2. While the supernatant-1 gave significant proportions of its different constituents, reduced amounts of the same elements are found in supernatant-2 where this reduction reached 61% for sodium, 69% for silicon and a strong reduction was noted to aluminium 99%. Nevertheless these amounts are still sufficient to synthesise Al-MCM-41 nanomaterials.

4.3.2 X-ray diffraction

Figure.4.1 summarizes the XRD patterns of volclay, fused-Na-volclay at 550 °C and residual-1.

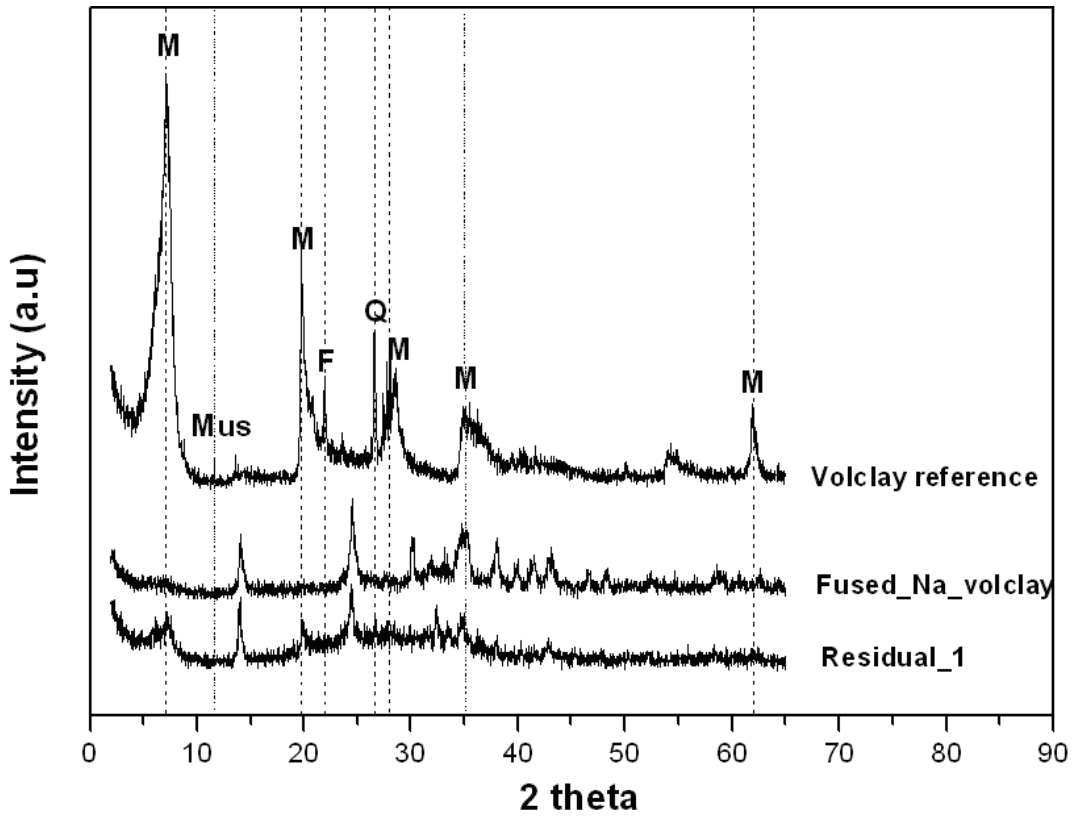

Fig.4.1. XRD patterns of volclay as reference, fused-Na-volclay (1:1.2 volclay: NaOH) and residual-1; (M) montmorillonite, (F) feldspars, (Q) quartz and (Mus) muscovite

The major mineral phases deduced from XRD in volclay are montmorillonite, quartz and muscovite. Disappearance of the peaks that characterize montmorillonite, muscovite and quartz confirm that the alkaline fusion of volclay dissolved all of these species and resulted in the precipitation of a sodium silicate (Fig.4.1) and led to deduce that the fusion process by intermediary of sodium hydroxide generate new phases called sodium silicate (Na_2SiO_2) and sodium aluminate equation 1 and 2 respectively. The chemical equation describing this process is:

$2NaOH + SiO_2 \longrightarrow Na_2SiO_3 + H_2O$ Eq. 1

$2NaOH + Al(OH)_3 \longrightarrow Al(OH)_4^- + Na^+$ Eq. 2

The disappear of all mineral phases of volclay indicates that the fusion results in structural disturbances through the breaking of unstable bonds. Adams., (1987) found that the heating of the montmorillonite with small monovalent cations much above 100 °C leads to decrease in the interlayer spacing (collapse of the clay layers). These observations were also reported by our previous work (2009). The XRD pattern of calcined samples of the MCM-41 synthesized by using supernatant-1 and supernatant-2 (Fig.4.2) allowed identification of the peaks representing the (100), (110), (200) and (210) planes corresponding to an hexagonal structure with symmetry P6mm space group, which are typical of a MCM-41 product. The value of the unit cell parameter a_o of the hexagonal pore arrangement for sample synthesized from the supernatant-1 is higher with 4.50 nm than that found for the supernatant-2 with 4.41 nm. Usually this difference is attributed to the decrease in the pore size and/or in the wall thickness of the nanostructure by polymerization of the silica and/or aluminium. Referring to the results obtained from N_2-gas sorption and XRD; this difference is due to both pore diameter and wall thickness. The wall thickness in both samples synthesized from supernatant-1 and 2 present a slight difference, when the pore size Dp is calculated by using equation 3:

$$Dp=1.213*d_{100}*(2.2*V_{meso}/(1+2.2*V_{meso}))^{1/2} \quad \text{Eq. 3}$$

Where V_{meso} is the mesopore volume (taken at a relative pressure p/po equal to 0.7) and d_{100} the interplanar space of the (100) plane. However this difference becomes consistence when the pore size Dp is calculated by using DFT/Monte Carlo method. Kruk et al., (1997) found that the pore diameters estimated on the basis of theoretical and experimental predictions (nonlocal density functional theory) (W_{DFT}), primary mesopore volume and surface area ($W_{4V/S}$), geometrical considerations (W_d), and BJH method follow this order: $W_{DFT} > W_d > W_{4V/S} > W_{BJH\ des} > W_{BJH\ ads}$.

Although, the values of wall thickness calculated by using NLDFT approach were found to be less as compared to BJH model or to geometric relation.

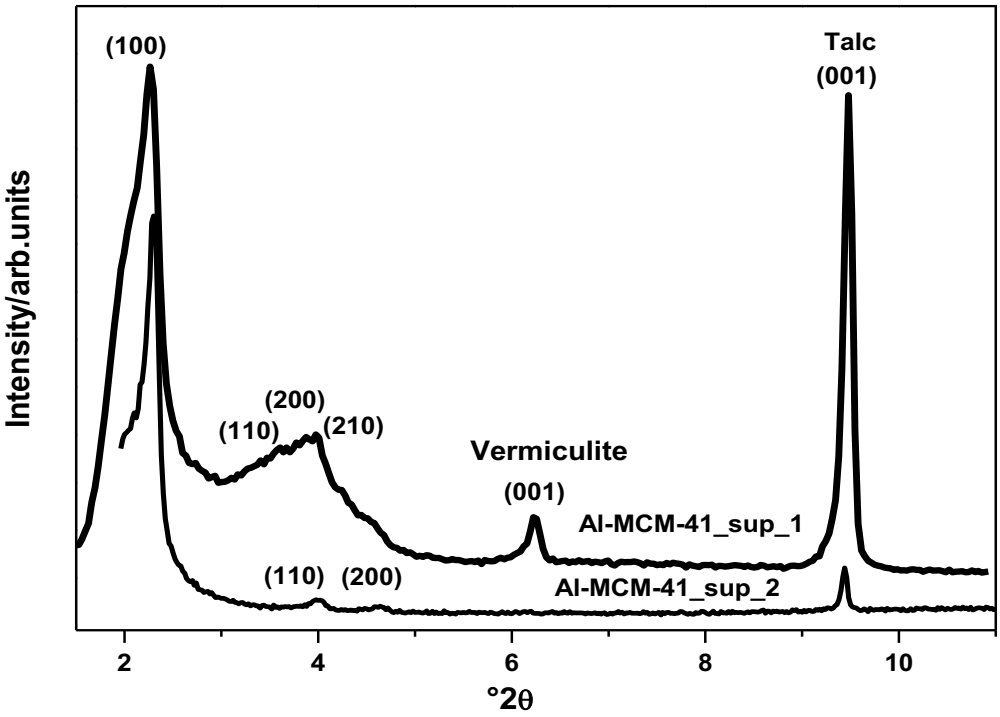

Fig.4.2. XRD pattern of Al-MCM-41 synthesized from supernatant-1 and 2, talc/vermiculite mixture was applied as internal standard for peak position correction

This result can be explained by the decreased of sodium amount in supernatant-2 of around 61% which favours an increase in the polymerized Si-fraction (Table 4.3). Unlike many authors who worked with the same technique of the fusion process to synthesise zeolites, found that a high concentration of Na-ions in the precursor solutions favours the formation of zeolites and hinders the formation of the Al-MCM-41 structure (Shigemoto et al., 1992). This study found firstly that the amount of sodium in both supernatant-1 and supernatant-2 is not critical and exhibited no effect on the synthesis of MCM-41 nanomaterials, and secondly the adjustment of pH value of solution by acid to 9.5 mixture solution after the addition of surfactant is very important for the formation of uniform mesopores, otherwise, the formation of the ordered mesoporous structure would be affected. The acid treatment shifts the polymerization/depolymerization equilibrium of the silicate species to a higher degree of condensation. It helps to close the silica-wall around the micelle and to strengthen it by the formation of covalent Si–O–Si bonds (Luechinger et al., 2003). In the case, when acid is added to a mixture solution without surfactant, the pH value of system will reduce and subsequently influence the interaction between cationic surfactant and anionic silicate species in the mixture, leading to the poor polymerization of inorganic silicate species.

4.3.3 Nitrogen adsorption studies

The N_2 sorption isotherms for the calcined MCM-41 samples synthesized at 100 °C are shown in Fig.4.3. The isotherms are of type IV according to the classification of IUPAC (Sing et al., 1985).

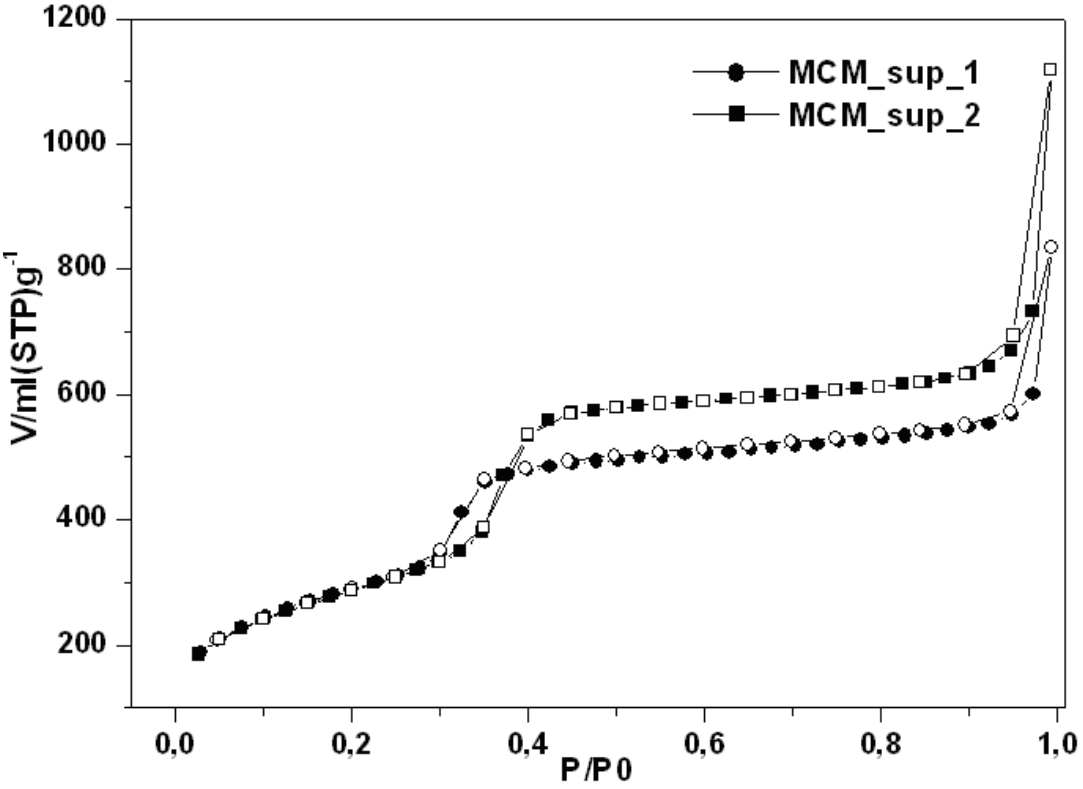

Fig.4.3. N_2 adsorption-desorption isotherm of MCM-sup-1 (●) and MCM-sup-2 (■). Full symbols adsorption, open symbols desorption

The capillary condensation step of the sample obtained from supernatant-1 and supernatant-2 lie in the interval between 0.3 and 0.4 p/p_o. The sharpness in this step indicates a large uniformity of the mesopore size distribution. (Fig.4.4).

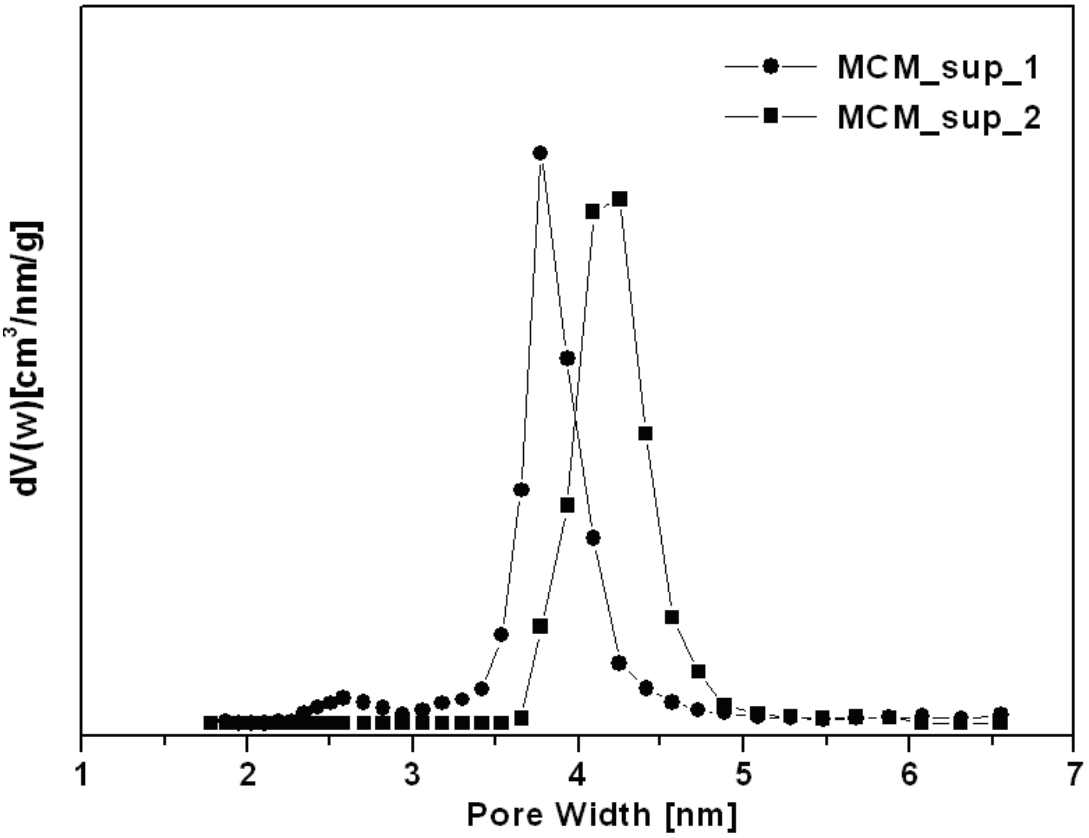

Fig.4.4. Pore size distributions of MCM-sup-1 and MCM-sup-2 derived from N_2-adsorption isotherms calculated by DFT/Monte-Carlo method

The specific surface area of the calcined MCM-41 sample from supernatant-2 is 1044 m^2/g. For the sample obtained from supernatant-2 pore size Dp of 3.67 nm is calculated by equation 1 inserting a value for V_{meso} taken at a relative pressure equal to 0.7. Pore size determined by DFT/Monte Carlo method is 4.2 nm. (Table 4.4).

Table 4.4. Structural properties of the samples

Sample	a_0 (nm)	d_{100} (nm)	S_{BET} (m^2/g)	V_{meso} (cm^3/g)	D_{DFT} (nm)	D_p (nm)	bp (N_2) (nm)	bp (XRD) (nm)
Al-MCM-41 supernatant-1	4.53	3.89	1060	0.77	3.78	3.85	0.72	0.65
Al-MCM-41 supernatant-2	4.41	3.82	1044	0.77	4.25	3.67	0.16	0.74

a_0: unit cell; S_{BET}: specific surface area; V_{meso}: mesoporous volume; D_{DFT} : DFT Method Pore Size Distribution; Dp: Pore Size Distribution calculated at 0.7 p/p_0 by this equation : $Dp=1.213*d_{100}*(2.2*V_{meso}/(1+2.2*V_{meso}))^{1/2}$; bp: wall thickness

4.3.4 Environmental scanning electron microscopy

The SEM images of the particle morphologies of the Al-MCM-41 samples synthesized from the laboratory reagents Ludox as silicon source and sodium aluminate as aluminium source (a and b), from supernatant-2 (c and d) and supernatant-1 (e and f) are shown in Figure.4.5.

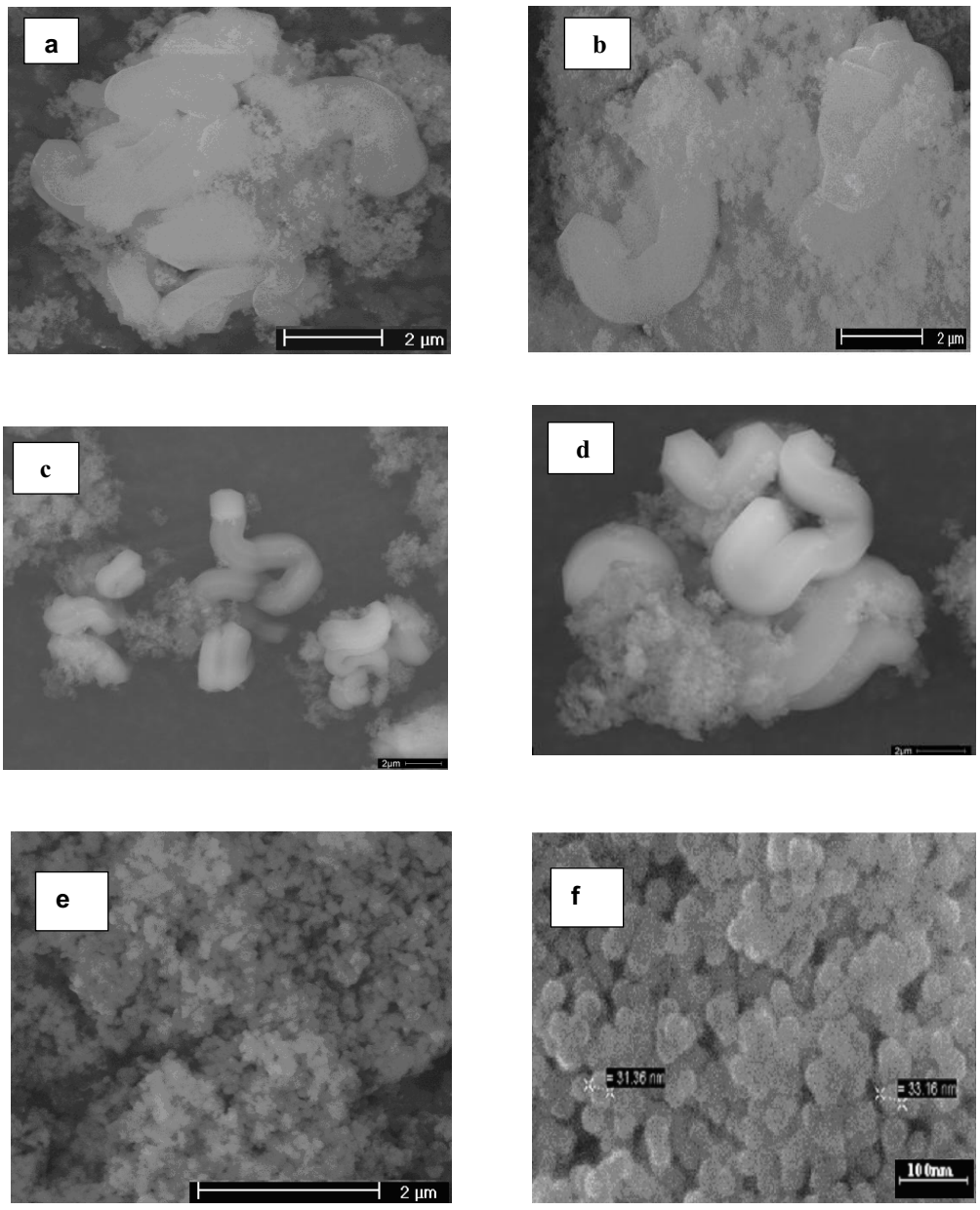

Fig.4.5. ESEM of Al-MCM-41 sample synthesised from laboratory reagents (a,b), supernatant-2 (c,d) and supernatant-1 (e, f)

It was found that the Al-MCM-41 tubes obtained from laboratory grade reagents are conserved in the morphology of Al-MCM-41 from supernatant-2; the acid treatment favours the formation of covalent Si–O–Si bonds within and between the silica walls of the mesostructure during both synthesis and calcination. This strengthening of the silica walls leads to the observed improvement in the long-range ordering and hydrothermal stability (Luechinger et al., 2003). In contrast, no tubes are found in the sample derived from supernatant-1. The major difference between these three samples is the Si/Al ratio. The first two samples show a high ratio of around 50 for the lab grade reagents and 300 for supernatant-2 processed samples, whereas samples synthesised from supernatant-1 exhibit a Si/Al-ratio of 15. This indicates a strong influence of aluminium content on morphology. Aluminium seems to block the Si polymerization sites, thus leading to a reduced growth in all dimensions. This finding is supported by the low values of the line width of the (100) peak ca. 0.128 compared to supernatant-1 ca. 0.408 favouring a tube like arrangement of the meso-porous channels for samples with a low Al-content as present in supernatant-2. Nevertheless the co-existence of some aggregations of spherical particles is shown in all samples.

4.4 Conclusion

The second water treatment is adequate to extract silica and aluminium from residual-1 without any additional fusion process. The originally fused clay, however, can be used more than one time. The physical proprieties of the new Al-MCM-41, such as pore diameter, pore volume, wall thickness and S_{BET} are similar to the Al-MCM-41 produced from the fused material. It can be concluded that the alkaline fusion of a clay in general and volclay in particular, is the key to replace laboratory grade reagents in the synthesis of most nanomaterials not only MCM-41 and therefore their production cost can be strongly reduced.

Chapter 5.

The synthesis of MCM-41 nanomaterial from Algerian Bentonite: the effect of the mineral phase contents of clay on the structure properties

5.1 Introduction

The mesoporous molecular sieves collectively known as M41S, a fascinating class of solids contain uniform one-dimensional channels 2 – 10 nm in diameter (Beck et al., 1992; Kresge et al., 1992 and Behrens 1993) and a highly specific surface area of up to 1000 m^2/g. These materials, of which MCM-41 is the best studied member, are prepared using aggregates of a surfactant to serve as the template, instead of single organic molecules as with the conventional sieves. Many attempts for preparation are focused on the use of a natural source instead of the laboratory reagents. Singer et al., (1995) proposed to convert the coal fly ash by hydrothermal activation methods to zeolites using alkaline solutions (mainly NaOH and KOH solution) which are analogue to the formation of natural zeolites from volcanic deposits. In 1999, Chang et al., have studied the conversion of the coal fly ash to a mesoporous materials aluminosilicate in the hexagonal phase type MCM-41 with a very important incorporation of aluminium (Si/Al = 13.4). Kumar and coworkers (2001) synthesized MCM-41 and SBA-15 with a specific surface area of 842 m^2/g and 483 m^2/g respectively from coal fly ash using the fusion method. Wakihara et al., (2004) introduced for the first time an alkaline fusion to synthesis the conventional zeolites similar to chabazite or mordenite. This method improved the conversion rate of aluminium-silicate phases and resulted in very interesting types of zeolites. Kang et al., (2005) reported the synthesis of Al-MCM-41 by using water glass (or silicate sodium) as Si source and metakaolin as only Al sources. Recently in our previous work 2009, we have synthesized an Al-MCM-41 by using volclay as aluminosilicate source with a high specific surface area about ca. 1060 m^2/g. In this study, we report the effect of the mineral phase contents of Algerian bentonite on the physical properties of MCM-41 compared with the MCM-14 synthesized from volclay.

The synthesis of Al-MCM-41 from a natural Algerian bentonite as silica and aluminium source use CTABr as template.

5.2 Experimental

5.2.1 Starting materials

The natural bentonite used in this study was extracted from Maghnia mine (Hammam Boughrara, 600 km west of the capital Algiers); its chemical composition is listed in Table 5.1.

Table 5.1. Chemical composition of volclay and Algerian bentonite

Wt.%	SiO_2	Al_2O_3	Fe_2O_3	TiO_2	CaO	MgO	Na_2O	K_2O	LOI
Volclay	56.5	18.6	3.6	0.1	1.1	2.3	1.8	0.5	15.4
Algerian bentonite	60.5	18.6	2.3	0.1	1.0	3.8	1.2	0.9	12.1

The main components of bentonite sample are silicon and aluminium, with fewer amounts of other elements including Fe, Ca, and Na.

5.2.2 Synthesis of Al-MCM-41

For the synthesis of mesoporous material, we adopt the alkaline fusion which consist on the extraction of the Si and Al species by mixing the Algerian bentonite with sodium hydroxide powder in a weight ratio of bentonite to NaOH of 1: 1.2 and heated at 823 K for 1 h in air. The fused mass obtained is cooled to room temperature and milled overnight. The fused bentonite was then mixed with water in a weight ratio of 1: 4 and stirred for 1 day at room temperature. The resultant suspension was separated by centrifugation to obtain the supernatant. In a typical MCM-41, 0.867 g of hexadecyltrimethylammonium bromide (C_{16}TMABr), 15 ml water and 0.75 g aq. NH_4OH were combined with 40 ml of the supernatant and stirred at room temperature during 1 h at pH 9.5. The crystallization procedure was done at a temperature of 373 K. The powder samples were washed, dried and heat-treated to 823 K for up to 8 h with a heat rate of 2 °C/min.

5.2.3 Characterization

Powder X-ray diffraction (XRD) patterns were carried using a Bruker AXS diffractometer using CuKα (wavelength = 0.15404 nm) radiation, with scanning step 0.035 °2θ between 2° and 80 °2θ. The chemical composition were analysed by X-ray fluorescence (XRF) (Philips PW2400). The approximate crystallite sizes of the sample were calculated using the Debye–Scherrer equation based on (100) diffraction peak (°2θ ≈ 2°-3°). The IR spectra were measured using a Bruker Equinox55 with a resolution of 4 cm^{-1} and KBr pillets. The structure, size morphology and local chemical composition of the mesoporous

aluminosilicates were examined by analytical transmission electron microscopy (TEM) attached with an EDXS (energy dispersive analysis by X-ray spectroscopy) using a Philips CM20. N_2 and water vapour adsorption-desorption isotherms were obtained an automatic adsorbometre conceived and realized in LEM-GRESD. For the N_2 adsorption-desorption the sample was outgassed at 473 K over 24 h prior to adsorption. The specific surface area was determined by the BET (Brunauer et al., 1938) formula from data in the relative pressure range from 0.04 to 0.2.

5.3 Results and discussion

5.3.1 X-ray diffraction and chemical composition

Fig.5.1 summarizes the XRD patterns of the bentonite (a) and the fused bentonite (b) at 823 K. The major mineralogical compositions deduced from XRD that exist in bentonite are montmorillonite, quartz and muscovite. (Fig.5.1a).

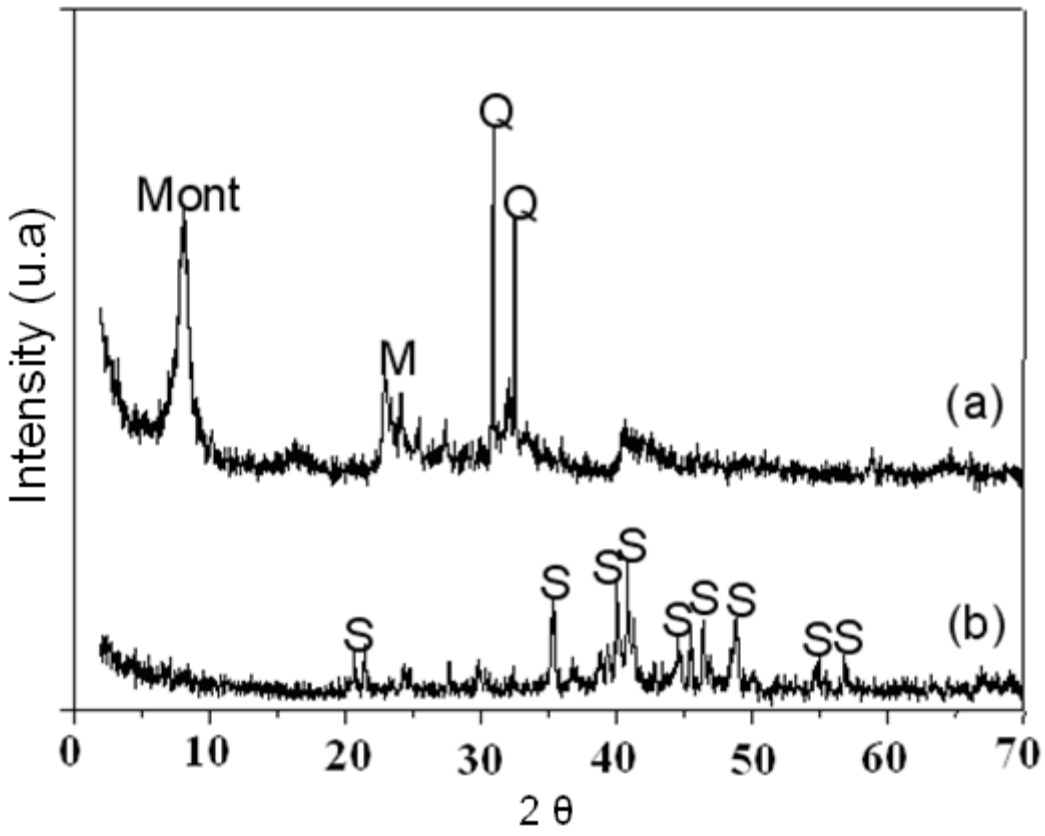

Fig.5.1. XRD patterns of the bentonite (a) and the fused bentonite (b) at 823 K. Mont: montmorillonite, M: muscovite, Q: quartz and S: sodium silicate

Disappearance of the peaks that characterize montmorillonite, muscovite and quartz confirm that the alkaline fusion of bentonite dissolves the totality of this species to a large amount of sodium silicate (Fig.5.1b) and led to deduce that the fusion process by intermediary of sodium hydroxide generate new phases called s sodium silicate (Na_2SiO_2) and sodium aluminate equation 1 and 2 respectively. The chemical equation describing this process is:

$2NaOH + SiO_2 \longrightarrow Na_2SiO_3 + H_2O$ Eq. 1

$2NaOH + Al(OH)_3 \longrightarrow Al(OH)_4^- + Na^+$ Eq. 2

In the case of muscovite, the breakdown of the muscovite under alkaline condition at low temperature led to other clay minerals like as kaolinite and illite, the latter underwent the same effect (i, e) the decomposition of their structures to obtain sodium silicate because they are still always under alkaline fusion and high temperature and in the other hand the amount of the muscovite in the bentonite is ranged between 3 ± 1 wt.%.

Disappearance of all mineral phases of Algerian bentonite indicates that the fusion causes collapse of the structure which results in structural disturbances through the breaking of unstable bonds. Adams (1987) found that the heating of the montmorillonite with small monovalent cations much above 100 °C leads to a decrease of the interlayer spacing (collapse of the clay layers). These observations were also reported by our previous work (2009). The powder X-ray diffraction patterns of as-synthesized and calcined Al-MCM-41 samples are illustrated in Fig.5.2.

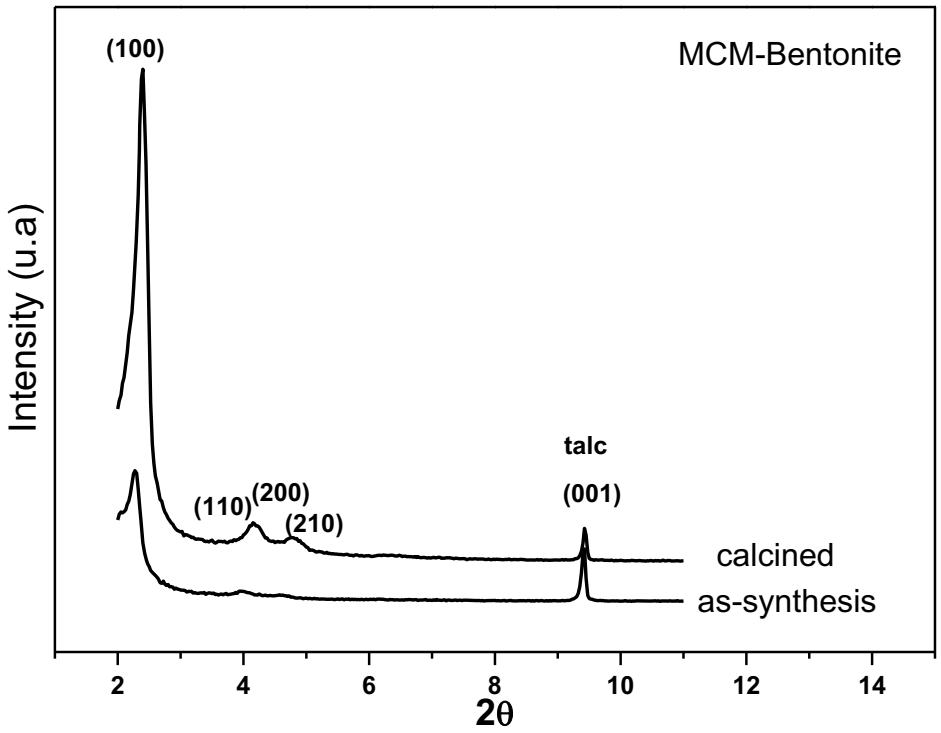

Fig.5.2. XRD patterns of the as-synthesis and calcined MCM-bentonite samples, talc was applied as internal standard for peak position correction

According to the large °2θ range scanned (°2θ =10-40°), no characteristic peaks of amorphous silicon phase and impurities like quartz and cristobalite, which are usually present in the naturally occurring clay were observed. Therefore, major amounts of silicon and aluminium extracted from the Algerian bentonite was consumed to produce Al-MCM-41. The characteristic Bragg Peak (100) was observed in the low-angle X-ray patterns, which is characteristic for a hexagonal pore structure typical of Al-MCM-41 (Wang et al., 1999). Moreover, more appreciable characteristic Bragg peaks (110), (200) and (210) were observed which flag a better structuring of the hexagonal channels of Al-MCM-41 (Beck et al., 1992).

A high Na^+ ion concentration in the precursor solution, which is constituted of silicon and aluminium extracted from volclay by alkaline fusion, is known to favour the formation of zeolites and hinder the formation of MCM-bentonite phase (Shigemoto et al., 1993). The adjustment of the pH during the synthesis is important due the high concentration of Na^+ ions present in the supernatant of fused bentonite. It is also observed that the value of synthesis pH influences strongly the quality of the obtained MCM-bentonite. This observation is in agreement with that found by Luechinger et al., (2003). The Bragg peaks (100), (110) and (200) of the resultant sample MCM-bentonite calcined becomes stronger after calcinations at 550 °C than the ones obtained from as-synthesis one , showing that the ordering of the sample was enhanced. The unit cell of calcined material decreases from 4.50 to 4.40 nm compared to the one of the as-synthesis one. This phenomenon was caused by the removal of the surfactant from the channels, and by condensation of silanol groups on the walls.

The powder XRD patterns of the samples synthesised from volclay and bentonite calcined are depicted in Fig.5.3. The XRD pattern of Al-MCM-41calcined sample from bentonite consists of one very strong peak and three weak peaks corresponding to (100) at 2.3 °2θ, (110), (200) and (210) at 2θ values ranging from 3 to 6° , where that one from volclay exhibits the same peaks (100), (110), (200) and (210). Referring to the XRD of both samples, it is deduced that the sample synthesized from Algerian bentonite presents a better crystallinity compared to that one from volclay. This can be attributed to the aluminium content in the MCM-volclay framework Si/Al ca. 17 and in MCM-bentonite Si/Al ca. 44, Adjdir et al., (2009) found that when the aluminium content into silicate framework increase the crystallinity of this sample decreases. In the other hand the chemical composition of bentonite contains less amount of aluminium compared to volclay, consequently the extraction of aluminium from Algerian bentonite could be less and hence the aluminium content is less.

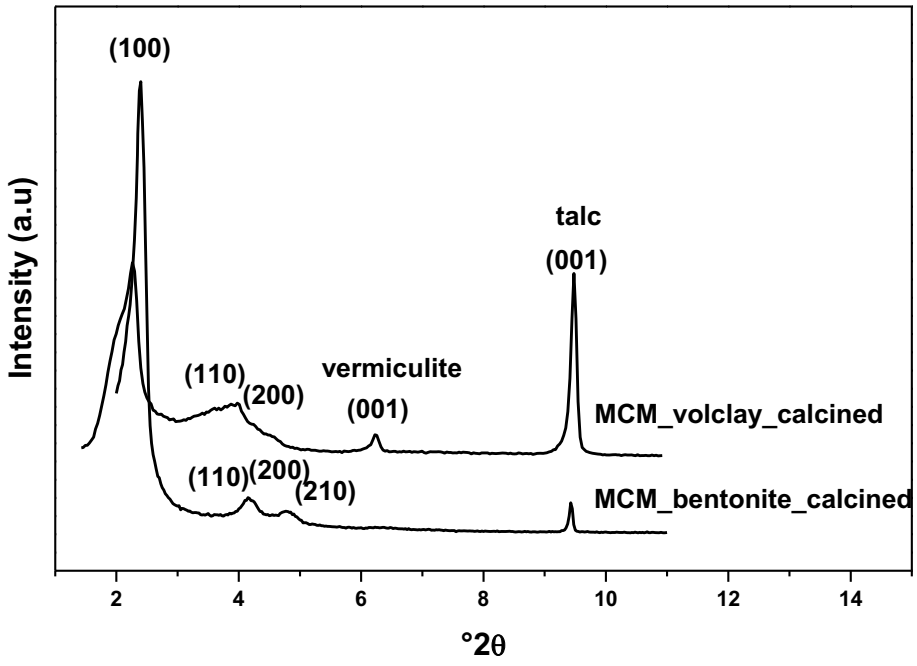

Fig.5.3. XRD patterns of MCM-volclay-calcined and MCM-bentonite-calcined, talc/muscovite mixture was applied as internal standard for peak position

This approach is confirmed by the FWHM (Full Width at Half Maximum) of both samples, in the case of MCM-bentonite, the FWHM has a value of 0.295°, the FWHM of MCM-41 volclay however is 0.416°. The fusion is a decomposition of crystals to a disordered structure. This change is followed by collapse of the structure and formation of sodium silicate instead. According to Taylor (1962), in the absence of salts, the dehydroxylation of clays involves the migration of protons from inside the structure to surfaces or boundaries and their combination with OH groups present in these regions to form water. The reaction is facilitated by the volatilization of the water. In this process the clay structure loses one positively and one negatively charged species, hence, no charge imbalance is produced. Only some vacant OH sites are produced. Natale and Helmy (1992) found that dehydroxylation is different from the reaction that was apparently operative in the presence of NaOH; here, protons migrated and volatile products formed. In this reaction structural hydroxyls were not lost; hence, a charge imbalance and a diffusion potential were created, which forced the movement of sodium ions into the crystal along the electric potential created by the movement of the protons in the opposite direction. Because of its size (much greater than a proton) and its 8- to 10-fold coordination with oxygen in silicates, the movement of sodium into the clay structure at fusion temperature requires drastic changes in the oxygen packing. The presence of sodium,

therefore, produces a distortion of the clay structure and the loss of the crystallographic properties of the clay, namely, the production of a disordered structure and the disappearance of the XRD pattern of the mineral phases.

5.3.2 Nitrogen adsorption studies

Fig.5.4. shows the N_2 adsorption/desorption isotherm for Al-MCM-41 from Algerian bentonite and Table 5.2 summarizes the textural proprieties of this sample.

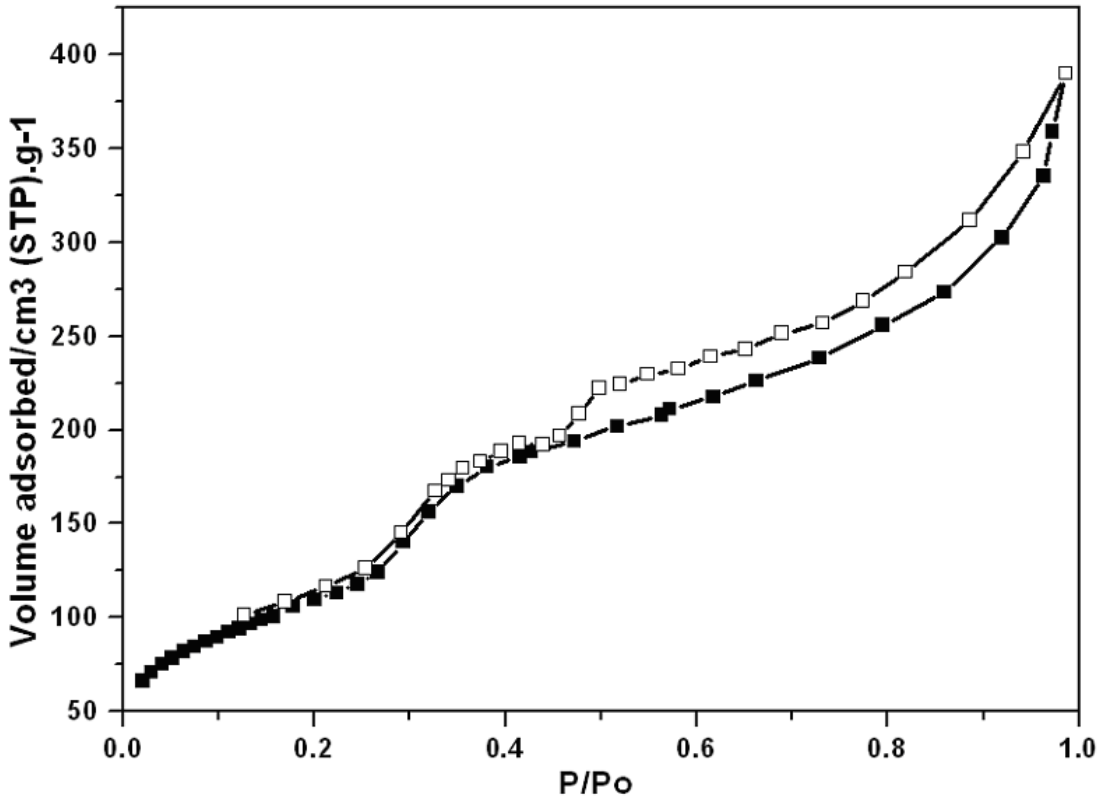

Fig.5.4. N_2-adsorption-desorption isotherm of Al-MCM-41 from bentonite calcined standard method (■) adsorption branch, (□) desorption branch

Table 5.2. Structural characteristics of the calcined Al-MCM-41

sample	d_{100} (nm)	a_0 (nm)	FWHM °2θ	$Dp_{(XRD)}$ (nm)	S_{BET} (m^2/g)	V_{meso} (m^2/g)	bp (nm)
MCM-volclay	3.89	4.53	0.295	3.85	1060	0.77	0.68
MCM-bentonite	3.65	4.40	0.416	3.80	464	0.72	0.60

Lattice parameter from XRD using the formula, $a_o = 2/(3)^{1/} * d_{100}$. Determined by a geometrical method (Kruk *et al.,* 1997 and Dabadie *et al.,* 1996) by supposing that the MCM-41 exhibits a hexagonal arrangement of cylindrical pores; FWHM: full width at half maximum. The pore diameter is given by: DpXRD = C*d_{100}* [ρ *Vp/(1+ ρ *Vp)]1/2. Where Vp is pore volume, ρ is density of the pores walls 2.2 $cm^3.g^{-1}$for silica materials (Dabadie *et al.,* 1996 and Iler, 1979), d_{100} is interplanar spacing and C is a constant depending on the pore geometry (*C = 1.213* for a geometry cylindrical (*Beck et al.*, 1992).. bp is pore wall thikness, a_o-D_{DRX}.

The obtained isotherm is typical for Al-MCM-41 phase. The corresponding isotherm is of type IV, characteristic of the mesoporous solids according to the IUPAC nomenclature (Sing et al., 1985). The type IV isotherm is defined by three stages: at low relative pressures, a slow increase of nitrogen corresponding to monolayer-multilayer adsorption on the pore walls. At intermediate relative pressures, a sharp step indicative of capillary condensation within mesopores. In the last stage, at high relative pressures, a final plate with a slight inclination associated with multilayer adsorption on external surface of the particles. The isotherm presents the sharp capillary condensation step at p/p_o 0.3, typical of a uniform mesoporous material with a pore size at around 3.8 nm. The specific surface area of Al-MCM-41 was ca. 464 m^2/g with a pore volume of 0.72 cm^3/g calculated at 0.42 p/p_0. This p/p_0 value was chosen to eliminate the adsorbate volume which can occur between the platy particles (Table 5.2).

The lower specific surface area obtained is probably due to particle size. The particle size of MCM-volclay is ca. 19.8 nm, whereas the particle size of MCM-bentonite is 28 nm calculated by Debye-Scherrer equation. The similar result was found by Kumar et al., and in our previous work Adjdir et al., (2009).

The wall thickness in the case of MCM-volclay is around (0.80 nm) and higher than that found for MCM-bentonite (ca. 0.60 nm). This can be explain by the incorporation of aluminium species (Hui et al., 2006) where the Si/Al ratio of MCM-volclay is much higher than of MCM-bentonite, and by the length bond of Si-O (158 pm) is weaker than of Al-O (183.6 pm) in MCM-41.

5.3.3 FT-IR analysis

The FT-IR spectra of Al-MCM-41 (Fig.5.5,Table 5.3) exhibited bands in the region between 950 and 1200 cm^{-1} which could be assigned to antisymmetric stretching of ≡Si−O−T≡ (T ═ Si or Al) bonds. Bands in the 600-800 cm^{-1} region will involve the corresponding symmetric vibrations. The absorption band at 465 cm^{-1} corresponds to bending vibration of ≡T−O− (T ═ Si or Al). The as-synthesis sample exhibits additional bands below 3000 cm^{-1} which could be attributed to alkaline stretching adsorption of the surfactant, these bands are disappeared from the calcined sample which gives the prove that the calcinations removed the surfactant from the pores. All these features are typical of aluminosilicate of MCM-41 structure Bernard et al., (1985).

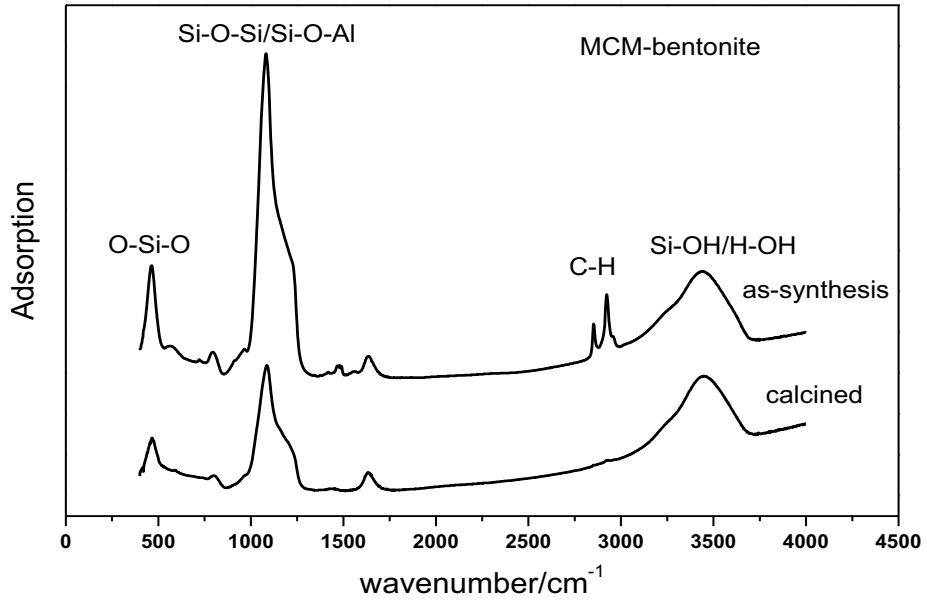

Fig.5.5. FT-IR spectra of Al-MCM-41 calcined and as-synthesized from bentonite

Table 5.3. IR band positions of the Al-MCM-41

Sample	O-Si-O Bending	Si-O-Si sym-stretch	Si-O-Si/Si-O-Al Anti-sym stretching				n-C-H and d-C-H (surfactant) As-syn		Si-OH and H_2O groups
	cm^{-1}	cm^{-1}	cm^{-1}	cm^{-1}	cm^{-1}	cm^{-1}	cm^{-1}	cm^{-1}	cm^{-1}
MCM-bent-as-sy	465.5	810.3	1048.1	1093.0	1143.1	1216.4	2921	2851	3500
MCM-bent-cal	465.5	810.3	1048.1	1093.0	1143.1	1216.4			3500

In addition MCM-bentonite calcined was studied by transmission microscopy (TEM). After the heat treatment at 550 °C of Algerian bentonite with sodium hydroxide, the microstructural as well as the compositional uniformity is lost when compared to the untreated Algerian bentonite. (Fig.5.6.a).

5.3.4 Transmission electron microscopy

The EDXS analysis for the crystalline phase of MCM-bentonite-cal and its amorphous phase led to a Si/Al ratio of 50 and 12.4 respectively. These values confirm the incorporation of the aluminium in the wall of MCM-41 which led to small wall thickness compared to MCM-volclay whereas the amorphous phase did not reacted to produce an MCM-41. This result also confirms that only a part of aluminium was reacted to produce an MCM-41.

The transmission electron microscopy of the Al-MCM-41 synthesized from bentonite is presented in Fig.5.6.b. This image confirms that the material has uniform pore system and clear hexagonal patterns of the pores or honeycomb-like structure. This result is well correlated with the XRD, and by the electronic diffraction the unit cell of Al-MCM-41 is well defined. The value of the unit cell is equal to 4.2 nm and agrees nicely with the one obtained by XRD with 4.4 nm.

Selected area electron diffraction pattern (SAED) in Fig.5.6.b inset showing a high symmetry along the two possible orientations of p6mm plan group obtained for the sample, proving the hexagonal arrangement of the nanomaterials pores.

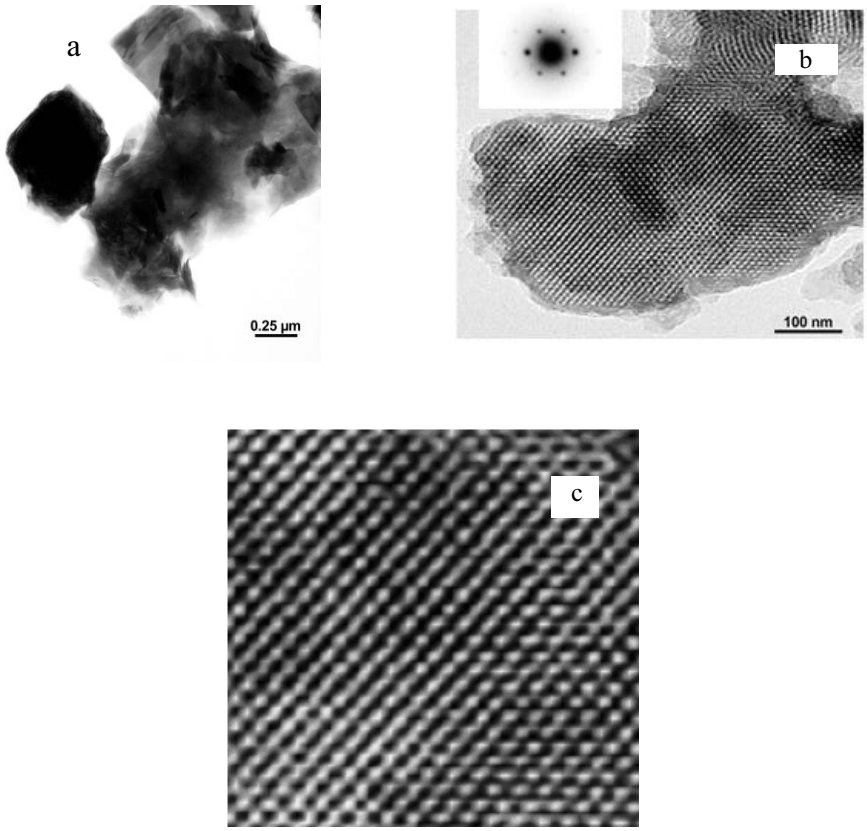

Fig.5.6. TEM- images of bentonite-fused (a). Images of MCM-bentonite calcined (b) and selected area electron diffraction patterns is shown as inset in (b).Images of MCM-bentonite calcined (c) with 200% magnification of image (b)

5.4 Conclusion

In conclusion, it is shown that the Algerian Bentonite can be used as an aluminosilicate source for the synthesis of Al-MCM-41. The mineral phase content of both clays used can inflect the aluminium content of the final product.

A solid with a symmetrical hexagonal pore structure typical of Al-MCM-41 was observed for the sample synthesized from Algerian bentonite at pH = 9.5. The adjustment of the pH of the mixture after addition of the all reagents decreased the Na^+ ion concentration in the solution and therefore increased the reactivity of the silicon and aluminium to obtain the final MCM product.

The N_2-sorption isotherm was of type IV, characteristic of a mesoporous solid. The wall thickness and mesoporous volume of the MCM-41 from Algerian bentonite are typical for materials of MCM-41 type. TEM image confirms that the material has uniform pore system with hexagonal patterns. EDXS revealed that hexagonal phase had a Si/Al ratio of 50 whereas for the amorphous phase a Si/Al ratio of 13.5 was determined. These values are much higher than the Si/Al ratio of 4.7, which was measured for the bentonite. The purely mesoporous aluminosilicate was free from impurities such as Fe, Ca or K.

Summary

The use of the synthetic zeolite and MCM-41 is restricted due to prohibitive production costs. Also the achievement of quality characteristics like high structuring, physical properties, and content of aluminium incorporated by the use of laboratory reagents could become a high priced task and difficult.

The incorporation of aluminium and boron separately in the MCM-41 framework by the use of laboratory reagents affects the crystallinity of the materials and it is shown that the incorporation of aluminium in the MCM-41 framework is limited to $SiO_2/Al_2O_3 = 25$.

This work put forth the hypothesis that the use of natural sources as precursor for the synthesis of nanomaterials, either mesoporous or microporous, is promising and can resolve these problems.

The first chapter of this work is devoted to give the reader a chronological overview on the use of the waste and natural sources such as coal fly and bottom ashes, rice husk and clay as silicon and aluminium precursor by the use a new process called alkaline fusion in the synthesis of nanomaterials.

The results obtained are very promising, the natural sources, such as volclay; Algerian bentonite and other sources are considerate as an alternatives to be used as silicon and aluminium precursor. The use of the alkaline fusion process reduces the treatment cost (time and temperature) and therefore preserves the environment.

The use of a natural source and specially volclay would reduce the costs of silicon and aluminium source (1 kg of silicon and aluminium from volclay costs around 0.03 € whereas the same amount of silicon from ludox and aluminium from sodium aluminates cost around 350 € without take in consideration the energy cost. However, the second supernatant recoups the energy fee). Therefore, the price of the mesoporous or microporous synthesis from the volclay as silicon and aluminium precursor should be the cheapest one.

The choice of volclay, which is constituted of (Na-rich) smectite 60 wt.%, (Ca-rich) smectite 20 wt.%, quartz 10.5 wt.%, muscovite/illite 3 wt.% and K-feldspar 4 wt%, where quartz, muscovite/illite and K-feldspar are considered as impurities, is based on its high aluminium content and its high availability. In addition, volclay is cheaper than laboratory reagents.

The combination between the alkaline fusion process and the volclay, the amount of the silicon and aluminium extracted is significant to that found by any sources till now (see chapter 1).

Chapter 2 treats the synthesis of mesoporous materials from laboratory reagents and the effect of the substitution of aluminium and boron on the final structure and compare these different results elsewhere in this work.

Isomorphous substitution of boron and aluminium in MCM-41 framework was successfully carried out. The best structure was allocated to Al- and B-MCM-41 for a mass ratio equal to 150. A hexagonal structure characteristic for a mesoporous material produced from laboratory reagents was still obtained for a SiO_2/Al_2O_3 or B_2O_3 ratio of 25. A higher content of Al or B did not further increase the quality of the product and may not result in hexagonal structures.

The use of clay minerals can be considered as an alternative to increase the aluminium content in the mesoporous materials with the preservation of the hexagonal structure. This can be realised by applying the alkaline fusion as new process to extract the silicon and aluminium oligomers from volclay and other clay sources (e.g. an Algerian bentonite). The 3rd chapter discusses the methods used to extract both silicon and aluminium from volclay and to test the effect of the NaOH treatment (pellet, powder or solution). The form of NaOH (pellet or powder) which exhibits a marked difference in pricing didn't play any effect on the fusion process. However, the treatment nature (alkaline fusion treatment or in solution of NaOH) played an important role in the extraction of silicon and aluminium oligomers. The Al-MCM-41 synthesized by the use of volclay under alkaline and mild thermal treatment gave a mesoporous materials called Al-MCM-41-sup-1 with a high specific surface area around 1060 m^2/g, a pore volume of about 0.77 cm^3/g and pore sizes centred at 3.78 nm compared to the Al-MCM-41 synthesized from laboratory reagent (chapter 2). The Si/Al ratio in Al-MCM-41-sup-1 was smaller than that produced by the use of laboratory reagents, Si/Al ratios are 17 and 63 respectively. According to these results, the incorporation of high aluminium amount along with the preservation of the structure is possible only by the use of the natural material and by adopting the alkaline fusion process.

To increase the efficiency of this new synthesis-method, a second water treatment (without any additional fusion process of the residual-1) was tested to extract silica and aluminium. The Al-MCM-41 synthesized from the supernant-2 gave a high physical and structural quality compared to that one produced from laboratory reagents. The incorporation of the aluminium, maintaining the Al-MCM-41structure of the samples, from the first and second supernatant was higher than that found in Al-MCM-41 from laboratory reagent. It can be concluded that the alkaline fusion of a clay in general and volclay in particular is the key to

replace laboratory grade reagents in the synthesis of most nanomaterials not only MCM-41 and therefore their production costs can be strongly reduced.

The alkaline fusion process can be used for different kinds of clay minerals to extract the silicon and aluminium oligomers as confirmed in chapter 5.

Algerian bentonite can be used as an aluminosilicate source for the synthesis of Al-MCM-41. The mineral phase content of this kind of bentonite used can inflect the aluminium content of the final product. A solid with a symmetrical hexagonal pore structure typical of Al-MCM-41 was observed for the sample synthesized from Algerian bentonite.

Zeolite path (Fig.1 flow sheet) was also considered, first results which are very promising showed that the most phases obtained are attributed to the so called NaP zeolite species ($Na_6Al_6Si_{10}O_{32}\cdot 12H_2O$, belonging to the Gismondine series). According to X-ray diffraction, the use of supernatant-1 without the addition of any other reagents gave a pure NaP zeolite.

Future work

As discussed earlier, the demand of mesoporous materials which have physical and structural properties better than that found in zeolite have increased. However, their use in large scale processes is very limited because of their high cost. The natural source can bring the solution. Further studies will be released to elucidate a way to decrease more and more their production costs and to make them available for a wide use. Many scientists have tried to use the waste sources as low cost materials in order to reduce its significant quantity and to make them profitable. Among these wastes which do not have attracted much consideration, we find used glass and used ceramic. These two sources are rich on silicon and aluminium and can be used as precursor for different kind of mesoporous. Another source which is abundant and can be used as silicon is sand. Up to now, no attempt to use these new silicon and aluminium sources has been conducted.

The following suggestions for future work are presented:

1. The alkaline fusion parameters such as temperature, time and the amount of NaOH have to be optimized.
2. Used glass, used ceramic and sand should be tested as silicon and aluminium source.
3. The amount of silicon and aluminium extracted is worthwhile to be increased by optimization of the fused clay and water ratio.
4. The use of supernatant for the synthesis of different zeolites is important to be investigated.

5. The effect of the dilution of the supernatant-1 and 2 to obtain different kind of zeolite should be examined.

6. The possibility to reduce the crystallization time of zeolites from days to hours should be examined.

7. The use of the mesoporous materials produced from clay could be used as drug delivery system, and in combination with surface functionalization employing active silanes, it can be also used for biosensoring devices, molecular transport, reaction nanovessels, and of course due to the high specific area, as catalyst for different applications.

References

Adams, J.M., 1987. Synthetic Organic Chemistry Using Pillared, Cation-Exchanged and -Treated Montmorillonite Catalysts. Applied Clay Science. 2, 309-342.

Adjdir, M., Ali-Dahmane, T., Weidler, P.G., 2010. Short review on mesoporous materials from waste and natural source. In preparation.

Adjdir, M., Ali-Dahmane, T., Weidler, P.G., 2009. The structural comparison between Al-MCM-41 and B-MCM-41. C. R. Chimie. 12, 793-800.

Adjdir, M., Ali-Dahmane, T., Weidler, P.G., Friedrich, F., Scherer, T., 2009. The synthesis of Al-MCM-41 from volclay — A low-cost Al and Si source. Applied Clay Science. 46, 185–189.

Adjdir, M., Ali-Dahmane, T., Friedrich, F., Scherer, Eckhardt, D., Weidler, P.G., 2009. The synthesis of MCM-41 nanomaterials from volclay II: Increasing process efficiency by iterative water treatment. Applied Clay Science. Submitted.

Ali-Dahmane, T., Adjdir, M., Hamacha, R., Villieras, F., Bengueddach, A., Weidler, P.G., 2010. The synthesis of MCM-41 nanomaterial from Algerian Bentonite: The effect of the mineral phase contents of clay on the structure properties. Applied clay science. Accepted.

Akasaka, H., Yukutake, H., Nagata, Y., Funabiki, T., Mizutani, T., Takagi, H., Fukushima, Y., Juneja, L.R., Nanbu, H., Kitahata, K., 2009. Selective adsorption of biladien-ab-one and zinc biladien-ab-one to mesoporous silica. Microporous and Mesoporous Materials. 120, 331–338.

Angelos, S., Liong, M., Choi, E., Zink, J.I., 2008. Mesoporous silicate materials as substrates for molecular machines and drug delivery. Chemical Engineering Journal. 137, 4–13.

Badamali, S.K., Sakthivel, A., Selvam, P., 2000. Influence of aluminium sources on the synthesis and catalytic activity of mesoporous AlMCM-41 molecular sieves. Catal. Today. 63, 291-295.

Baker, J.M., Dore, J.C., Behrens, P., 1997. Nucleation of ice in confined geometry. J. Phys. Chem. B 101. 6226-6229.

Bai, N., Chi, Y., Zou, Y., Pang, W., 2002. Characterization of GaAs/thiol/electrolyte interface. Mater. Lett. 54, 37– 42.

Bajpai, P.K., Rao, M.S., Gokhale, K.V.G.K., 1981. Synthesis of mordonite type zeolite using silica from rice husk ash. Ind. End. Chem. Prod. Res. Dev. 20, 721–726.

Beck, J.S., Chu, C.T.-W., Johnson, I.D., Kresge, C.T., Leonowicz, M.E., Roth, W.J., Vartuli, J.W., 1991. WO Patent. 91/11390.

Beck, J.S., Vartuli, J.C., Roth, W.J., Leonowicz, M.E., Kresge, C.T., Schmitt, K.D., Chu, C. T.-W., Olson, D.H., Sheppard, E.W., McCullen, S.B., Higgins, J.B., Schlenker, J.L., 1992. A new family of mesoporous molecular sieves prepared with liquid crystal templates. J. Am. Chem. Soc. 114, 10834-10843.

Behrens, P., 1993. Mesoporous Inorganic Solids. Advanced Materials. 5, 127-132.

Benhamou, A., Baudu, M., Derriche, Z., Basly, J.P., 2009. Aqueous heavy metals removal on amine-functionalized Si-MCM-41 and Si-MCM-48. J. Hazard. Mater. 171, 1001-1008

Bhagiyalakshmi, M., Yun, L.J., Anuradha, R., Jang, H.T., 2009. Synthesis of chloropropylamine grafted mesoporous MCM-41, MCM-48 and SBA-15 from rice husk ash: their application to CO_2 chemisorption. J. Porous. Mater. 17, 475-484.

Borade, R.B., Clearfield, A., 1995. Synthesis of aluminum rich MCM-41. Catal. Lett. 31, 267-272.

Bonneviot, L., Kaliaguine, S., 1995. Zeolites. A Refined Tool for Designing Catalytic Sites, (Eds.), Elsevier, Amsterdam. 543.

Branton, P.J., Hall, P.G., Sing, K.S.W., 1993. Physisorption of nitrogen and oxygen by MCM-41, a model mesoporous adsorbent. J. Chem. Soc. Chem. Commun. 1257-1258.

Brunauer, S., Emmett, P.H., Teller, E., 1938. Adsorption of Gases in Multimolecular Layers. J. Am. Chem. Soc. 60, 309-319.

Burke, M., 2007. CCP experts gather in India. In: Ash at work. USA: American Coal Ash Association. 2, 17–19.

Catlow, C.R.A., Bell, R.G., Gale, J.D., and Lewis, D.W., 1995. Modelling of Structure and Reactivity in Zeolites. (Ed,), Academic Press, London. 97, 87-100.

Chandrasekar, G., Ahn, W-S., 2008. Synthesis of cubic mesoporous silica and carbon using fly ash. Journal of Non-Crystalline Solids. 354, 4027–4030.

Chang, H-L., Chun, C-M., Aksay, I.A., Shih, W-H., 1999. Conversion of Fly Ash into Mesoporous Aluminosilicate. Ind. Eng. Chem. Res. 38, 973-977.

Chakraverty, A., Mishra, P., Banerjee, H.D., 1988. Investigation of combustion of raw and acid-leached rice husk for production of pure amorphous white silica. J. Mater. Sci. 23, 21-24.

Chakraverty, A., Banerjee, H.D., Mishra, P., 1990. Production of amorphous silica from rice husk in a vertical furnace. AMA Agric. Mech. Asia Afr. Lat. Am. 21, 69-75.

Chen, C.Y., Li, H-X., Davis, M.E., 1993. Studies on mesoporous materials I. Synthesis and characterization of MCM-41. Micropor. Mater. 2, 17-26.

Cheng, C.F., Park, D.H., Klinowski, J., 1997. Optimal parameters for the synthesis of the mesoporous molecular sieve [Si]-MCM-41. J. Chem. Soc., Faraday Trans. 93, 193-197.

Chevalier, Y., Zemb, T., 1990. The structure of micelles and microemulsions. Rep. Prog. Phys. 53, 279-371.

Chiola, V., Ritsko, J.E., Vanderpool, C.D., 1971. US Patent. 3 556 725.

Chu, C.T.-W., Kuehl, G.H., Lago, R.M., Change, C.D., 1985. Isomorphous substitution in zeolite frameworks : II. Catalytic properties of [B]ZSM-5 J. Catal. 93. 451-458.

Chumee, J., Grisdanurak, N., Neramittagapong, A., Wittayakun, J., 2009. Characterization of platinum–iron catalysts supported on MCM-41 synthesized with rice husk silica and their performance for phenol hydroxylation. Sci. Technol. Adv. Mater. 10, 015006.

Conradt, R., Pimkhaohkam, P., Leela-Adisorn, U., 1992. Nano-structured silica from rice husk. Journal of Non-Crystalline Solids. 145, 75-79.

Corma, A., Kan, Q., Navarro, M.T., Perez-Pariente, J., Rey, F., 1997. Synthesis of MCM-41 with Different Pore Diameters without Addition of Auxiliary Organics. Chem. Mater. 9, 2123-2126.

Dabadie, T., Ayral, A., Guizard, C., Cot, L., Lacan, P., 1996. Synthesis and characterization of inorganic gels in a lyotropic liquid crystal medium. Part 2. —Synthesis of silica gels in lyotropic crystal phases obtained from cationic surfactants. Journal of Materials Chemistry. 6, 1789-1794.

Dai, Z., Fang, M., Bao, J., Wang, H., Lu, T., 2007. An amperometric glucose biosensor constructed by immobilizing glucose oxidase on titanium-containing mesoporous composite material of no. 41 modified screen-printed electrodes. Analytica Chimica Acta. 591, 195–199.

Della, V.P., Kühn, I., Hotza, D., 2002. Rice husk ash as an alternate source for active silica production. Materials Letters. 57, 818-821.

Diaz, J.F., and Balkus, K.J., 1996. Enzyme immobilization in MCM-41 molecular sieve. Journal of Molecular Catalysis B: Enzymatic. 2, 115–126.

Eswaramoorthi, I., Dalai, A.K., 2006. Synthesis, characterisation and catalytic performance of boron substituted SBA-15 molecular sieves. Microporous and Mesoporous Materials. 93, 1-11.

Fan, J., Yu, C., Gao, F., Lei, J., Tian, B., Wang, L., Luo, Q., Tu, B., Zhou, W., and Zhao, D., 2003. Cubic mesoporous silica with large controllable entrance sizes and advanced adsorption properties. Angewandte Chemie-International Edition 42, 115, 3254–3258.

Franke, O., Schulz-Ekloff, G., Rathousky, J., Starek, J., Zukal, A., 1993. Unusual type of adsorption isotherm describing capillary condensation without hysteresis. J. Chem. Soc.,Chem. Commun. 724-726.

Galarneau, A., Di Renzo, F., Fajula, F., Mollo, L., Fubini, B., Ottaviani, M.F., 1998. Kinetics of formation of micelle-templated silica mesophases monitored by electron paramagnetic resonance. J. Coll. Interface Sci. 201, 105-117.

Gao, Y., Konovalova, T.A., Xu, T., Kispert, L.D., 2002. Electron transfer of carotenoids imbedded in MCM-41 and Ti-MCM-41: EPR, ENDOR and UV–Vis studies. The Journal of Physical Chemistry B. 106, 10808–10815.

Gross, A.F., and Tolbert, S.H., Wu, J., 1999. Host-guest chemistry using an oriented mesoporous host: alignment and isolation of a semiconducting polymer in the nanopores of ordered silica matrix. J. Phys. Chem. B. 103, 2374-2384.

Grisdanurak, N., Chiarakorn, S., Wittayakun, J., 2003. Utilization of mesoporous molecular seive synthesis from natural source rice husk silica to chlorinated volatile organic compounds (CVOCs) adsorption. Korean Journal of Chemical Engineering. 20, 950-955.

Guggenheim, S., 1995. Definition of clay and clay mineral: joint report of the AIPEA nomenclature and CMS nomenclature committees. Clays and Clay Minerals. 43, 255-256.

Halina, M., Ramesh, S., Yarmo, M.A., Kamarudin, R.A., 2007. Non-hydrothermal synthesis of mesoporous materials using sodium silicate from coal fly ash. Materials Chemistry and Physics. 101, 344–351.

He, J., Ma, K., Jin, J., Dong, Z., Wang, J., Li, R., 2009. Preparation and characterization of octyl-modified ordered mesoporous carbon CMK-3 for phenol adsorption. Microporous and Mesoporous Materials. 121, 173–177.

Heilmann, A., Teuscher, N., Kiesow, A., Janasek, D., and Spohn, U., 2003. Nanoporous aluminum oxide as a novel support material for enzyme biosensors. Journal of Nanoscience and Nanotechnology. 3, 375–379.

Höller, H., and Wirsching, U., 1985. Zeolites formation from fly ash. Fortschr. Mineral. 63, 21–43.

Hu, Y., Martra, G., Zhang, J., Higashimoto, S., Coluccia, S., Anpo, M., 2006. Characterization of the local structures of Ti-MCM-41 and their photocatalytic reactivity for the decomposition of NO into N_2 and O_2. The Journal of Physical Chemistry B. 110, 1680–1685.

Hui, K.S., Chao, C.Y.H., 2006. Synthesis of MCM-41 from coal fly ash by a green approach: Influence of synthesis pH. Journal of Hazardous Materials B. 137, 1135–1148.

Iler, R.K., 1979. The Chemistry of Silica. Wiley. New York. 6.

IUPAC. 1957. Reporting Physisorption Data for Gas/Solid Systems. Pur, Appl. Chem. 87, 603.

Jie, L., Jie, F., Yu, C., Zhang, L., Jiang, S., Tu, B., and Zhao, D., 2004. Immobilization of enzymes in mesoporous materials: controlling the entrance to nanospace. Microporous and Mesoporous Materials. 73, 121–128.

Jullaphan, O., Witoon, T., Chareonpanich, M., 2009. Synthesis of mixed-phase uniformly infiltrated SBA-3-like in SBA-15 bimodal mesoporous silica from rice husk ash. Materials Letters. 63 1303–1306.

Kang, F., Wang, Q., and Xiang, S., 2005. Synthesis of mesoporous Al-MCM-41 materials using metakaolin as aluminum source. Materials Letters. 59, 1426-1429.

Ketcome, N., Grisdanurak, N., Chiarakorn, S., 2009. Silylated rice husk MCM-41 and its binary adsorption of water–toluene mixture. J. Porous. Mater. 16, 41–46.

Kosslick, H., Tuan, V.A., Fricke, R., Peuker, C., Pilz, W., Storek, W., 1993. Synthesis and characterization of Ge-ZSM-5 zeolites. J. Phys. Chem. 97, 5678-5684.

Kresge, C.T., Leonowicz, M.E., Roth, W.J., Vartuli, J.C., and Beck, J.S., 1992. Ordered mesoporous molecular sieves synthesized by a liquid-crystal template mechanism. Nature. 359, 710-712.

Kruk, M., Jaroniec, M., Sayari, A., 1997. Adsorption Study of Surface and Structural Properties of MCM-41 Materials of Different Pore Sizes. J. Phy. Chem. 101, 583-589.

Kumar, P., Mal, N., Oumi, Y., Yamana, K., and Sano, T., 2001. Mesoporous materials prepared using coal fly ash as the silicon and aluminium source. J. Mater. Chem. 11, 3285–3290.

Lam, K.F., Fong, C.M., and Yeung, K.L., 2007. Separation of Precious Metals using Selective Mesoporous Adsorbents. Gold Bulletin. 40, 192-198.

Lowell, S., Shields, J.E., Thomas, M.A., Thommes, M., 2004. Characterization of Porous Solids and Podwers: Surface Area, Pore Size and Density. (Ed,), Springer. 16, 347.

Lee, K.P., Showkat, A.M., Gopalan, A.I., Kim, S.H., Choi, S.H., 2005. Synthesis of poly(diphenylamine) nanotubes in the channels of MCM-41 through self-assembly. Macromolecules. 38, 364–371.

Li, J., Zhou, C., Xie, H., Ge, Z., Yuan, L., Li, X., 2006. Titanium-containing mesoporous materials: synthesis and application in selective catalytic oxidation. Journal of Natural Gas Chemistry. 15, 164–177.

Liu, B., Hu, R., and Deng, J., 1997. Characterization of immobilization of an enzyme in a modified Y zeolite matrix and its application to an amperometric glucose biosensor. Analytical Chemistry. 69, 2343–2348.

Liu, B., Cao, Y., Chen, D., Kong, J., and Deng, J., 2003. Amperometric biosensor based on a nanoporous ZrO2 matrix. Analytica Chimica Acta. 478, 59–66.

Liou, T.–H., 2004. Preparation and characterization of nano-structured silica from 44 rice husk. Materials Science and Engineering A. 364, 2, 313-323.

Liu, S., He, H., Luan, Z., Klinowski, J., 1996. Solid-state NMR studies of the borosilicate mesoporous molecular sieve MCM-41. J. Chem. Soc., Faraday Trans. 92, 2011-2015.

Liu, H., Bao, X., Wei, W., Shi, G., 2003. Synthesis and characterization of kaolin/NaY/MCM-41 composites. Microporous and Mesoporous Materials. 66, 117–125.

Llewellyn, P.L., Ciesla, U., Decher, H., Stadler, R., Schüth, F., and Unger, K.K., 1994. MCM-41 and related materials as media for controlled polymerization processes. Stud. Surf. Sci. Catal. 84 , 2013-2020.

Loewenstein, W., Lowenstein, M., 1953. The distribution of aluminum in the tetrahedra of silicates and aluminates. American Mineralogist. 92-96.

Loy, D.A., Mather, B., Straumanis, A.R., Baugher, C., Schneider, D.A., Sanchez, A., Shea, K.J., 2004. Effect of the pH on the gelation time of hexylene-bridged polysilsesquioxanes. Chem. Mater. 16, 2041-2043.

Luechinger, M., Frunz, L., Pirngruber, G.D., Prins, R., 2003. A mechanistic explanation of the formation of high quality MCM-41 with high hydrothermal stability. Microporous Mesoporous Mater. 64, 203-211.

McBain, J.W., Soldate, A.M., 1942. The Solubility of Propylene Vapor in Water as Affected by Typical Detergents. J. Amer. Chem. Soc. 64, 1556-1557.

Melo, R.A.A., Giotto, M.V., Rocha, J., and Urquieta-González, E.A., 1999. MCM-41 ordered mesoporous molecular sieves synthesis and characterization. Mat. Res. 2, 173-179.

Meyers, B.L., Ely, S.R., Kutz, N.A., Kaduk, J.A., and Van den Bossche, E., 1985. Determination of structural boron in borosilicate molecular sieves via X-ray diffraction. J. Catal. 91, 352-355.

Milkey, R.G., 1960. Infrared spectra of some tectosilicates. Amer. Min. 45, 990-1007.

Mokaya, R., 2001. Hydrothermally-induced morphological transformation of mesoporous MCM-41 silica. Microporous and mesoporous Materials. 44-45, 119-127.

Moller, K., Bein, T., 1998. Inclusion Chemistry in Periodic Mesoporous Hosts. Chem. Mater. 10, 2950- 2963.

Moreno, N., Querol, X., Ayora, C., Alasteuey, A., Fernández-Preira, C., Janssen Jurkovicová, M., 2001. Potential Environmental application of Pure Zeolitic Material synthesized from Fly Ash. Journal of Envir. Eng. Sci. 127, 996-1002.

Natale, I.M., and Helmy, A.K., 1992. Montmorillonite-salt interactions at 550° C. Clays and Clay Minerals. 40, 206-211.

Nur, H., Guan, L.C., Endud, S., Hamdan, H., 2004. Quantitative measurement of a mixture of mesophases cubic MCM-48 and hexagonal MCM-41 by 13C CP/MAS NMR. Materials Letters. 58, 1971-1974.

Nur, H., Hamid, H., Endud, S., Hamdan, H., Ramli, Z., 2005. Iron-porphyrin encapsulated in poly(methacrylic acid) and mesoporous Al-MCM-41 as catalysts in the oxidation of benzene to phenol. Materials Chemistry and Physics. 96, 337-342.

Oberhagemann, U., Jeschke, M., Papp, H., 1999. Synthesis of highly ordered boron-containing B–MCM-41 and pure silica MCM-41. Micropor. Mesopor. Mater. 33, 165-172.

Occelli, M.L., Biz, S., Auroux, A., Ray, G.J., 1998. Effects of the nature of the aluminum source on the acidic properties of some mesostructured materials. Micropor. Mesopor. Mater. 26, 193-213.

Parala, H., Winkler, H., Kolbe, M., Wohlfart, A., Fischer, R.A., Schmechel, R., von Seggern, H., 2000. Confinement of CdSe Nanoparticles Inside MCM-41. Advanced Materials. 12, 1050–1055.

Patel, M., Prasanna, P., 1987. SEM studies on silica from plant materials. X-Ray Spectrometry. 16, 57-60.

Pauwels, B., Tendeloo, G.V., Thoelen, C., Rhijn, W.V., Jacobs, P.A., 2001. Structure determination of spherical MCM-41 particles. Adv. Mater. 13, 1317-1320.

Poh, N.E., Nur, H., Muhid, M.N.M., Hamdan, H., 2006. Sulphated AlMCM-41 Mesoporous solid Brønsted acid catalyst for ibenzoylation of biphenyl. Catalalysis Today. 114, 257-262.

Perathoner, S., Lanzafame, P., Passalacqua, R., Centi, G., Schlgöl, R., Su, D.S., 2006. Use of mesoporous SBA-15 for nanostructuring titania for photocatalytic applications. Microporous and Mesoporous Materials. 90, 347–361.

Proctor, A., Kalapathy, U.,and Shultz, J., 2000. A simple method for production of pure silica from rice hull ash. Bioresource Technology. 73, 257-262.

Queiroz, A.U.B., Aikawa, L.T., 1994. French Patent. 2694000.

Rayalu, S., Labhasetwar, N.K., Khanna, P., 2000. U. S. Patent no. 6027708.

Real, C., Alcala, M.D., Criado, J.M., 1996. Preparation of silica from rice husk. Journal of the American Ceramic Society. 79, 2012-2016.

Rosen, M.J., 1989. Surfactants and interfacial phenomena. 2(Ed,), John Wiley & Sons, New York.

Ryoo, R., Kim, J.M., 1995. Structural Order in MCM-41 controlled by Shifting Silicate Polymerization Equilibrium. J. Chem. Soc. Chem. Commun. 711-712.

Salonen, J., Lehto, V.P., 2008. Fabrication and chemical surface modification of mesoporous silicon for biomedical applications. Chemical Engineering Journal. 137, 162–172.

Sanhueza, V., Lopez-Escobar, L., Kelm, U., and Ruby Cid., 2006. Synthesis of a mesoporous material from two natural sources. J. Chem. Technol. Biotechnol. 81, 614–617.

Sasaki, T., Kajino, T., Li, B., Sugiyama, H., and Takahashi, H., 2001. New pulp biobleaching system involving manganese peroxidase immobilized in a silica support with controlled pore sizes. Applied and Environmental Microbiology. 67, 2208–2212.

Sayari, A., Moudrakovski, I., Danumah, C., Ratcliffe, C.I., Ripmeester, J.A., Preston, K.F., 1995. Synthesis and nuclear magnetic resonance study of boron-modified MCM-41 mesoporous materials. J. Phys. Chem. 99, 16373-16379.

Sayari, A., 1996. Catalysis by crystalline mesoporous molecular sieves. Chem. Mater. 8, 1840- 1852.

Selvam, P., Bhatia, S.K., Sonwane, C.G., 2001. Recent advances in processing and characterization of periodic mesoporous MCM-41 silicate molecular sieves. Ind. Eng. Chem. Res. 40, 3237-3261.

Shanbhag, G.V., Kumbar, S.M., Halligudis, B., 2008. Chemoselective synthesis of β-amino acid derivatives by hydroamination of activated olefins using AlSBA-15 catalyst prepared by post-synthetic treatment. Journal of molecular catalysis. A, Chemica. 284, 16-23.

Shigemoto, N., Shirakami, K., Hirano, S., and Hayashi, H., 1992. Preparation and characterization of zeolites from coal ash. Nippon Kagaku Kaishi. 484–492.

Shigemoto, N., Hayashi, H., Miyaura, K., 1993. Selective formation of Na-X zeolite from coal fly ash by fusion with sodium hydroxide prior to hydrothermal reaction. Journal of Materials Science. 28, 4781-4786.

Shimizu, Y., Hyodo, T., Egashira, M., 2004. Mesoporous semiconducting oxides for gas sensor application. Journal of the European Ceramic Society. 24, 1389–1398.

Sidheswaran, P., Bhat, A.N., 1997. Impact of zeolitic water content on exchange of calcium ions. Thermochimica Acta. 298, 55–58.

Sing, J.W., Everett, D.H., Haul, R.A.W., Moscou, L., Pierotti, R.A., Rouquérol, J., and Siemieniewska, T., 1985. Reporting Physisorption Data for Gas/Solid System. Pure Appl. Chem. 57, 603-619.

Singer, A., Bergaut, V., 1995. Cation Exchange Properties of Hydrothermally Treated Coal Fly Ash. Environ. Sci. Technol. 29, 1748-1753.

Sherman, J.D., 1999. Synthetic zeolites and other microporous oxide molecular sieves. Proc. Natl. Acad. Sci. USA. 96, 3471-3478.

Stave, M.S., and Nicholas, J.B., 1995. Density functional studies of zeolites. II: structure and acidity of [T]-ZSM-5 models (T = B, Al, Ga, and Fe). J. Phys. Chem. 99, 15046-15061.

Steudel, A., 2008. Selection strategy and modification of layer silicates for technical applications. Faculty of Civil Engineering, Geo- and Environmental Sciences of Fridericiana university Karlsruhe (TH).

Sun, Y., Liu, X.W., Su, W., Zhou, Y., Zhou, L., 2007. Studies on ordered mesoporous materials for potential environmental and clean energy applications. Applied Surface Science. 253, 5650–5655.

Sundaramurthy, V., Lingappan, N., 2003. The catalytic effect of boron substituted ZSM-5 and MCM-41 molecular sieves on 1-octene isomerisation. Microporous and Mesoporous Materials. 65, 243-255.

Scholle, K.F.M.G.J., Kentgens, A.P.M., Veeman, W.S., Frenken, P., Van der Velden, G.P.M., 1984. Proton magic angle spinning nuclear magnetic resonance and temperature programmed desorption studies of ammonia on the acidity of the framework hydroxyl groups in the zeolite H-ZSM-5 and in H-boralite. J. Phys. Chem. 88, 5-8.

Surachai Artkla. 2008. Catalysts supported on MCM-41 synthesized from rice husk silica: titanium oxide for photodegradation of organic pollutants and potassium oxide for transesterification of palm olein oil. Degree of Doctor of Philosophy in Chemistry Suranaree University of Technology.

Szostak, R., 1989. Molecular Sieves. Van Nostrand Reinhold, New York.

Tanford, C., 1980. The hydrophobic effect: Formation of micelles and biological membranes. Wiley, New York.

Taylor, H.F.W., 1962. Homogeneous and inhomogeneous mechanisms in the dehydroxylation of minerals. Clay Min. Bull. 5, 45-55.

Trong, On.D., Kapoor, M.P., Bonneviot, L., Kaliaguine, S., Gabelica, Z., 1996. Structural State of Boron and Catalytic Properties of MFI-Titanium Boralites. J. Chem. Soc. Faraday Trans. 92, 1031-1038.

Ulagappan, N., Rao, C.N.R., 1996. Evidence for supramolecular organization of alkane and surfactant molecules in the process of forming mesoporous silica. Chem. Commun. 2759-2760.

Valerio, G., Plevert, J., Goursot, S., and di Renzo, F., 2000. Modeling of boron substitution in zeolites and implications on lattice parameters, Phys. Chem. Chem. Phys. 2, 1091–1094.

Vallet-Regi, M., Ramila, A., del Real, R.P., Perez-Pariente, J., 2001. A new property of MCM-41: Drug delivery system. Chem. Mater., 13, 308-311.

Vidya, K., Dapurkar, S.E., Selvam, P., Badamali, S.K., Kumar, D., Gupta, N.M., 2002. Encapsulation, characterization and catalytic properties of uranyl ions in mesoporous molecular sieves. J. Mol. Catal. A. 181, 91-97.

Voegtlin, A.C., Matijasic, A., Patarin, J., Sauerland, C., Grillet, Y., Huve, L., 1997. Room-temperature synthesis of silicate mesoporous MCM-41-type materials: Influence of the synthesis pH on the porosity of the materials obtained. Micropor. Mater. 10, 137–147.

Wakihara, T., Sugiyama, A., Okubo, T., 2004. Crystal growth of faujasite observed by atomic force microscopy. Microporous Mesoporous Mater. 70, 7-13.

Wang, A., & Kabe, T., 1999. Fine-tuning of pore size of MCM-41 by adjusting the initial pH of the synthesis mixture. Chem. Commun. 2067-2068.

Wu, X.W., M, H-W., Li, J-H., Zhang, J., Li, Z-H., 2007. The synthesis of mesoporous aluminosilicate using microcline for adsorption of mercury(II). Journal of Colloid and Interface Science. 315, 555–561.

Wu, C.G., and Bein, T., 1994. Conducting carbon wires in ordered, nanometer-sized channels. Science. 266, 1013-1015.

Xu, X.H., Lu, P., Zhou, Y.M., Zhao, Z.Z., Guo, M.Q., 2009. Laccase immobilized on methylene blue modified mesoporous silica MCM-41 /PVA. Materials science & engineering C. Biomimetic and supramolecular systems. 29, 2160-2164.

Yalcin, N., Sevinc, V., 2001. Study on silica obtained from rice husk. Ceramics International. 27, 219-224.

Yanagisawa, T., Shimizu, T., Kudora, K., and Kato, C., 1990. The Preparation of Alkyltriinethylaininonium–Kaneinite Complexes and Their Conversion to Microporous Materials. Bull. Chem. Soc. Jpn. 63, 988.

Yang, H., Tang, A., Ouyang, J., Li, M., and Mann, S., 2010. From Natural Attapulgite to Mesoporous Materials: Methodology, Characterization and Structural Evolution. J. Phys. Chem. B. 114, 2390–2398.

Yang, H., Deng, Y., Du, C., Jin, S., 2010. Novel synthesis of ordered mesoporous materials Al-MCM-41 from bentonite. Applied Clay Science. 47, 351–355.

Zhao, D., Huo, Q., Feng, J., Chmelka, B.F., Stucky, G.D., 1998. Nonionic Triblock and Star Diblock Copolymer and Oligomeric Surfactant Syntheses of Highly Ordered, Hydrothermally Stable, Mesoporous Silica Structures. J. Am. Chem. Soc. 120, 6024-6036.

Zhao, Y.X., Ding, M.Y., Chen, D.P., 2005. Adsorption properties of mesoporous silicas for organic pollutants in water. Analytica Chimica Acta. 542, 193–198.

Zhang, X-F., Zhang, Z., 2001. Progress in Transmission Electron Microscopy 2. Springer Series in Surface Sciences. 39, 307.

Zhu, H.Y., Ding, Z., and Barry, J.C., 2002. Porous Solids from Layered Clays by Combined Pillaring and Templating Approaches. J. Phys. Chem. B. 106, 11420-11429.

http://www.acaa-usa.org/.

http://www.ecoba.com/ecobaccpprod.html.